

JOURNAL OF THE ANATOMICAL SOCIETY OF INDIA

Print ISSN: 0003-2778

GENERAL INFORMATION

About the Journal

Journal of the Anatomical Society of India (ISSN: Print 0003-2778) is peer-reviewed journal. The journal is owned and run by Anatomical Society of India. The journal publishes research articles related to all aspects of Anatomy and allied medical/surgical sciences. Pre-Publication Peer Review and Post-Publication Peer Review Online Manuscript Submission System Selection of articles on the basis of MRS system Eminent academicians across the globe as the Editorial board members Electronic Table of Contents alerts Available in both online and print form. The journal is published quarterly in the months of January, April, July and October.

Scope of the Journal

The aim of the *Journal of the Anatomical Society of India* is to enhance and upgrade the research work in the field of anatomy and allied clinical subjects. It provides an integrative forum for anatomists across the globe to exchange their knowledge and views. It also helps to promote communication among fellow academicians and researchers worldwide. The Journal is devoted to publish recent original research work and recent advances in the field of Anatomical Sciences and allied clinical subjects. It provides an opportunity to academicians to disseminate their knowledge that is directly relevant to all domains of health sciences.

The Editorial Board comprises of academicians across the globe.

JASI is indexed in Scopus, available in Science Direct.

Abstracting and Indexing Information

The journal is registered with the following abstracting partners:

Baidu Scholar, CNKI (China National Knowledge Infrastructure), EBSCO Publishing's Electronic Databases, Ex Libris – Primo Central, Google Scholar, Hinari, Infotrieve, Netherlands ISSN center, ProQuest, TdNet, Wanfang Data

The journal is indexed with, or included in, the following:

SCOPUS, Science Citation Index Expanded, IndMed, MedInd, Scimago Journal Ranking, Emerging Sources Citation Index.

Impact Factor[®] as reported in the Journal Citation Reports[™] (Clarivate Analytics, 2021): 0.26

Information for Authors

Article processing and publication charges will be communicated by the editorial office. All manuscripts must be submitted online at <https://review.jow.medknow.com/jasi>.

Subscription Information

A subscription to JASI comprises 4 issues. Prices include postage. Annual Subscription Rate for non-members-

Rates of Membership (with effect from 1.1.2022)		
	India	International
Ordinary membership	INR 1500	US \$ 100
Couple membership	INR 2250	
Life membership	INR 8000	US \$ 900
Subscription Rates (till 31 st August)		
Individual	INR 6000	US \$ 650
Library/Institutional	INR 12000	US \$ 1000
Trade discount of 10% for agencies only		
Subscription Rates (after 31 st August)		
Individual	INR 6500	US \$ 700
Library/Institutional	INR 12500	US \$ 1050

The Journal of Anatomical Society of India (ISSN: 0003-2778) is published quarterly. Subscriptions are accepted on a prepaid basis only and are entered on a calendar year basis. Issues are sent by standard mail. Priority rates are available upon request.

Information to Members/Subscribers

All members and existing subscribers of the Anatomical Society of India are requested to send their membership/existing subscription fee for the current year to the Treasurer of the Society on the following address: Prof (Dr.) Punit Manik, Treasurer, ASI, Department of Anatomy, KGMU, Lucknow - 226003. Email: punitamanik@yahoo.co.in. All payments should be made through an account payee bank draft drawn in favor of the **Treasurer, Anatomical Society of India**, payable at **Lucknow** only, preferably for **Allahabad Bank, Medical College Branch, Lucknow**. Outstation cheques/drafts must include INR 70 extra as bank collection charges.

All complaints regarding non-receipt of journal issues should be addressed to the Editor-in-Chief, JASI at editorjasi@gmail.com. The new subscribers may, please contact wklrhpmedknow_subscriptions@wolterskluwer.com.

Requests of any general information like travel concession forms, venue of next annual

conference, etc. should be addressed to the General Secretary of the Anatomical Society of India.

For mode of payment and other details, please visit www.medknow.com/subscribe.asp

Claims for missing issues will be serviced at no charge if received within 60 days of the cover date for domestic subscribers, and 3 months for subscribers outside India. Duplicate copies cannot be sent to replace issues not delivered because of failure to notify publisher of change of address. The journal is published and distributed by Wolters Kluwer India Pvt. Ltd. Copies are sent to subscribers directly from the publisher's address. It is illegal to acquire copies from any other source. If a copy is received for personal use as a member of the association/society, one cannot resale or give-away the copy for commercial or library use.

The copies of the journal to the subscribers are sent by ordinary post. The editorial board, association or publisher will not be responsible for non receipt of copies. If any subscriber wishes to receive the copies by registered post or courier, kindly contact the publisher's office. If a copy returns due to incomplete, incorrect or changed address of a subscriber on two consecutive occasions, the names of such subscribers will be deleted from the mailing list of the journal. Providing complete, correct and up-to-date address is the responsibility of the subscriber.

Nonmembers: Please send change of address information to subscriptions@medknow.com.

Advertising Policies

The journal accepts display and classified advertising. Frequency discounts and special positions are available. Inquiries about advertising should be sent to Wolters Kluwer India Pvt. Ltd, advertise@medknow.com.

The journal reserves the right to reject any advertisement considered unsuitable according to the set policies of the journal.

The appearance of advertising or product information in the various sections in the journal does not constitute an endorsement or approval by the journal and/or its publisher of the quality or value of the said product or of claims made for it by its manufacturer.

Copyright

The entire contents of the JASI are protected under Indian and international copyrights. The Journal, however, grants to all users a free, irrevocable, worldwide, perpetual right of access to, and a license to copy, use, distribute, perform and display the work publicly and to make and distribute derivative works in any digital medium for any reasonable non-commercial purpose, subject to proper attribution of authorship and ownership of the rights. The journal also grants the right to make small numbers of printed copies for their personal non-commercial use.

Permissions

For information on how to request permissions to reproduce articles/information from this journal, please visit www.jasi.org.in.

Disclaimer

The information and opinions presented in the Journal reflect the views of the authors and not of the Journal or its Editorial Board or the Publisher. Publication does not constitute endorsement by the journal. Neither the JASI nor its publishers nor anyone else involved in creating, producing or delivering the JASI or the materials contained therein, assumes any liability or responsibility for the accuracy, completeness, or usefulness of any information provided in the JASI, nor shall they be liable for any direct, indirect, incidental, special, consequential or punitive damages arising out of the use of the JASI. The JASI, nor its publishers, nor any other party involved in the preparation of material contained in the JASI represents or warrants that the information contained herein is in every respect accurate or complete, and they are not responsible for any errors or omissions or for the results obtained from the use of such material. Readers are encouraged to confirm the information contained herein with other sources.

Addresses

Editorial Office

Dr. Vishram Singh, Editor-in-Chief, JASI
OC-5/103, 1st floor, Orange County Society,
Ahinsa Khand-I, Indirapuram, Ghaziabad,
Delhi, NCR- 201014.
Email: editorjasi@gmail.com

Published by

Wolters Kluwer India Pvt. Ltd
A-202, 2nd Floor, The Qube,
C.T.S. No.1498A/2 Village Marol, Andheri (East),
Mumbai - 400 059, India.
Phone: 91-22-66491818
Website: www.medknow.com

Printed at

Nikeda Art Printers Pvt. Ltd.,
Building No. C/3 - 14,15,16, Shree Balaji Complex, Vehele Road,
Village Bhatale, Taluka Bhiwandi, District Thane - 421302, India.

JOURNAL OF THE ANATOMICAL SOCIETY OF INDIA

Print ISSN: 0003-2778

EDITORIAL BOARD

Editor-in-Chief

Dr. Vishram Singh, MBBS, MS, PhD (hc), FASI, FIMSA
Adjunct Professor, Department of Anatomy, KMC, Mangalore, Manipal Academy of Higher Education, Manipal, Karnataka

Joint-Editor

Dr. Murlimanju B.V
Associate Professor, Department of Anatomy, KMC, Mangalore, Manipal Academy of Higher Education, Manipal, Karnataka

Managing Editor

Dr. C. S. Ramesh Babu
Associate Professor, Department of Anatomy, Muzaffarnagar Medical College, Muzaffarnagar, Uttar Pradesh

Associate Editor

Dr. D. Krishna Chaitanya Reddy
Assistant Professor, Department of Anatomy, Kamini Academy of Medical Sciences and Research Center, Hyderabad

Section Editors

Clinical Anatomy

Dr. Vishy Mahadevan, PhD, FRCS(Ed), FRCS
Prof of Surgical Anatomy, The Royal College of Surgeons of England, London, UK

Histology

Dr. G.P. Pal, MS, DSc, Prof & Head, Department of Anatomy, MDC & RC, Indore, India

Gross and Imaging Anatomy

Dr. Srijit Das, Department of Human and Clinical Anatomy, College of Medicine and Health Sciences, Sultan Qaboos University, Muscat, Oman

Medical Education

Dr. Deepa Singh
Professor, Department of Anatomy, HIMS, Swami Rama Himalayan University, Jolly Grant, Dehradun, Uttarakhand

Neuroanatomy

Dr. T.S. Roy, MD, PhD
Prof & Head, Department of Anatomy, AIIMS, New Delhi

Embryology

Dr. Gayatri Rath, MS, FAMS
Professor and Head, Department of Anatomy, NDMC Medical College, New Delhi

Genetics

Dr. Rima Dada, MD, PhD
Prof, Department of Anatomy, AIIMS, New Delhi, India

Dental Sciences

Dr. Praveen B Kudva
Professor and Head, Department of Periodontology, Jaipur Dental College, Jaipur, Rajasthan

National Editorial Board

Dr. S.D. Joshi, Indore
Dr. G.S. Longia, Jaipur
Dr. A.K. Srivastava, Lucknow
Dr. Daksha Dixit, Belgaum
Dr. S.K. Jain, Moradabad
Dr. P.K. Sharma, Lucknow
Dr. S. Senthil Kumar, Chennai
Dr. Daisy Sahani, Chandigarh
Dr. N. Damayanti Devi, Imphal

Dr. Renu Chauhan, Delhi
Dr. Ashok Sahai, Agra
Dr. Ramesh Babu, Muzaffarnagar
Dr. T.C. Singel, Ahmedabad
Dr. P.K. Verma, Hyderabad
Dr. S.L. Jethani, Dehradun
Dr. Surajit Ghatak, Jodhpur
Dr. Brijendra Singh, Rishikesh
Dr. P. Vatsala Swamy, Pune

International Editorial Board

Dr. Yun-Qing Li, China
Dr. In-Sun Park, Korea
Dr. K.B. Swamy, Malaysia
Dr. Syed Javed Haider, Saudi Arabia
Dr. Pasuk Mahaknkrauh, Thailand
Dr. Tom Thomas R. Gest, USA

Dr. Chris Briggs, Australia
Dr. Petru Matusz, Romania
Dr. Min Suk Chung, South Korea
Dr. Veronica Macchi, Italy
Dr. Gopalakrishnakone, Singapore
Dr. Sunil Upadhyay, UK

JOURNAL OF THE ANATOMICAL SOCIETY OF INDIA

Print ISSN: 0003-2778

EXECUTIVE COMMITTEE

Office Bearers

President

Dr. Brijendra Singh (Rishikesh)

Vice President

Dr. G. P. Pal (Indore)

Gen. Secretary

Dr. S.L. Jethani (Dehradun)

Joint. Secretary

Dr. Jitendra Patel (Ahmedabad)

Treasurer

Dr. Punita Manik (Lucknow)

Joint-Treasurer

Dr. R K Verma (Lucknow)

Editor-in-Chief

Dr. Vishram Singh (Mangalore)

Joint-Editor

Dr. Murlimanju B.V (Mangalore)

Members

Dr. Avinash Abhaya (Chandigarh)
Dr. Sumit T. Patil (Portblair)
Dr. Mirnmoy Pal (Agartala)
Dr. Manish R. Gaikwad (Bhubaneswar)
Dr. Sudhir Eknath Pawar (Ahmednagar)
Dr. Rekha Lalwani (Bhopal)
Dr. Anshu Sharma (Chandigarh)
Dr. Rakesh K Diwan (Lucknow)
Dr. A. Amar Jayanthi (Trichur)
Dr. Ranjan Kumar Das (Baripada)

Dr. Rajani Singh (Rishikesh)
Dr. Anu Sharma (Ludhiana)
Dr. Pradeep Bokariya (Sevagram)
Dr. B. Prakash Babu (Manipal)
Dr. Ruchira Sethi (Varanasi)
Dr. Ashok Nirvan (Ahmedabad)
Dr. S K Deshpande (Dharwad)
Dr. Sunita Athavale (Bhopal)
Dr. Sharmistha Biswas (Kolkatta)

JOURNAL OF THE ANATOMICAL SOCIETY OF INDIA

Volume 71 | Issue 4 | October-December 2022

CONTENTS

EDITORIAL

Philately, World Postage Stamps, History of Medicine, and Anatomists

Vishram Singh, B. V. Murlimanju, Rajanigandha Vadgaonkar259

ORIGINAL ARTICLES

Morphologic and Morphometric Evaluation of the Carotid Artery Wall: A Cadaver-Based Light and Scanning Electron Microscopic Study

Hilal Nakkas, Ferda Topal Celikkan, Nihal Apaydm, Oya Evirgen261

Anatomical Variations of the Human Ossicular Chain in South Indian Population: Morphometry and Morphology

Giridhar Dasegowda, Padmalatha Kadirappa, Hema Nanjundaraju, Seema Shimoga Raja, Rachana Suresh.....266

Stereological and Comparative Evaluation of the Carpal Tunnel in Patients with Carpal Tunnel Syndrome Using Magnetic Resonance Images

Gürsel A. K. Güven, Mehmet Emirzeoglu, Murat Terzi, Mustafa Bekir Selçuk, Bünyamin Sahin.....272

Correlation of Cephalo-Facial Parameters with Body Height in Indian and African Students of a University in North India

Sreekala C. Nair, Prajna Paramita Samanta, Poonam Kharb.....279

Numerical Chromosomal Aberrations in Acute Lymphoblastic Leukemia in North Indians

Indu Shri, Rakesh Kumar Verma, Archana Rani, Navneet Kumar.....283

Anthropometric Parameters of Idiopathic Familial Short Stature Females and its Correlation with Height and Comparison with the Control Group

Karishma Sharma, Rishita Chandra, Brijendra Singh, Shashi Ranjan Mani Yadav, Manisha Naithani, Surekha Kishore, Vivek Mishra, Kriti Mohan, Prashant Kumar Verma.....288

Evaluation of the Brain Indexes of Subjects with and without Brain Atrophy Using Computed Tomography

Mahmut Öksüzler, Sema Polat, Mahmut Tunç, Duygu Vuralli, Pinar Göker295

Ambiguity of the Radiographs around the Elbow Joint: Anatomical Variant versus Degenerative Changes

Vojtech Kunc, Vladimir Kunc, Katerina Kuncova, David Kachlik, Lubomir Kopp.....303

Effect of Different Doses of Aluminum Chloride on Neurodegeneration in Hippocampus Region of the Rat Brain

Amit Massand, Mallika Basera, Sonal Grace, Reshma Kumarachandra, K. Sudha, Rajalakshmi Rai, Murlimanju BV, K. Sowndarya307

The Relationship between Isolated Unilateral Concha Bullosa and Mastoid Air Cell Volumes

Fatih Yüksel, Mehmet Erkan Kahraman, Isa Deniz311

CASE REPORTS

Unusual Multiple Arterial Variations of the Upper Limb

Buse Naz Çandır, Latif Sağlam, İlke Ali Gürses, Özcan Gayretli.....317

Milder and Later Presentation of Trisomy 13: A Case Report and Literature Review

Rashmi. N, H. S. Kiran, H. S. Rajani321

continued...

**Case Report of Persistent Left Superior Vena Cava with Absent Papillary
Muscle – Unusual Coexistence**

Divya Umamaheswaran, Jayagandhi Sakkarai, Rema Devi.....324

INSTRUCTIONS TO AUTHOR329

Philately, World Postage Stamps, History of Medicine, and Anatomists

Philately deals with the study and assortment of postal stamps. However, there are no barriers for the connection between the history of medicine and philately. It is very much exciting to see the portraits of people of world-famous anatomists, medical reputation, medical inventions, welfare organizations of medicine, and diseases as postal stamps. Postal departments all over the world have supported the efforts of governments in creating awareness and spreading information on health topics and programs. Great Britain has issued the first stamp globally in the year 1840.^[1] In India, from 1837 onward, the East India Company used hand-struck stamps. However, the first stamp in India was printed in 1854 by Victoria-George VI during British India. Before the era of telephones, computers, and mobile phones, postal letters were the best and only method of communication nationally and internationally. Postage stamps are the token offered for postal charges and they are also utilized to spread essential information about history, culture, awareness, and achievements.^[2] The hobby of postal stamp collection is now changed to digital philately due to advanced technology. A total of 48,159 stamps from 184 countries are registered in the World Association for the Development of Philately (WADP).^[2] In 1970, France released a postal stamp featuring a French professor of pharmacy, Pierre Joseph Pelletier, and his student, Joseph Coventou, who together prepared pure salts of quinine and tested them clinically. This postal stamp was released to celebrate the 150th anniversary of the discovery of quinine.^[3] The highest number of entries in the WADP is by France (1258), followed by Japan (1106), and the other top entries included the USA (1096), Portugal (1029), Belgium (994), Great Britain (987), Australia (954), Hungary (915), Spain (849), and Romania (846). Indian stamps totaled 554 entries, and the least entry in the WADP Numbering System is by the Democratic Republic of the Congo.^[2]

During the 7th international conference of anatomy, which was held in New York City, USA, in 1960, Oscar V. Batson, who identified the vertebral venous system, was remembered.^[4] Aristotle was published on a postal stamp from Greek and Galen in Yemen.^[5] Leonardo da Vinci, who was instrumental in patenting the cross-sectional anatomy, was given on a stamp in France [Figure 1a]. Andreas Vesalius [Figure 1b]^[5] is considered the founder of modern anatomy, and World Anatomy Day is celebrated on every year, October 15, which is the death anniversary of

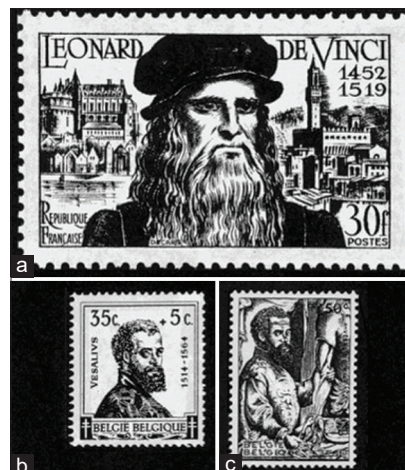


Figure 1: (a) Leonardo da Vinci in a French stamp; (b) Andreas Vesalius, the founder of modern anatomy; (c) the woodcut portrait of Andreas Vesalius, which shows the dissection of an upper limb^[5]

him. World Anatomy Day is an initiative of “International Federation of Association of Anatomists.” The picture of Andreas Vesalius, which shows the surgical dissection of the upper extremity, was reproduced [Figure 1c].^[5] Niels Stensen, who identified the duct of the parotid gland, was commemorated in Denmark in 1969.

Although philately will not cover the whole historical anatomists and medicine, whatever published pictures on the postal stamps will introduce the world famous academicians and scientists into the fascinating medical field and the history of human anatomy.^[5]

Vishram Singh, B. V. Murlimanju, Rajanigandha Vadgaonkar

Department of Anatomy, Kasturba Medical College, Mangalore, Manipal Academy of Higher Education, Manipal, Karnataka, India

Address for correspondence: Dr. B. V. Murlimanju, Department of Anatomy, Kasturba Medical College, Mangalore - 575 004, Karnataka, India. E-mail: flutemist@gmail.com

References

1. Rajasoorya C. Stamping with stamps – Medical history and postage stamps. Singapore Med J 2020;61:503-4.
2. Hirwade MA, Nawlakhe UA. Postage stamps and digital philately: Worldwide and Indian scenario. Int Inf Libr Rev 2012;44:28-39.
3. Paidhungat JV. Medical philately (medical personalities on

stamps). J Assoc Physicians India 2001;49:909.

4. Sauer ME. Anatomists on postage stamps. Anat Rec 1950;106:314.
5. O’Rahilly R. Philatelic introduction to the history of anatomy. Clin Anat 1997;10:337-40.


This is an open access journal, and articles are distributed under the terms of the Creative Commons Attribution-NonCommercial-ShareAlike 4.0 license, which allows others to remix, tweak, and build upon the work non-commercially, as long as appropriate credit is given and the new creations are licensed under the identical terms.

Article Info

Received: 27 October 2022

Accepted: 28 October 2022

Available online: ***

Access this article online	
Quick Response Code: 	Website: www.jasi.org.in
	DOI: 10.4103/jasi.jasi_152_22

How to cite this article: Singh V, Murlimanju BV, Vadgaonkar R. Philately, world postage stamps, history of medicine, and anatomists. J Anat Soc India 2022;XX:XX-XX.

Morphologic and Morphometric Evaluation of the Carotid Artery Wall: A Cadaver-Based Light and Scanning Electron Microscopic Study

Abstract

Introduction: A variety of changes occur on the elastic artery wall with age. Ultrastructural studies made in this area are mostly animal based. We aimed to evaluate wall changes and three-dimensional organization of the elastic lamellae with aging in humans. **Material and Methods:** Common carotid arteries were obtained from 17 human cadavers which were grouped as G1 ($n = 6$), 30–39 years; G2 ($n = 5$), 40–49 years; and G3 ($n = 6$), >50 years of age. Samples were evaluated under light and scanning electron microscopes. **Results:** Examination of G1 revealed intimal thickening and foamy cell infiltration. G2 and G3 had plaques bulging into the lumen and interlamellar space was widened. The lamellae were more straight. There was a positive correlation between intimal thickness and age. Elastic fiber content decreased with aging. Scanning electron microscopic analysis confirmed the findings. G1 and G2 had a smooth surfaced internal elastic lamina with uniform fenestrations whereas G3 contained numerous irregular fenestrae. **Discussion and Conclusion:** With this study, we showed some other wall structure changes beside plaque formation by aging. Which layer is affected the most was not clear at previous clinical studies because using ultrasonography (USG) cannot address the layer. Microscopic evaluation of this study revealed that when a wall thickening is detected by USG, it is due to intimal thickening. The specific vessel layer structural changes are important for proper treatment.

Keywords: Carotid artery, intima–media thickness, light microscopy, scanning electron microscopy

Introduction

Elastic type of communicating arteries, such as aorta and common carotid artery (CCA), absorb the energy caused by a large amount of systolic blood. During diastole, this absorbed energy recurs and helps transmit the diastolic blood by keeping the vascular tonus.^[1] Endothelial dysfunction leads to the failure of barrier function and the accumulation of low-density lipoprotein cholesterol in the subendothelium forming atherosclerotic lesions. Fragmentation of elastic lamellae due to mechanical and enzymatic factors (e.g., matrix metalloproteinase-2 activity), decreasing ratio of elastin/collagen content of the artery wall, and decreasing tonus and degeneration of vascular smooth muscle cells (VSMCs) involve a variety of changes on large elastic artery wall with aging.^[1-3] All these changes lead to intimal–medial thickening and atherosclerosis.^[4-7] They also induce hypertension and cardiovascular diseases (CVDs) such as myocardial infarct,

cerebrovascular ischemia, and stroke.^[2,8,9]

It is shown with large-scale follow-up studies that increased intima–media thickness (IMT) gives an opinion about future vascular events independently of conventional risk factors and it is predictive in younger group as much as in older subjects.^[6,10-12] Ultrasonography (USG) is a widely used noninvasive diagnostic technique for measuring IMT and assessing atherosclerotic status, but unfortunately USG examination is mostly inadequate to predict which layer is mostly affected in elastic arteries.^[4,8,13] The new development in ultrasonographic technology tries to deal with this problem such as *in vivo* intravascular USG gives more useful information about arterial wall structure but commonly not preferred as it is an invasive method.^[14] In literature, scanning electron microscopic (SEM) technique was used to observe the endothelial layer and three-dimensional configuration of arterial wall components such as extracellular matrix, collagen fibers, elastin lamellae, and VSMCs.^[3,15] In the present study, we

Hilal Nakkas,
Ferda Topal
Celikkan¹,
Nihal Apaydin²,
Oya Evirgen¹

Department of Histology
and Embryology, Faculty of
Medicine, Ankara Yildirim
Beyazit University, Departments
of ¹Histology and Embryology
and ²Anatomy, Faculty of
Medicine, Ankara University,
Ankara, Turkey

Article Info

Received: 01 October 2021

Revised: 13 June 2022

Accepted: 16 August 2022

Available online: ***

Address for correspondence:

Dr. Hilal Nakkas,
Department of
Histology-Embryology, Ankara
Yildirim Beyazit University
School of Medicine, Ihsan
Dogramaci Boulevard, 3rd Km.
Cankaya, Ankara, Turkey.
E-mail: gokturkhillal@gmail.com

Access this article online

Website: www.jasi.org.in

DOI:
10.4103/jasi.jasi_168_21

Quick Response Code:



How to cite this article: Nakkas H, Celikkan FT, Apaydin N, Evirgen O. Morphologic and morphometric evaluation of the carotid artery wall: A cadaver-based light and scanning electron microscopic study. J Anat Soc India 2022;XX:XX-XX.

This is an open access journal, and articles are distributed under the terms of the Creative Commons Attribution-NonCommercial-ShareAlike 4.0 License, which allows others to remix, tweak, and build upon the work non-commercially, as long as appropriate credit is given and the new creations are licensed under the identical terms.

For reprints contact: WKHLRPMedknow_reprints@wolterskluwer.com

aimed to evaluate the structure and the morphometry of the intimal, subintimal, medial layers, and three-dimensional organization of the elastic lamellae in CCA wall of human cadavers with respect to age.

Material and Methods

Sample collection and processing

The study was conducted in the Department of Histology and Embryology and the Department of Anatomy at Ankara University. The cadavers used in this study were donated to Ankara University Faculty of Medicine for anatomical education, research, and clinical skill training. The history of health which includes cardiovascular system risk factors such as arterial pressure, blood biochemistry, CVDs and causes of death of all cadavers were not determined. The research protocol was approved by the Human Research Ethics Committee of Ankara University Faculty of Medicine (Decision number: I2-174-21). All the tissue-handling procedures were conducted according to the principles outlined in the Declaration of Helsinki. CCA segments of 3 cm in length were obtained from 17 adult (15 men and 2 women) human cadavers that were grouped with respect to age as G1 ($n = 6$), 30–39 years; G2 ($n = 5$), 40–49 years; and G3 ($n = 6$), >50 years. All obtained CCA segments were divided into two pieces and processed for light microscope and SEM analysis.

Tissue processing and morphometric analysis

The fixed (with 4% formaldehyde solution) CCA tissue samples taken from cadavers were dehydrated through the increasing concentrations of ethanol series and embedded in paraffin blocks. The paraffin sections (4 μm) were stained with H and E (H and E) for routine examination. For the evaluation of elastic lamella and collagenous fibrous tissue, the sections were stained with orcein and indigo carmine (by Frankel's method). The intimal thickening, lipid accumulation, inflammation, continuity of elastic lamellae, course of elastic lamellae, and internal elastic lamina (IEL) continuity of the CCA vessel wall were assessed and scored as (-), no changes; (+), mild; (++) moderate; and (+++), severe.

For morphometric analysis, digital 8-bit RGB images from sections of all groups were obtained with an AxioCam MRc5 Camera mounted on the light microscope (Zeiss Axio Scope A1, Oberkochen, Germany) at $\times 40$ magnification lens. The morphometric measurements were made by Photoshop CS5© image analysis software. Intimal thickness (IT) was defined as the distance from the luminal surface of the endothelium to the inner border of IEL. Intimal area (IA) was calculated by subtracting the luminal area from internal elastic area. Medial area (MA) was defined as the area between IEL and adventitia. By marking brownish colored areas of the orcein and indigo carmine stained cross sections at $\times 40$ magnification, the intimal, medial and intimal + medial elastin content ratio

of the vessel wall were analyzed and calculated.^[16] All measurements were performed in a blinded fashion to groups by a senior histologist.

Scanning electron microscopic analysis

For the SEM examination, two consecutive 0.5–1 mm segments from each specimen were first incubated in 90% formic acid at 45°C for 4 days to obtain maceration of the cellular elements. Segments were, then, postfixed with 0.5% tannic acid and 1% osmium tetroxide (OsO_4) and dehydrated. One segment of each sample was kept as whole and the other one was frozen in liquid nitrogen and fractured. All segments were dried in the critical point dryer, sputter-coated with gold palladium (Emitech K550x, England), and observed under SEM (Leo 438VP, Germany) operated at 1218 kV. Pictures were directly acquired in digital format as 1024 \times 768 pixels grayscale tagged image file format images.

Statistical analysis

Statistics were obtained using the ready-to-use program of SPSS version 11.0 (SPSSInc., Chicago, IL, USA). All the values were expressed as mean \pm standard deviation. The obtained results were assessed by one-way analysis of variance and Tukey's tests. $P < 0.05$ was considered statistically significant.

Results

Light microscopic examination of G1 revealed intimal foamy cell (macrophages loaded with lipid) infiltration. IEL was intact and elastic fibers were interposed within VSMCs. Elastic fibers lied in parallel undulant arrays [Figure 1a and b]. G2 had atherosclerotic plaques bulging into the artery lumen, which contained cholesterol crystals within the fibrous tissue and cellular infiltration [Figure 1c and d]. Atherosclerotic plaques in G3 were crescentic in shape and they were protruded, obstructing nearly half of the lumen [Figure 1e, e', e'']. G2 and G3 had fragmentations and duplications of the IEL, particularly at the site of the atherosclerotic plaque [Figure 1d' and f']. Interlamellar space was widened and lamellae were more straight, rather than wavy [Figure 1d and f]. All these evaluations according to the morphological parameters are summarized in Table 1. Elastic fiber content decreased with increasing age; the difference between groups was not

Table 1: Morphologic evaluation

	G1	G2	G3
Intimal thickening	+	++	+++
Lipid accumulation	-	+	++
Inflammation	+	-	+
Continuity of elastic lamellae	Continuous	Fractures	Fractures
Course of elastic lamellae	Wavy	Wavy/straight	Straight
IEL fracture	+	++	+++

IEL: Internal elastic lamina. (-): no changes; (+): mild; (++) moderate; (+++): severe.

statistically significant [Table 2]. Intima was thinner in G1 compared with other groups with respect to age and the difference was statistically significant ($P < 0.05$) [Table 3]. The area of intima in G1 was significantly ($P < 0.01$) decreased than those of G2 and G3. There was no statistically significant difference in the area of media between the groups [Table 4].

SEM analysis showed that in G1, IEL contains occasional porous structures and elastic fibrils which were tightly intertwined. In G2, at the site of atherosclerotic location, elastic lamina had a fibrillar appearance. In G3, elastic lamellae of tunica media were thinned, occasionally discontinuous, and were running in a straight course [Figure 2a-f]. While IEL of age groups G1 and G2 contained few round fenestrations of uniform size, the group G3 showed numerous, larger, and irregular polymorphous fenestrae [Figure 3a-c].

Discussion

In the present study, the light and SEM evaluation of common carotid arteries obtained from 17 adult donated cadavers demonstrated morphometric and morphologic alterations of the vessel wall in groups with respect to age. Light microscopic examination demonstrated that the increase in intima thickness detected in G2 and G3 than G1 seems to be suggestive of an adaptive response against blood flow and pressure with age as it is reported in

previous studies.^[2,4,7,13,17] IEL was shown to be intact in G1, but there were fragmentations and duplications, especially in the regions of atherosclerotic lesions and crescentic intimal thickenings in G2 and G3. This is suggestive of continuous mechanical stress with increasing age that may

Table 2: Elastic fiber ratio in intima, media, and intima+media

	Intima (%±SD ^a)	Media (%±SD ^a)	Intima + media (%±SD)
G1	60.17±0.19	46.2±0.12	50±0.11
G2	36.36±0.28	47.03±0.09	46.18±0.12
G3	31.88±0.30	42.04±0.13	40.62±0.07

^aNot statistically significant. SD: Standard deviation

Table 3: Intimal thickness

	IT (µm)
G1 (n=6)	45.88*
G2 (n=5)	159.52
G3 (n=6)	161.68

*IT $P < 0.05$, there were statistically significant difference.

IT: Intimal thickness

Table 4: The area of intimal area and medial area

	Σ of MA (mm ²)	Σ of IA (mm ²)
G1	27.8	1.57*
G2	16.5	5.79
G3	22.0	5.57

*Intimal area, $P < 0.01$, there was statistically significant difference.

MA: Medial area, IA: Intimal area

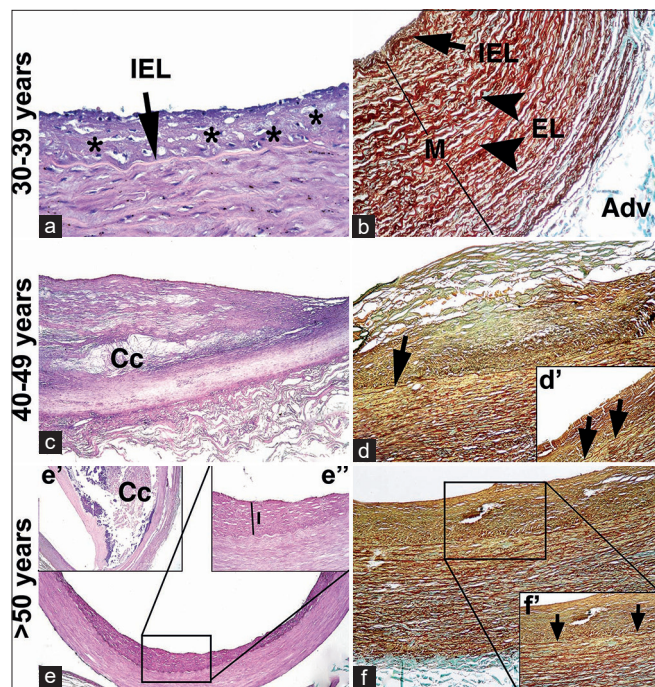


Figure 1: Light microscopic images of carotid arteries in the age groups (G1, G2, G3). (a and b); IEL (arrow): Internal elastic lamina, EL (arrow head): Elastic lamellae, M: Media, Adv: Adventitia, *: Foamy Cell (macrophage). (c and d); arrow: fracture of EL; Cc: Cholesterol crystals. (e and f) inlets: Arrows: Fragmentation, Cc: Cholesterol crystals, I: Intima. Stain: a, c, e: Hematoxyline and Eosin; b, d, f: Orcein. Magnification: a, b, c, d, e, f: ×40; d', e', e'', f': ×100 (with immersion oil)

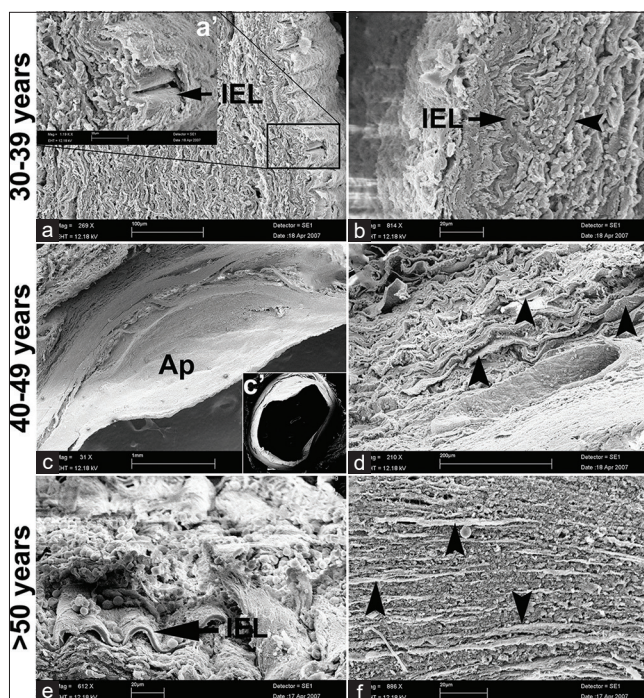


Figure 2: Scanning electronic microscopic images of carotid arteries in the age groups (G1, G2, G3). At (a, b, d, e and f); IEL (arrows): Internal elastic lamina, arrow head: Elastic lamellae, at (c); Ap: Atheroma plaque. a': High magnification of IEL; c': Low magnification of bulging atheroma plaque

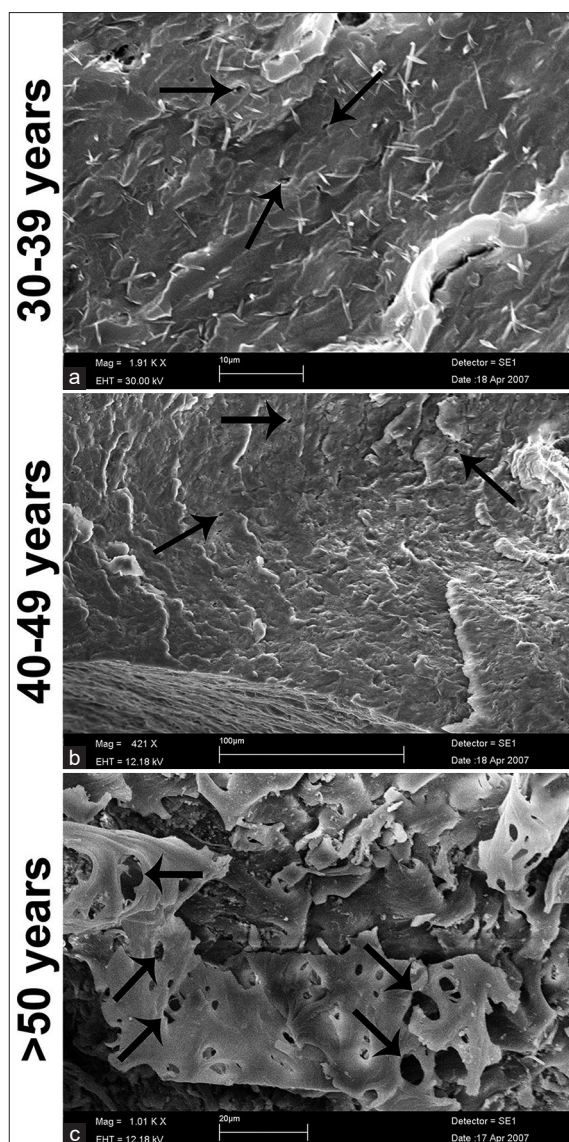


Figure 3: Scanning electron microscopic micrographs of carotid arteries in the age groups (G1, G2, and G3). At (a and b) micrographs uniform size fenestrations and smooth surfaced IEL(Internal elastic lamina) of G1, G2 groups is shown. (c); Irregular fenestrations of IEL in G3 group. Thin arrows: Fenestrae

cause IEL fractures, thus contributing to the formation of atherosclerotic plaques.^[5,11,18] In literature, higher value of intima media thickness reflects early atherosclerotic disease and estimated as a risk factor for cardiovascular and cerebrovascular diseases such as myocardial infarction, stroke, and death.^[6,12,19,20] Iwakiri *et al.* stated that the measurement of both CCA-intima media thickness and coronary artery intima/media ratio is significantly higher in death patients with CVD than in those without CVD.^[17]

It is important to address which layer is getting thicker because the atherosclerosis (accumulation of lipids) can cause intima thickening whereas hypertrophy of VSMCs can cause medial thickening.^[21] In our study, we found an increase in IA of the vessel wall that can be due to cell infiltration which is positively correlates with age; however,

the MA was decreased in G2 and G3 groups when compared to G1, and the difference was not statistically significant as shown in Table 4. While the IA increases with age, there is a decrease seen in MA. It reverse interaction seems to be related with atherosclerotic changes and cell infiltration within intimal layer that is proceeding to medial layer and also elastic lamellae disruption and VSMCs loss in media layer.

In older age groups (G2 and G3) the elastic lamellae has more straighter course and interlamellar space has been increased. This may be due to loss of VSMCs and compensation of this area by fibrous tissue. In some recent studies, it is shown that the decrease of elastin and increase of collagen quantity lead the carotid artery to become stiffer with aging.^[1-3] We indicated that the ratio of elastic fiber in intima, media and intima + media of CCA wall decreased with age, but there were no statistically significant difference between the groups. Furthermore, with SEM, we observed that elastin lamella in older age groups showed larger and irregular fenestrae. This may indicate the elastic fiber loss in vessel wall rather than insufficient repairing and renewal of elastin, because the quantity of elastin from the early development remains constant in many vital organs due to its very long half-life and very low turnover.^[22]

To assess the vessel wall status for cardio and cerebrovascular risk factors is important for treatment. The USG is a noninvasive and inexpensive vessel wall thickness measurement method, but this method cannot distinguish intima from media as it gives the sum of arterial wall thickness, especially in elastic arteries.^[9,11,23] In recent years, USG has been developed to assess individual intima and media thickness measurement such as high-resolution B-mode ultrasound and intravascular USG which is an invasive method, but these techniques require more expensive device and qualified employee.^[24]

The limitations of the present study are (i) we could not obtain the medical history and causes of death of all the donated cadavers that were used in this study; (ii) as the medical education of anatomy turns to virtual anatomy instead of cadaveric dissection, the number of donated cadavers is getting lower by time; this limits our cadaver numbers in the groups of the present study; and (iii) also in the present study, due to the low number of cadavers, the male and female distribution was not equal in the groups for comparing the gender differences in the aging effect on the carotid wall.

Conclusion

SEM and light microscopic observations of CCA in human cadavers revealed that IT and IA were increased with age in our study. Light microscopic observation of the CCA wall showed IEL e fragmentation and duplication, more straighter course of elastic lamellae, and atherosclerotic

plaques. SEM observation of CCA revealed that numerous, larger, and irregular polymorphous fenestrae are interpreted as inadequacy in repairing and renewal of elastin in vessel wall. In this study, based on both the morphometric results and SEM observations of CCA, we suggest that the vessel wall thickening in elastic arteries is more likely to be due to intimal layer rather than medial layer.

Financial support and sponsorship

Nil.

Conflicts of interest

There are no conflicts of interest.

References

- Greenwald SE. Ageing of the conduit arteries. *J Pathol* 2007;211:157-72.
- Lakatta EG. Cardiovascular ageing in health sets the stage for cardiovascular disease. *Heart Lung Circ* 2002;11:76-91.
- Ferraraccio F, Esposito S, Santé P, Cerasuolo F, Agozzino M, Agozzino M, *et al.* Scanning electron microscopy of aortic medial changes in aortic ascending dilatation. *Ultrastruct Pathol* 2004;28:137-40.
- Raspanti M, Protasoni M, Manelli A, Guizzardi S, Mantovani V, Sala A. The extracellular matrix of the human aortic wall: Ultrastructural observations by FEG-SEM and by tapping-mode AFM. *Micron* 2006;37:81-6.
- Sims FH. The initiation of intimal thickening in human arteries. *Pathology* 2000;32:171-5.
- Persson J, Formgren J, Israelsson B, Berglund G. Ultrasound-determined intima-media thickness and atherosclerosis. Direct and indirect validation. *Arterioscler Thromb* 1994;14:261-4.
- Jogestrand T, Eiken O, Nowak J. Relation between the elastic properties and intima-media thickness of the common carotid artery. *Clin Physiol Funct Imaging* 2003;23:134-7.
- Johnson CP, Baugh R, Wilson CA, Burns J. Age related changes in the tunica media of the vertebral artery: Implications for the assessment of vessels injured by trauma. *J Clin Pathol* 2001;54:139-45.
- Katakami N, Matsuoka TA, Shimomura I. Clinical utility of carotid ultrasonography: Application for the management of patients with diabetes. *J Diabetes Investig* 2019;10:883-98.
- Kokubo Y, Watanabe M, Higashiyama A, Nakao YM, Nakamura F, Miyamoto Y. Impact of intima-media thickness progression in the common carotid arteries on the risk of incident cardiovascular disease in the suita study. *J Am Heart Assoc* 2018;7:e007720.
- Tschiderer L, Klingenschmid G, Seekircher L, Willeit P. Carotid intima-media thickness predicts carotid plaque development: Meta-analysis of seven studies involving 9341 participants. *Eur J Clin Invest* 2020;50:e13217.
- Lorenz MW, von Kegler S, Steinmetz H, Markus HS, Sitzer M. Carotid intima-media thickening indicates a higher vascular risk across a wide age range: Prospective data from the Carotid Atherosclerosis Progression Study (CAPS). *Stroke* 2006;37:87-92.
- Schmidt-Trucksäss A, Grathwohl D, Schmid A, Boragk R, Upmeyer C, Keul J, *et al.* Structural, functional, and hemodynamic changes of the common carotid artery with age in male subjects. *Arterioscler Thromb Vasc Biol* 1999;19:1091-7.
- Manninen HI, Räsänen H, Vanninen RL, Berg M, Hippeläinen M, Saari T, *et al.* Human carotid arteries: Correlation of intravascular US with angiographic and histopathologic findings. *Radiology* 1998;206:65-74.
- Walski M, Chlopicki S, Celary-Walska R, Frontczak-Baniewicz M. Ultrastructural alterations of endothelium covering advanced atherosclerotic plaque in human carotid artery visualised by scanning electron microscope. *J Physiol Pharmacol* 2002;53:713-23.
- Thiripurasundari R, Sreekumari K, Aravindan KP. Autopsy-based morphometric study of coronary atherosclerosis in young adults. *Indian J Med Res* 2019;150:592-7.
- Iwakiri T, Yano Y, Sato Y, Hatakeyama K, Marutsuka K, Fujimoto S, *et al.* Usefulness of carotid intima-media thickness measurement as an indicator of generalized atherosclerosis: Findings from autopsy analysis. *Atherosclerosis* 2012;225:359-62.
- Watase H, Sun J, Hippe DS, Balu N, Li F, Zhao X, *et al.* Carotid artery remodeling is segment specific: An *in vivo* study by vessel wall magnetic resonance imaging. *Arterioscler Thromb Vasc Biol* 2018;38:927-34.
- Perwaiz Khan S, Gul P, Khemani S, Yaqub Z. Determination of site-specific carotid-intima media thickness: Common carotid artery and carotid bifurcation in hypercholesterolemia patients. *Pak J Med Sci* 2013;29:1249-52.
- Limbu YR, Rajbhandari R, Sharma R, Singh S, Limbu D, Adhikari CM, *et al.* Carotid intima-media thickness (CIMT) and carotid plaques in young Nepalese patients with angiographically documented coronary artery disease. *Cardiovasc Diagn Ther* 2015;5:1-7.
- Sillescu H. Carotid intima-media thickness and/or carotid plaque: What is relevant? *Eur J Vasc Endovasc Surg* 2014;48:115-7.
- Le Page A, Khalil A, Vermette P, Frost EH, Larbi A, Witkowski JM, *et al.* The role of elastin-derived peptides in human physiology and diseases. *Matrix Biol* 2019;84:81-96.
- Zhang Y, Guallar E, Malhotra S, Astor BC, Polak JF, Qiao Y, *et al.* Carotid artery wall thickness and incident cardiovascular events: A comparison between US and MRI in the Multi-Ethnic Study of Atherosclerosis (MESA). *Radiology* 2018;289:649-57.
- Kim GH, Youn HJ. Is carotid artery ultrasound still useful method for evaluation of atherosclerosis? *Korean Circ J* 2017;47:1-8.

Anatomical Variations of the Human Ossicular Chain in South Indian Population: Morphometry and Morphology

Abstract

Introduction: The middle ear consists of the malleus, incus, and stapes. The otologic surgeons need to have a thorough knowledge of anatomical details and variations to provide better operative results and for surgical maneuvers. The present study aimed to analyze the morphological variation and morphometry of the ear ossicles and compare the parameters with those reported in previous studies. **Material and Methods:** The study was conducted on 28 mallei, 26 incus, and 20 stapes obtained from the cadavers allotted for dissection. Measurements were documented, and the morphological variations were analyzed. **Results:** The average of the parameters showed that the malleus was 7.59 mm in total length with an angle of 130°; the manubrium was 4.65 mm, the total length of the head and neck was 5.01 mm, and the average weight was 21.50 mg. The incus had a total length and width of 6.37 and 4.89 mm, respectively; a maximal distance of 5.97 mm between the tips with an angle of 101° and weighed an average of 23.81 mg. The stapes had a total length of 3.36 mm, with the stapedia base being 2.83 mm in length and 1.41 mm in width, and weighed an average of 3.16 mg. **Discussion and Conclusion:** The ossicular chain shows great variations in measurements and morphology. Hence, a thorough anatomical knowledge of the human ossicular chain is required for clinicians for surgical maneuvers and for designing prosthetics to replace the adult middle ear ossicles.

Keywords: Anatomical variation, ear ossicles, incus, malleus, morphology, stapes

Introduction

The tympanic cavity of the temporal bone contains three ossicles (auditory ossicles); malleus, incus, and stapes.^[1,2] These ossicles form a chain connecting the tympanic membrane to the fenestra vestibuli (oval window). They have ligamentous connections with the walls of the middle ear cavity and are bound together by articulations. Malleus is the most lateral and is firmly attached to the tympanic membrane; the stapes is the most medial fixed to the fenestra vestibuli and is in direct contact with the perilymph; the intermediate between the two is the incus.^[3] This complex ossicular system acts like a bent lever to connect the vibrations of the outer tympanic membrane into intensified thrusts of stapes against the perilymph for a smooth and amplified transmission of sound.^[4-6]

Malleus, shaped like a hammer, consists of anterior and lateral processes, manubrium (handle), neck, and head with which it

articulates with incus at the incudomalleolar joint.^[7] Incus consists of a body, short and long process. At the tip of the long process lies a medially projecting mass known as the lenticular process, also referred to as the fourth ossicle, due to its incomplete fusion with the long process. The lenticular process articulates with stapes forming the incudo-stapedial joint. Stapes, the smallest bone in the body shaped like a miniature stirrup, consists of small buttons like head, a neck, two crura, and footplate (base).^[3,8]

Many congenital craniofacial, including temporal mandibular disorders, are known to form ossicular anomalies and associated symptoms as their definitive component.^[9] Acquired lesions such as chronic suppurative otitis media (CSOM) affect the ossicular chain and form a huge burden of disease in developing countries; thus, there is a higher demand for reconstructive surgeries using the ossicular prosthesis. The present study aims in providing valuable parameters of morphometry and morphological variation in the human ossicular chain.

This is an open access journal, and articles are distributed under the terms of the Creative Commons Attribution-NonCommercial-ShareAlike 4.0 License, which allows others to remix, tweak, and build upon the work non-commercially, as long as appropriate credit is given and the new creations are licensed under the identical terms.

For reprints contact: WKHLRPMedknow_reprints@wolterskluwer.com

How to cite this article: Dasegowda G, Kadirappa P, Nanjundaraju H, Raja SS, Suresh R. Anatomical variations of the human ossicular chain in south Indian population: Morphometry and morphology. J Anat Soc India 2022;XX:XX-XX.

Giridhar Dasegowda, Padmalatha Kadirappa, Hema Nanjundaraju, Seema Shimoga Raja, Rachana Suresh

Department of Anatomy, ESIC MC and PGIMSR, Bengaluru, Karnataka, India

Article Info

Received: 26 November 2021

Revised: 25 July 2022

Accepted: 02 September 2022

Available online: ***

Address for correspondence:

Dr. Giridhar Dasegowda,
Department of Anatomy, ESIC
MC and PGIMSR, Rajajinagar,
Bengaluru - 560 010,
Karnataka, India.
E-mail: giridhar.dasegowda@gmail.com

Access this article online

Website: www.jasi.org.in

DOI:
10.4103/jasi.jasi_192_21

Quick Response Code:



Material and Methods

The study was conducted on a total of 28 Malleus, 26 Incus, and 20 Stapes obtained from the cadavers of both sexes allotted for dissection for undergraduates at ESIC Medical College. IRB was waived for this study on ear ossicles from cadaver. Using the electric bone cutter, the calvaria was removed, exposing the brain. The brain was severed at the level of the medulla oblongata, and the dura mater was stripped to remove the brain. The roof of the middle ear was exposed by removing the tegmen tympani to create a small opening using a chisel and hammer. Malleus was identified by the round head and articulating with incus at the epitympanum; by fine manipulation, with forceps, both the ossicles were removed. A diagonal section through the arcuate eminence was taken on the temporal bone to expose the stapes and removed with forceps after fine manipulation. The ossicles damaged or eroded as a consequence of CSOM, or other diseases were excluded from the study.

The variations in the ossicular chain were observed under the magnification of the simple microscope. The measurements of length were obtained using the Digital Vernier Caliper with the least count of 0.01 mm, and the weight of ossicles was obtained using the Contech Analytical Balance with the least count of 0.01 mg. Photographs were obtained with the help of a stereoscopic microscope, and the measurements of angle were estimated using the photographs. Results were statistically analyzed using the version SPSS - 22 software (IBM Corp., Armonk, N.Y., USA), and $P < 0.05$ was considered statistically significant. The parameters taken were similar to studies conducted by Unur *et al.* and Sodhi *et al.*^[1,4,10]

The following measurements of Malleus were obtained, as shown in Figure 1.

1. Total length (A1) in mm: the maximum distance between the top of the head and the end of the manubrium

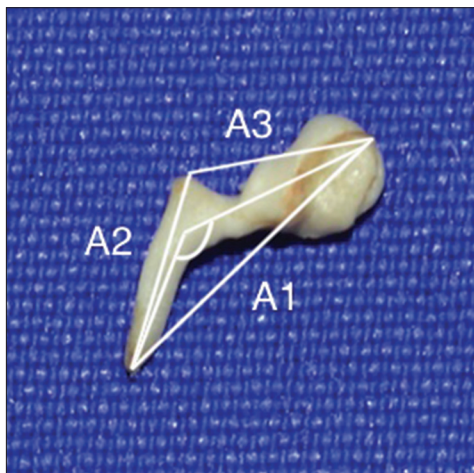


Figure 1: Measurements of malleus. (A1): Total length, (A2): Length of manubrium (A3): Length of head and neck

2. Length of manubrium (A2) in mm: the maximum distance between the end of the lateral process and the end of the manubrium
3. Length of the head and neck (A3) in mm: the maximum distance between the top of the head and the end of the lateral process
4. Angle of malleus: measured between the long axis of the malleus and that of the manubrium
5. Index: Length of the manubrium \times 100/total length.
6. Weight of the malleus (mg).

The following measurements of incus were obtained, as shown in Figure 2.

1. Total length (B1) in mm: Maximal distance between the superior edge of the body and the end of the long process
2. Total width (B2) in mm: Maximal distance between the superior edge of the body and the end of the short process
3. Maximal distance between the tips of the processes (B3) in mm
4. Angle of the incus measured between the processes
5. Index: Total width \times 100/total length of the incus
6. Weight of the incus (mg).

The following measurements of stapes were obtained, as shown in Figure 3.

1. Total height (C1) in mm: Maximum distance between the top of the head and the footplate
2. Length of footplate (C2) in mm: Maximum length of the long axis of footplate
3. Width of footplate (C3) in mm: Maximum width of the footplate.
4. Index: Length of footplate \times 100/total height
5. Weight of the stapes (mg).

Results

The data obtained in this study were determined in two categories: morphologic and morphometric. The morphometrical data obtained are tabulated in Table 1 for malleus, Table 2 for incus, and Table 3 for stapes. The

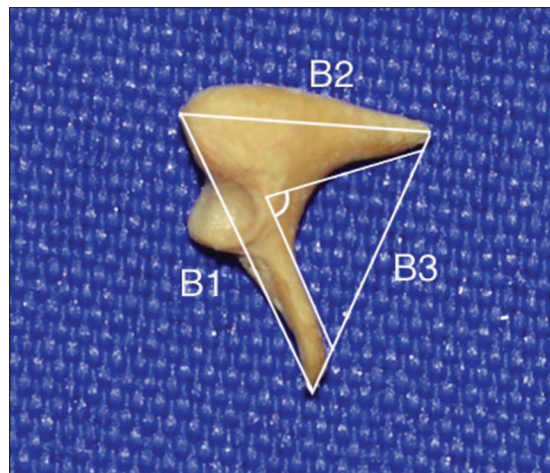


Figure 2: Measurements of Incus. (B1): Total length, (B2): Total width, (B3): Distance between the tips

morphological data were based on observation; the distal part of the manubrium (free ends) of the malleus showed variations between a straight line and curved anteriorly, as shown in Figure 4. The anterior and lateral process of malleus showed much variability in length. The inferior border of the short process of incus showed variation between a notch and a straight course (without notch), as shown in Figure 5. A wide angle and narrow-angle variation were noted with a well-developed corpus and less developed corpus, respectively, in incus, as shown in Figure 6. The variations of stapes noted were with respect to the length of the neck, growth on the footplate, and variations in the obturator foramen. The different shapes observed in stapes in the foramen were a circular, semicircular, tunnel, and square, as shown in Figure 7. Two stapes were noted with growth on the footplate, as shown in Figure 8.

Discussion

Vesalius de described malleus and incus in his monumental work “De humani corporis fabrica” in 1543.^[5]

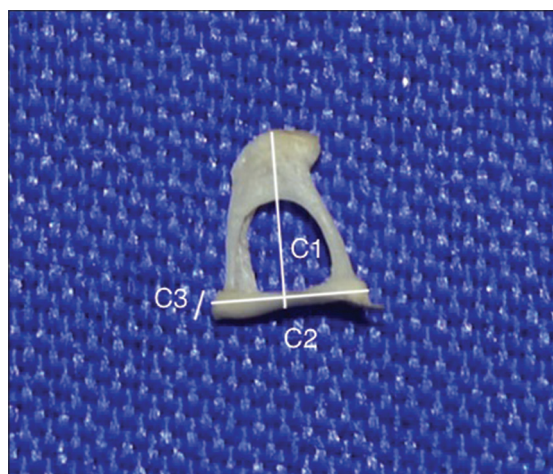


Figure 3: Measurements of stapes. (C1): Total height, (C2): Length of footplate, (C3): Width of footplate

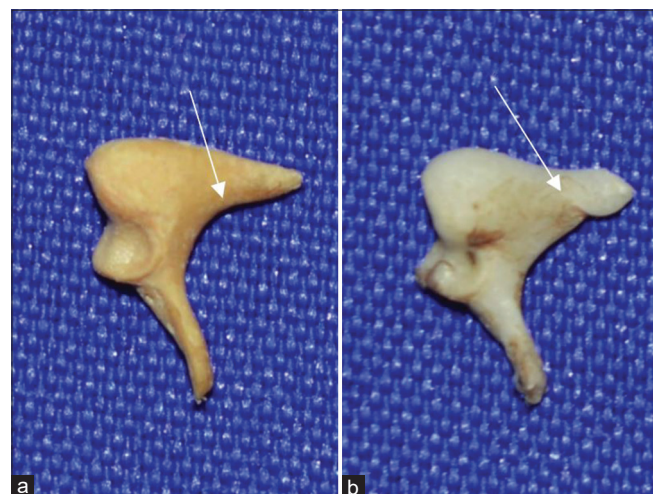


Figure 5: Straight (a): And notch (b): Course on inferior border of incus

Eustachius and Ingrassia were the first to describe stapes in 1546.^[11]

Lempert and Wolff described several unique features of the ear ossicles such as its embryological development, position in the tympanic cavity, and enveloping mucosa.^[12]

The present morphometric data of malleus, incus, and stapes obtained from the present study have been compared to the studies conducted previously, as shown in Table 4.

The parameters of malleus and incus were similar to the study conducted by Unur *et al.*, while the parameters of stapes were similar to the study by Farahani and Nooranipour.^[1,16] Among the ossicles, stapes was found to be the most variable. Similar results have been obtained

Table 1: Morphometric analysis of malleus (n=28)

	Mean	SD	P	Maximum	Minimum
Total length (mm)	7.59	0.48	0.005	8.35	6.42
Length of manubrium (mm)	4.65	0.27	0.006	5.07	3.64
Length of head and neck (mm)	5.01	0.19	0.006	5.36	4.15
Index	61.44	4.46	0.005	69.64	55.4
Angle (°)	130.27	9.22	0.005	152	120
Weight (mg)	21.5	2.21	0.005	25.2	16.3

SD: Standard deviation

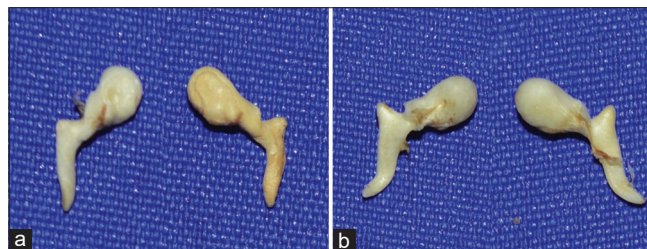


Figure 4: Free end of manubrium of malleus showing straight course (a) and curved anteriorly (b)

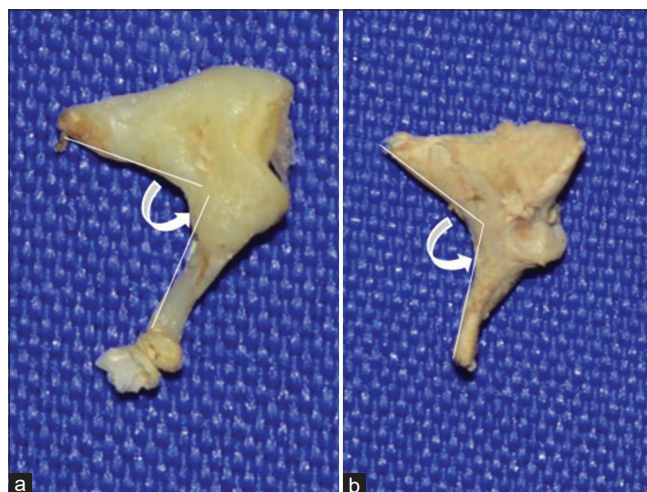


Figure 6: Narrow (a): And wide angle (b): Between the processes in incus

from the previous studies.^[7,17-20] Stapes has also shown variation in its positioning in the fossa of the oval window.^[21] In the present study, malleus showed variation in the course of manubrium, straight or a curved course. This goes in conjunction with the previous studies.^[1,8,18] A study conducted by Todd and Creighton observed a malleus with an absent lateral process and inflected manubrium.^[22] Such unusual findings were not obtained in the present study.

Table 2: Morphometric analysis of incus (n=26)

	Mean	SD	P	Maximum	Minimum
Total length (mm)	6.37	0.34	0.007	6.87	5.71
Total width (mm)	4.89	0.24	0.008	5.40	3.90
Maximum distance between the tips (mm)	5.97	0.31	0.007	6.45	5.27
Index	75.92	4.54	0.007	82.28	68.30
Angle (°)	101.06	10.51	0.008	125	84
Weight (mg)	23.81	3.58	0.004	29.80	15.40

SD: Standard deviation

Table 3: Morphometric analysis of stapes (n=20)

	Mean	SD	P	Maximum	Minimum
Total length (mm)	3.36	0.18	0.033	3.73	3.17
Length of footplate (mm)	2.83	0.16	0.007	3.05	2.57
Width of footplate (mm)	1.41	0.12	0.033	1.67	1.26
Index	84.26	5.12	0.033	90.79	76.13
Weight (mg)	3.16	0.50	0.033	3.8	2.6

SD: Standard deviation

Table 4: Comparison of morphometric data of ear ossicles with previous studies

Parameters	Present study	Arrensburg <i>et al.</i> , 1981 ^[13]	Unur <i>et al.</i> , 2002 (newborn ossicles) ^[11]	Sodhi <i>et al.</i> , 2017 ^[4]	Rathava <i>et al.</i> , 2014 ^[14]	Padmini and Rao, 2013 (fetal ossicles) ^[15]
Malleus						
Total length	7.56	7.8	7.69	7.83	7.81	5.54
Length of manubrium	4.65	4.4	4.70	4.65	4.59	3.03
Length of head-and-neck	5.01	-	4.85	5.01	5.0	2.79
Incus						
Total length	6.37	6.4	6.47	6.47	-	5.13
Total width	4.89	5.1	4.88	4.88	-	3.47
Distance between two processes	5.97	-	6.12	5.31	-	4.50
Stapes						
Total height	3.36	3.2	3.22	3.38	3.33	2.71
Length of footplate	2.83	2.8	2.57	2.78	2.78	2.36
Width of footplate	1.41	1.3	1.29	1.34	1.34	-

The morphological variation observed in the incus included a narrow or wide angle between the processes and the notch observed in the inferior border of the short process. The early development of the posterior ligament of the incus, which connects the fossa incudis to the short process, may result in the formation of the notch.^[8]

The global burden of hearing loss is at least 250 million people, according to a survey conducted by WHO in 2001. In India, close to 60 million population suffer from disabling hearing impairment. Conditions like cholesteatoma, Otitis media, an inflammatory condition of the middle ear cavity, and congenital malformations like incudo-stapedial anomalies, congenital absence of incus may require ossicular reconstruction surgeries.^[23,24] The two types of prosthesis used are partial ossicular replacement prosthesis and total ossicular replacement prosthesis.^[25] Homograft ossicular prosthesis obtained from cadavers has gained acceptance and has been found to provide superior audiologic results when compared to autograft.^[15] Another study reported that angiogenesis was predominant in allogeneic ossicles, whereas autogenetic ossicles showed angiogenetic and Appositional osteogenesis.^[26] Several studies have been conducted to describe fetal ossicles and its use as prostheses or homografts.^[6,27] However, few studies stated that custom manufacturing of prostheses for each patient could optimize prosthesis fit as large soft-tissue structural variations prevent a single middle ear model from being applicable to all ears.^[2,28]

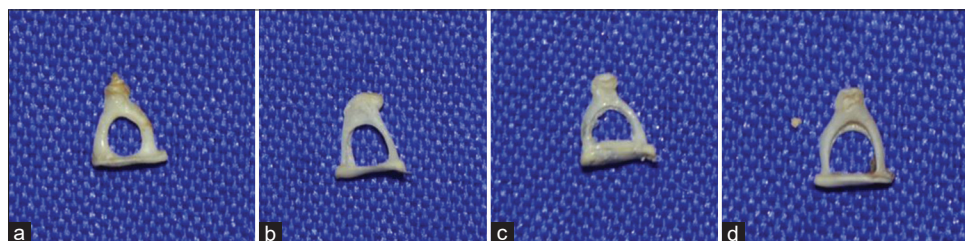


Figure 7: Morphological variations of the foramen of stapes. (a): Circular, (b): Square, (c): Semi-circular, (d): Tunnel

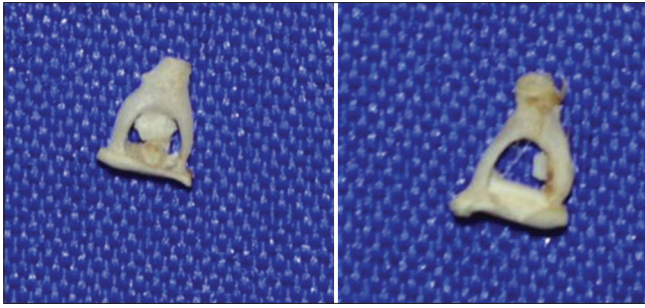


Figure 8: Growth on footplate on stapes

Middle ear ossicles have also been found to have anthropological importance. In lower animals, malleus and incus have been found to form a single unit called the maleo-incal complex.^[29] A study on the comparison of Neanderthal and modern humans stated that variation in ear ossicles is due to convergent brain expansion.^[30] Thus, these morphological variations provide anthropological evidence in evolution.

Conclusion

Auditory ossicles have been extensively studied since their discovery. The ossicles show great variation in their arrangement, morphology, and morphometry. Ossicles can be used as homograft; hence, there is a need to study and preserve them in ossicular banks. The morphometrical measurements and the morphological variations of ear ossicles observed have been reported in the present study. A thorough anatomical knowledge of the human ossicular chain and its variation is essential for clinicians to perform surgical maneuvers and to design prosthetics for ossicular replacement. The morphological differences observed are explained by the embryological variation in the development.

Acknowledgment

Our deepest gratitude is expressed to the following persons for their contribution in making the study possible. Dr. Simant Baliarsingh, Department of Biochemistry, for the assistance in data collection, and the staff of the Department of Anatomy for the advice and guidance.

Financial support and sponsorship

Nil.

Conflicts of interest

There are no conflicts of interest.

References

- Unur E, Ulger H, Ekinçi N. Morphometrical and morphological variations of middle ear ossicles in the newborn. *Erciyes Tip Dergisi* 2002;24:57-63.
- Sim JH, Puria S. Soft tissue morphometry of the malleus-incus complex from micro-CT imaging. *J Assoc Res Otolaryngol* 2008;9:5-21.
- Standring S. Gray's Anatomy. In: *The Anatomical Basis of Clinical Practice*. 40th ed. Edinburgh: Elsevier Churchill Livingstone; 2008. 623-52.
- Sodhi S, Singh Z, Lai J. Morphometric dimensions of human ear ossicles of males. *Natl J Med Res* 2017;7:47-51.
- Noussios G, Chouridis P, Kostretzis L, Natsis K. Morphological and morphometrical study of the human ossicular chain: A review of the literature and a meta-analysis of experience over 50 years. *J Clin Med Res* 2016;8:76-83.
- Nadeem G. Can fetal ossicles be used as prosthesis in adults? A morphometric study. *Int J Exp Clin Anat* 2013;6-7:52-57.
- Vinayachandra PH, Viveka S, Sudha MJ, Shetty B, Kuriakose S, Sagar S. Morphometry and variations of malleus with clinical correlations. *Int J Anat Res* 2014;2:191-94.
- Saha R, Srimani P, Mazumdar A, Mazumdar S. Morphological variations of middle ear ossicles and its clinical implications. *J Clin Diagn Res* 2017;11:C01-4.
- Kaneyama K, Segami N, Hatta T. Congenital deformities and developmental abnormalities of the mandibular condyle in the temporomandibular joint. *Congenit Anom (Kyoto)* 2008;48:118-25.
- Sodhi S, Singh Z, Davessar JL. Morphometry of human ear ossicles in females of North India. *Hum Biol Rev* 2018;7:172-182.
- Cappello F, Gerbino A, Zummo G. Giovanni filippo ingrassia: A five-hundred year-long lesson. *Clin Anat* 2010;23:743-9.
- Lempert J, Wolff D. Histopathology of the incus and the head of the malleus in cases of stapedial ankylosis. *Arch Otolaryngol (1925)* 1945;42:339-67.
- Arrensburg B, Harell M, Nathan H. The human middle ear ossicles, morphometry and taxonomic implications. *J Hum Evol* 1981;10:199-205.
- Rathava JK, Gohil DV, Satapara VK, Kukadiya UC, Trivedi PN, Patel MM, *et al.* Osteometric dimension of stapes. *J Res Med Den Sci* 2014;2:30-33.
- Padmini MP, Rao B. Morphological variations in human fetal ear ossicles – A study. *Int J Anat Res* 2013;1:40-42.
- Farahani RM, Nooranipour M. Anatomy and anthropometry of human stapes. *Am J Otolaryngol* 2008;29:42-7.
- Park HY, Han DH, Lee JB, Han NS, Choung YH, Park K. Congenital stapes anomalies with normal eardrum. *Clin Exp Otorhinolaryngol* 2009;2:33-8.
- Sarrat R, García Guzmán A, Torres A. Morphological variations of human ossicula tympani. *Acta Anat (Basel)* 1988;131:146-9.
- Wadhwa S, Kaul J, Agarwal A. Morphometric study of stapes and its clinical implications. *J Anat Soc India* 2005;54:1-9.
- Mudhol RS, Narahari S, Havaladar RR. Morphological and anthropometrical features of human ear ossicles: A 1-year cadaveric observational study. *J Anat Soc India* 2022;71:88-92.
- Djerić D, Savić D. Variations of the position of the stapes in the fossula of the round window and their surgical value. *Ann Otolaryngol Chir Cervicofac* 1988;105:313-5.
- Todd NW, Creighton FX Jr. Malleus and incus: Correlates of size. *Ann Otol Rhinol Laryngol* 2013;122:60-5.
- Kuhn JJ, Lassen LF. Congenital incudostapedial anomalies in adult stapes surgery: A case-series review. *Am J Otolaryngol* 2011;32:477-84.
- Wehrs RE. Congenital absence of the long process of the incus. *Laryngoscope* 1999;109:192-7.
- Olszewski J. The morphometry of the ear ossicles in humans during development. *Anat Anz* 1990;171:187-91.

26. Naujoks JH, Kempf HG. Histology and morphometry of explanted ear ossicles in man. *Laryngol Rhinol Otol (Stuttg)* 1986;65:374-6.
27. Sushma M, Kumari KL, Latha DA. A study on development of ear ossicles from prenatal to postnatal life of humans. *Int J Res Med Sci* 2016;4:4793-6.
28. Kamrava B, Roehm PC. Systematic review of ossicular chain anatomy: Strategic planning for development of novel middle ear prostheses. *Otolaryngol Head Neck Surg* 2017;157:190-200.
29. Martonos C, Damian A, Gudea A, Bud IT, Stan F. Morphological and morphometrical study of the auditory ossicles in chinchilla. *Anat Histol Embryol* 2019;48:340-5.
30. Stoessel A, David R, Gunz P, Schmidt T, Spoor F, Hublin JJ. Morphology and function of *Neandertal* and modern human ear ossicles. *Proc Natl Acad Sci U S A* 2016;113:11489-94.

Stereological and Comparative Evaluation of the Carpal Tunnel in Patients with Carpal Tunnel Syndrome Using Magnetic Resonance Images

Abstract

Introduction: In this study, the relation between carpal tunnel syndrome (CTS) severity and the carpal tunnel volume (CTV), volume and the volume fraction of the carpal tunnel contents on subjects with CTS and healthy individuals were examined. **Material and Methods:** 30 female patients diagnosed with CTS clinically and electrophysiologically and 16 healthy female patients were included in this study. In patient group, 50 and in control group 30 hand wrists were examined. CTS severity was ranked electrophysiologically. T1-weighted axial magnetic resonance images (MRIs) were examined by the Cavalieri principle. **Results:** CTV in the patient group ($4.26 \pm 0.57 \text{ cm}^3$) was found to be lower than that of the control group ($4.66 \pm 0.73 \text{ cm}^3$), while the volume ($0.41 \pm 0.07 \text{ cm}^3$) of the median nerve (Vnm) in the patient group was found to be higher than the control group ($P < 0.05$). Besides, the volume and volume fraction of the median nerve increase when the CTS severity increases ($r = 0.610$; $r = 0.778$). **Discussion and Conclusion:** Our study has shown that stereological studies with MRI are successful in determining the CTV in differentiating patients and healthy people. In addition, the volume and volume fraction of the median nerve were found to be quite effective in differentiating the severity of CTS. It is anatomically confirmed that when the severity of CTS increases, the space volume fraction of the carpal tunnel decreases.

Keywords: Carpal tunnel syndrome severity, carpal tunnel syndrome, magnetic resonance imaging, median nerve, volume fraction

Introduction

Carpal tunnel syndrome (CTS) is a common neuropathy that occurs by compression of the median nerve under the flexor retinaculum based on various pathological reasons. CTS mainly affects the 4%–5% of the age group of 40–60 years.^[1] The carpal tunnel composition and decrease of the space in the carpal tunnel, triggering situations that increase the pressure coming from inside and outside of tunnel, can cause CTS easily. Although it is well documented that CTS's cause is due to the median nerve compression, the biological mechanism underlying the compression remained unknown.^[2-4]

The stereological studies in accordance with Cavalieri principle help to estimate the volume of the biological structures. The content volume, volume fraction of that contents, or their fraction in proportion to the included total volume is evaluated in a scientific discipline with this approach. The unbiased and reliable results support

the diagnosis and effective treatment of the diseases.^[5,6]

The consensus about the criteria of CTS diagnosis in clinical fields is essential to provide effective treatment. The use of stereological techniques can also play an active role in explaining the morphology of the carpal tunnel and cases that are difficult to diagnose. Therefore, stereological studies done by cross-sectional imaging methods such as magnetic resonance (MR) and computed tomography are required substantially. In this study, we aimed to evaluate the effectiveness of stereological techniques in the diagnosis and severity of CTS.

Material and Methods

This study was approved by the Clinical Researches Local Ethics Committee. Volunteers were informed about the content, aim, and application of the study and their approvals were obtained. A questionnaire was conducted for the general health status of patients. Those who underwent trauma, steroid injection, and surgical operations

Gürsel A. K. Güven,
Mehmet
Emirzeoglu¹,
Murat Terzi²,
Mustafa Bekir
Selçuk³,
Bünyamin Sahin¹

Vocational School of Health Services, Ondokuz Mayıs University, Departments of ¹Anatomy, ²Neurology and ³Radiology, Faculty of Medicine, Ondokuz Mayıs University, Samsun, Turkey

Article Info

Received: 10 April 2021

Revised: 26 July 2022

Accepted: 13 September 2022

Available online: ***

Address for correspondence:

Prof. Mehmet Emirzeoglu,
Department of Anatomy, Faculty of Medicine, Ondokuz Mayıs University, Samsun, Turkey.
E-mail: memirze@omu.edu.tr

Access this article online

Website: www.jasi.org.in

DOI:
10.4103/jasi.jasi_71_21

Quick Response Code:



How to cite this article: Güven GA, Emirzeoglu M, Terzi M, Selçuk MB, Sahin B. Stereological and comparative evaluation of the carpal tunnel in patients with carpal tunnel syndrome using magnetic resonance images. J Anat Soc India 2022;XX:XX-XX.

This is an open access journal, and articles are distributed under the terms of the Creative Commons Attribution-NonCommercial-ShareAlike 4.0 License, which allows others to remix, tweak, and build upon the work non-commercially, as long as appropriate credit is given and the new creations are licensed under the identical terms.

For reprints contact: WKHLRPMedknow_reprints@wolterskluwer.com

on the wrist arthroscopy area were not included in the study. Patients who could not be evaluated due to moving their hands during MR were also excluded from the study. Carpal tunnel volume (CTV), the size differences of the tendons, and the median nerve between the patient and healthy groups with their fraction within the tunnel and their relations with CTS degree were examined in this study through the MR images (MRIs).

Thirty female patients with CTS participated in the study by performing physical examination and electrophysiological and clinical tests. The control group included 16 healthy female volunteers. In the patient group, 50 MRIs were obtained from bilateral wrists. In the control group, 16 right and 14 left MRIs of the wrist were obtained.

MRI imaging was performed using a 1.5-T scanner (Gyrosan Intera, Philips Healthcare, Best, the Netherlands). T1 weighted and three dimensional images were obtained. Axial T1-weighted turbo spin echo sequence: field of view [FOV]: 200 mm × 244 mm, (repetition time [TR]/echo time [TE]: 570/24 ms; 90° flip angle; 100% phase resolution; slice thickness: 3 mm; number of excitations [NEX]: 2; intersection gap: 0.3mm) and monitoring time was 10 min 18 s. The imaging was performed in the neutral position starting with radiocarpal articulation in the axial plane up to the proximal degree of metacarpal bones using by wrist coil. The imaging was performed in the neutral position starting with radiocarpal articulation in the axial plane up to the proximal degree of metacarpal bones using by wrist coil.

All patients were assessed by a neurologist with more than 10 years of experience. The cases with CTS were classified according to clinical assessment and the EMG (Electromyography) symptoms as mild CTS, moderate CTS, and severe CTS.^[7,8] Volume measurements were conducted according to the Cavalieri principle to measure the volume and volume fraction of the contents of the tunnel volume (V_t/CTV , V_{mn}/CTV) such as carpal tunnel, flexor tendons, and median nerve.^[9] The volume within a 3-cm segment of carpal tunnel was measured on 6–9 MR sections. Carpal tunnel was visible on 6–9 MR sections. Carpal tunnel was visible on 6–9 MR sections.

T1-weighted axial MRIs starting from distal of radius were taken in a way to include carpal tunnel completely which is located in proximal of metacarpals. Acquired MRIs were saved in DICOM format. In each section, the borders of the carpal tunnel, median nerve, and flexor tendon were analyzed by the ImageJ software, which is distributed freely by the National Institutes of Health of the USA. The borders of the carpal tunnel and median nerve were delineated using the polygon selection tool in the ImageJ. The sectional surface is the structures that were obtained automatically by the software [Figure 1a-c]. To calculate the projection area of the tendons, the image threshold of the sections was done and the sectional surface areas were measured [Figure 1d]. All measurements were repeated ten

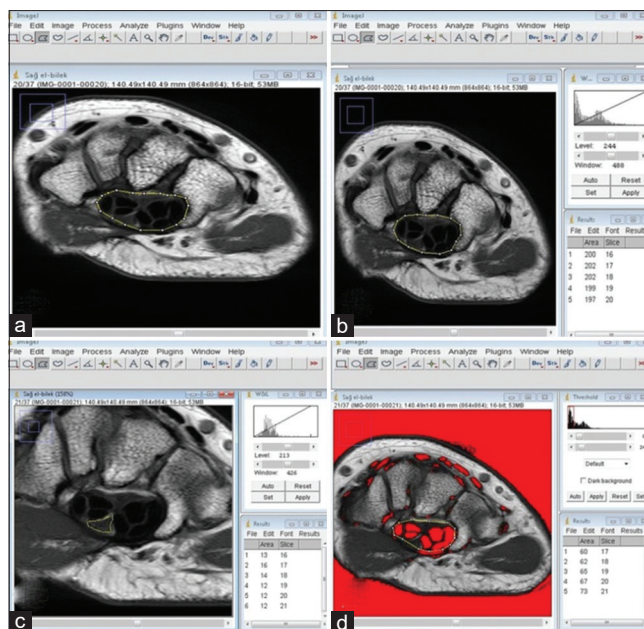


Figure 1: Measurement of volume and carpal tunnel contents using the ImageJ software. (a) Delineation of the boundaries of the carpal tunnel, (b) Measuring of the carpal tunnel surface area, (c) Measuring of the median nerve area, (d) Delineation of the boundaries of the flexor tendons in the carpal tunnel by threshold tool

times in each patient before starting the study. The two persons who made the measurements were blinded to the clinical evaluation and classification of electromyography. The obtained sectional cut surface areas were multiplied by the section thickness and the volumes of the total carpal tunnel, tendons, and median nerve were estimated using the Cavalieri principle. The following terms were used to determine the volume fraction of the median nerve and tendons to the CTV.

The volume fraction of the median nerve = $([V_{nm}/CTV] \times 100)$.

The volume fraction of tendon = $([V_t/CTV] \times 100)$.

The free space volume fraction within the total CTV was estimated as follows:

The space volume fraction of the carpal tunnel = $100 - ([V_{nm}/CTV] \times 100) + ([V_t/CTV] \times 100)$.

All the data were analyzed using the Statistical Package for the Social Sciences (SPSS v. 15). The carpal tunnel and canal content volume of the participants with mean values of volume fraction of flexor tendon and median nerve to the canal were calculated. The estimated data of the carpal tunnel, flexor tendons, and median nerve were controlled for the statistical distribution. Normal parametric statistics were used due to the normal distribution of the data. Student's *t*-test was used to compare results between the patient and control groups. One-way ANOVA and Tukey test were used for the evaluation of the severity types of CTS. The correlation was evaluated by Pearson and

Spearman coefficient of correlation according to the given convenience. Statistical significance level was accepted as $P \leq 0.05$.

Results

The mean age of the patient group was 51.07 ± 11.90 years (minimum 25, maximum 75) and the mean age of the control group was 48.56 ± 10.09 years (minimum 35, maximum 65). There was no difference in terms of age between the patient and control groups ($P > 0.05$). Fifty MRIs of wrists in the patient group and 30 MRIs of wrists in the control group were evaluated without regarding the left or right hand. The mean of total CTV in the patient group was found lower than the control group ($P < 0.05$). There was no difference in the mean of total tendon volumes between the groups ($P > 0.05$). The mean of median nerve volume in the patient group was higher than the control group [$P < 0.05$, Table 1]. The mean volume fraction of tendon volume and median nerve volume in the patient group was higher than the control group ($P < 0.05$). The mean volume fraction of space of the carpal tunnel in the patient group was lower than the control group [$P < 0.05$, Table 2].

The relation between carpal tunnel and canal content volume and volume fraction was evaluated according to the Spearman correlation coefficient calculation. There was a high positive correlation between CTV and tendon volume ($r = 0.658, P = 0.000$), median nerve volume and median

nerve volume fraction ($r = 0.778, P = 0.000$). A remarkable negative correlation was observed between the space of the carpal tunnel and the tendon volume fraction ($r = -0.963, P = 0.000$). There was a low negative correlation between the space of the carpal tunnel and the median nerve ($r = -0.375; P = 0.000$). A remarkable negative correlation was found between the space of the carpal tunnel and the median nerve volume fraction ($r = -0.612, P = 0.000$). In the patient group, 21 hand wrists (42%) with mild CTS, 24 hand wrists (48%) with moderate CTS, and 5 hand wrists (10%) with severe CTS were detected.

While there was no significant difference in tendon volumes ($P > 0.05$), significant differences were observed between CTV, median volume, median nerve volume fraction, and tendon volume fraction for CTS severity ($P < 0.05$). A significant difference was found between non-CTS and mild CTS for the mean CTV [$P < 0.05$; Figure 2]. The median nerve volumes of individuals without CTS were significantly different from other CTS severities and median nerve volume increased in concordance with CTS severity [$P < 0.05$; Figure 3]. Furthermore, a significant difference ($P = 0.007$) was observed between mild CTS and severe CTS [$P < 0.05$; Figure 3].

When we compared the volume fraction according to CTS severities, an increase was observed in the volume fraction of tendons and median nerve in concordance with the degree of severity among the CTS severities. Controversially, the space volume fraction of carpal tunnel decreased in concordance with CTS severity degree [$P < 0.05$; Figures 4-6].

Moderate correlation between CTS severity and median nerve volume ($r = 0.610, P = 0.000$), high correlation between CTS severity and median nerve volume fraction ($r = 0.778, P = 0.000$), weak positive correlation between CTS severity and tendon volume fraction ($r = 0.446, P = 0.000$), and moderate correlation

Table 1: The mean volumes of the carpal tunnel and tendons and median nerve and comparisons of volume values in patients with carpal tunnel syndrome (n=50) and control group (n=30)

Parameters	Groups	Total volume (cm ³ ±SD)	P
Carpal tunnel	CTS	4.26±0.57	0.008
	Control	4.66±0.73	
Tendons	CTS	1.90±0.33	0.646
	Control	1.87±0.31	
Median nerve	CTS	0.41±0.07	0.001
	Control	0.32±0.07	

SD: Standard deviation, CTS: Carpal tunnel syndrome

Table 2: Statistical comparison of volume fraction measured in patients with carpal tunnel syndrome (n=50) and control group (n=30)

Parameters	Groups	Total volume Volume fraction (%)	P
Tendons	CTS	44.74±5.50	0.001
	Control	40.24±4.58	
Median nerve	CTS	9.64±1.47	0.001
	Control	6.75±0.91	
Space of the carpal tunnel	CTS	45.62±6.01	0.001
	Control	53.02±4.51	

CTS: Carpal tunnel syndrome

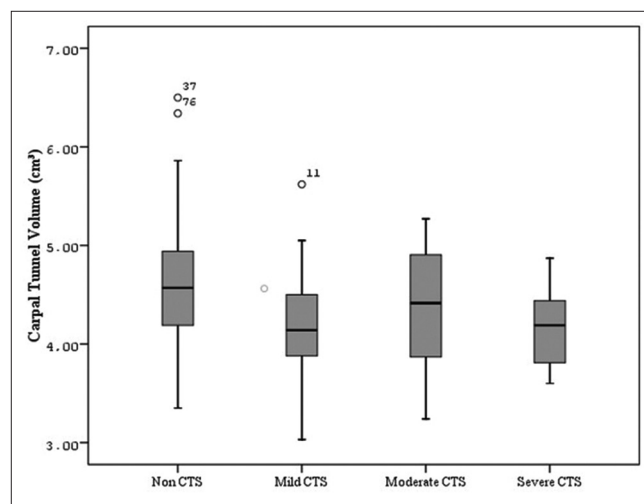


Figure 2: Mean CTV values regarding the severity of the CTS. CTV: Carpal tunnel volume, CTS: Carpal tunnel syndrome

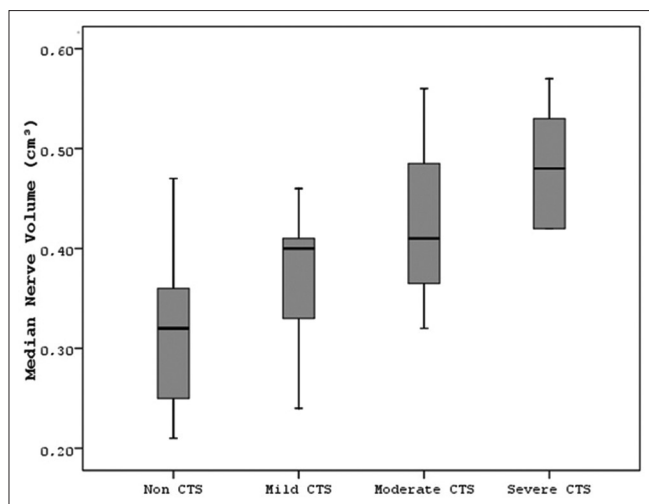


Figure 3: Mean median nerve volume values regarding the severity of the CTS. CTS: Carpal tunnel syndrome

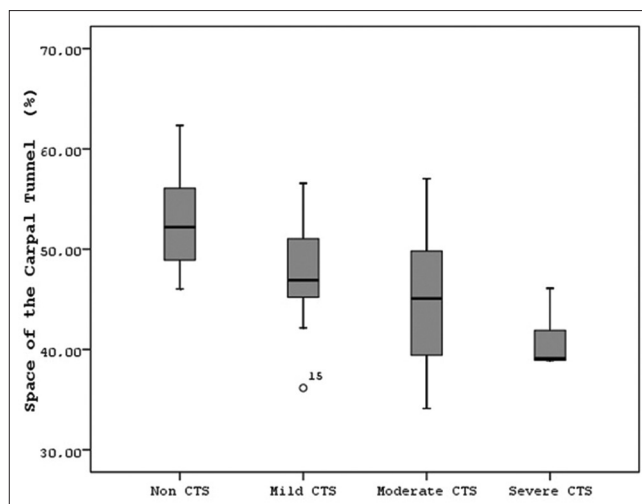


Figure 4: Mean space of the CTV fraction regarding the severity of the CTS. CTV: Carpal tunnel volume, CTS: Carpal tunnel syndrome

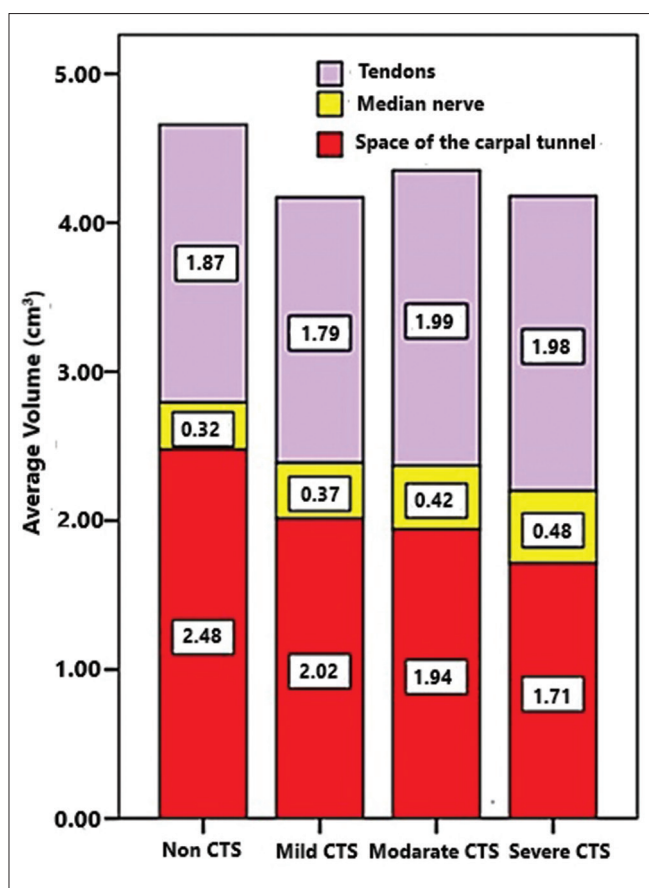


Figure 5: Mean volumes regarding the severity of the CTS. CTS: Carpal tunnel syndrome

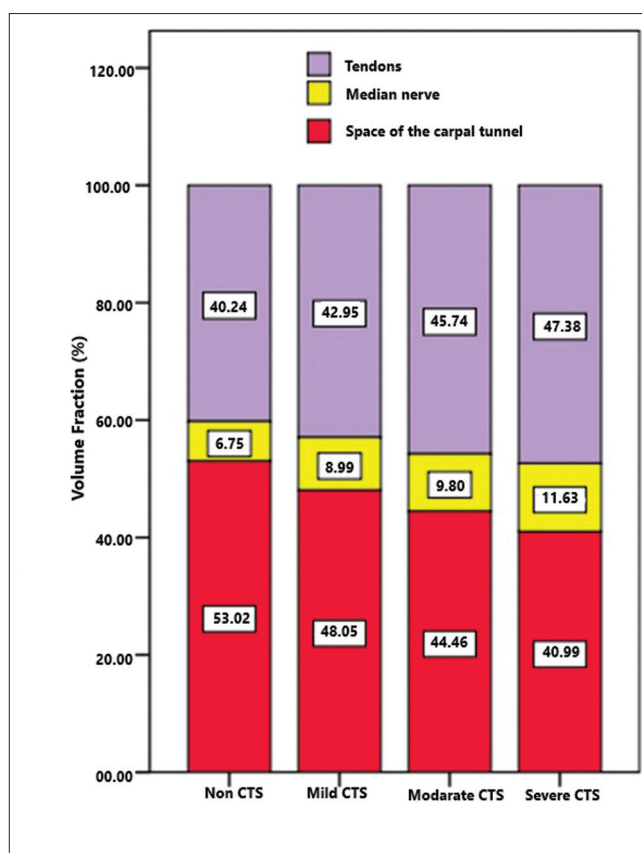


Figure 6: Mean volume fraction among CTS severities. CTS: Carpal tunnel syndrome

between CTS severity and space of canal volume fraction ($r = -0.616, P = 0.000$) were observed.

Discussion

In this study, the carpal tunnel volume and its structures (nervus medianus and tendons) were measured to

determine the severity of CTS. Carpal tunnel contents and the volume ratio values of these contents to the tunnel were obtained by stereological method. In this way, the 3-dimensional evaluation of the Carpal tunnel was made. Among these values, the most spectacular one is that the free space volume fraction of carpal tunnel decreased while the difference between volume and volume fractions

of median nerve increased as CTS severity increased. Accordingly, this is a compatible finding with the studies^[10,11] specifying an increase in carpal tunnel contents as a common characteristic of CTS. Besides, it is known that the volumes of carpal tunnel and contents within the tunnel affect the inner tunnel pressure.^[12,13] In literature, carpal tunnel area studies have been done, including predominantly nerve conduction studies and secondarily median nerve area.^[14-18] In addition, studies indicating the nervus medianus volume and CTV in patients with CTS are remarkable.^[14,19,20] Moreover, the fractions of the tunnel contents were researched in different studies.^[4,21] There are some studies analyzing CTS severity with Doppler ultrasonography (USG) or MRI in the literature.^[7,17,22,23] However, studies that find a mean volume value of median nerve depending on CTS severity or specify free space volume fraction of carpal tunnel quantitatively are not encountered. CTS severity may be determined by stereological methods without the need for a radiology specialist. The other finding of the study was that the volume of the carpal tunnel is found to be successful in differentiating sick and healthy people while unsuccessful in determining the severity of the CTS [Figure 2]. Moreover, this finding is quite compatible with the studies that indicate potential tendency to have smaller cross-sectional areas of carpal tunnel and increase in the fraction of the tendon to the tunnel in CTS etiology.^[24-26] Since the CTV of patients with CTS is less, it is very important to reduce the treatment cost of CTS as a result of early diagnosis in people who are genetically susceptible to CTS.

In our study, it was determined that the median nerve volume was higher and the CTV was lower in the patient group compared to the control group. While the volume value of the carpal tunnel achieved by Pacek *et al.*^[27] with the study on cadavers is quite lower than our study, the volume of the carpal tunnel and the contents achieved by Richman and Cobb again with the study on cadavers is observed as close to our data.^[4,28] Ablove *et al.* calculated the volume of the carpal tunnel as 4600 mm³.^[29] It is also noteworthy that the CTV values obtained by Pierre-Jerome *et al.* were quite high compared to our values and other measured volume values.^[30,31] We thought that these differences are because of heterogeneous studies, studies done by different operators, patient characteristics,^[32] studies on cadavers, and different study groups. In our study, it was found that the volume fraction of tendons and median nerves increased and the carpal tunnel space decreased because of the small volume of the carpal tunnel in patients with CTS according to the volume fractions [Tables 2 and 3]. Bower *et al.* stated that the volume of the carpal tunnel on neutral position is 3737 mm³ and the fraction of the canal contents to the carpal tunnel (CTCv/CTV) is 40%–43% by analyzing the MRIs of the right (the dominant one) wrist positions (flexion, extension, and neutral) of 4 healthy women and 4 healthy men.^[3] We think that the volume

of the right wrist carpal tunnel in the neutral position is smaller than our values because of the fact that the number of our cases is higher. While Bower *et al.* achieved the fraction of the carpal tunnel contents, we achieved the fraction of the canal free space. Oge *et al.* found that the fractions of the content area (tendon + median nerve/the area of the carpal tunnel) increase in patients with carpal tunnel, but the volume of the carpal tunnel is not different in both patients and healthy people.^[21]

It may be considered that idiopathic CTS might depend on the incompatibility of the median nerve and the volume of the carpal tunnel since the increase of internal pressure in carpal tunnel results in edema in the nerve and circulatory disorder.^[10] In addition, Uchiyama *et al.* stated that the increasing area of the carpal tunnel may depend on the flexor tendons and the median nerve.^[33]

If we look at the volume and the volume fraction according to the CTS severity, it is observed that the estimation of the volume of the carpal tunnel was successful at distinguishing patients and healthy people but unsuccessful at distinguishing CTS severity [Figure 2]. Furthermore, the volume and the volume fraction of the median nerve were quite effective in distinguishing CTS severity [Figure 5 and Table 3]. While the severity of CTS increased, the difference between volume fractions of the tendons increased in accordance with healthy people [Figure 5]. The volume fractions of the tendons were important in order to determine the severity of the CTS [Figure 6 and Table 3]. When the CTS severity increased, the free space of the carpal tunnel decreased [Figure 6 and Table 3]. No volumetric study about CTS severity is encountered in the literature. Moreover, it is observed that all the other studies about the volume and the volume fractions have been done on cadavers or only healthy people until today. Furthermore, in the studies on cadavers, there are some striking elements such as a small number of cadavers, not specifying the gender or age of cadavers, a chronic illness that may trigger CTS, a neurological table, uncertainty of etiologic factors like wrist trauma, and an insufficient number of participants in some studies.^[4,12,27,28] Using the Cavalieri method, a practical, fast, and quantitative examination about morphological changes on wrists became possible.^[34] Obtaining volume and volume ratio data using MRI images, being one of the first studies to determine the diagnosis and severity of Carpal tunnel syndrome, and the specificity of the working operator reveal the strengths of our study. The situations that limit our study are deficient for reaching the intended number of cases according to the nonexistence of a routine MRG protocol in CTS, scanning each person in the same MR device, and excluding people that have bad quality MRIs.

Conclusion

This study may be extended more by increasing the number of cases as men and women to analyze the volume and the volume fraction of the carpal tunnel, the contents, and free

Table 3: The relation between carpal tunnel and canal content volume and volume fraction in patients with CTS (n=50)

	Carpal tunnel volume	Tendons volume	Median nerve volume	Tendons volume fraction	Median nerve volume fraction	Space of the carpal tunnel
CTS severe						
<i>r</i>	-0.204	0.152	0.610	0.446	0.778	-0.616
<i>P</i>	0.070	0.179	0.000*	0.000*	0.000*	0.000*
Carpal tunnel volume						
<i>r</i>	1.000	0.658	0.368	-0.278	-0.280	0.318
<i>P</i>		0.000*	0.001	0.013	0.012	0.004
Tendons volume						
<i>r</i>		1.000	0.461	0.528	0.037	-0.461
<i>P</i>			0.000*	0.000	0.747	0.000*
Median nerve volume						
<i>r</i>			1.000	0.174	0.778	-0.375
<i>P</i>				0.122	0.000	0.001*
Tendons volume fraction						
<i>r</i>				1.000	0.376	-0.963
<i>P</i>					0.001	0.000*
Median nerve volume fraction						
<i>r</i>					1.000	-0.612
<i>P</i>						0.000*
Space of the carpal tunnel						
<i>r</i>						1.000
<i>P</i>						

CTS: Carpal tunnel syndrome. *0.01 is statistically significant ($P=0.000<0.01$)

space fractions over wrist positions (flexion, extension, and neutral) depending on the CTS severity. The studies on Doppler USG and MRI reviewing the CTS severity are important for obtaining standard data. In this present study, CTVs and the structures within (median nerve and tendons) and the fraction values of these contents to the tunnel were analyzed for the first time.

According to our results, it has been observed that estimating CTV is a successful method in determining the susceptibility to CTS. As the severity of CTS increases, the difference between the median nerve volume and volume fraction increases and the free space of the carpal tunnel decreases. Thus, it was anatomically confirmed that as the severity of CTS increases, the free space of the carpal tunnel decreases. Consensus on diagnostic criteria for CTS is essential in clinical areas to provide effective treatment. The use of stereological techniques may also play an essential role in exploring the morphology of the carpal tunnel and cases that are difficult to diagnose.

Financial support and sponsorship

This study was supported by Ondokuz Mayıs University Graduate Student Research Projects Fund (Project No. PYO.TIP. 1904.11.004.). The funder had no role in study design, data collection and analysis, decision to publish, or preparation of the manuscript.

Conflicts of interest

There are no conflicts of interest.

References

1. Aroori S, Spence RA. Carpal tunnel syndrome. *Ulster Med J* 2008;77:6-17.
2. McCabe SJ, Uebele AL, Pihur V, Rosales RS, Atroschi I. Epidemiologic associations of carpal tunnel syndrome and sleep position: Is there a case for causation? *Hand (N Y)* 2007;2:127-34.
3. Bower JA, Stanisiz GJ, Keir PJ. An MRI evaluation of carpal tunnel dimensions in healthy wrists: Implications for carpal tunnel syndrome. *Clin Biomech (Bristol, Avon)* 2006;21:816-25.
4. Cobb TK, Dalley BK, Posteraro RH, Lewis RC. Establishment of carpal contents/canal ratio by means of magnetic resonance imaging. *J Hand Surg Am* 1992;17:843-9.
5. Kalkan E, Cander B, Gul M, Girisgin S, Karabagli H, Sahin B. Prediction of prognosis in patients with epidural hematoma by a new stereological method. *Tohoku J Exp Med* 2007;211:235-42.
6. Sahin B, Ergur H. Assessment of the optimum section thickness for the estimation of liver volume using magnetic resonance images: A stereological gold standard study. *Eur J Radiol* 2006;57:96-101.
7. Mohammadi A, Ghasemi-Rad M, Mladkova-Suchy N, Ansari S. Correlation between the severity of carpal tunnel syndrome and color Doppler sonography findings. *AJR Am J Roentgenol* 2012;198:W181-4.
8. Jarvik JG, Yuen E, Kliot M. Diagnosis of carpal tunnel syndrome: Electrodiagnostic and MR imaging evaluation. *Neuroimaging Clin N Am* 2004;14:93-102, viii.

9. Sahin B, Elfaki A. Estimation of the volume and volume fraction of brain and brain structures on radiological images. *Neuroquantology* 2012;10:87-97.
10. Gelberman RH, Hergenroeder PT, Hargens AR, Lundborg GN, Akeson WH. The carpal tunnel syndrome. A study of carpal canal pressures. *J Bone Joint Surg Am* 1981;63:380-3.
11. Phalen GS. Spontaneous compression of the median nerve at the wrist. *J Am Med Assoc* 1951;145:1128-33.
12. Mogk JP, Keir PJ. The effect of landmarks and bone motion on posture-related changes in carpal tunnel volume. *Clin Biomech (Bristol, Avon)* 2009;24:708-15.
13. Mogk JP, Keir PJ. Evaluation of the carpal tunnel based on 3-D reconstruction from MRI. *J Biomech* 2007;40:2222-9.
14. Crnković T, Trkulja V, Bilić R, Gašpar D, Kolundžić R. Carpal tunnel and median nerve volume changes after tunnel release in patients with the carpal tunnel syndrome: A magnetic resonance imaging (MRI) study. *Int Orthop* 2016;40:981-7.
15. Moran L, Perez M, Esteban A, Bellon J, Arranz B, del Cerro M. Sonographic measurement of cross-sectional area of the median nerve in the diagnosis of carpal tunnel syndrome: Correlation with nerve conduction studies. *J Clin Ultrasound* 2009;37:125-31.
16. Mohammadi A, Afshar A, Etemadi A, Masoudi S, Baghizadeh A. Diagnostic value of cross-sectional area of median nerve in grading severity of carpal tunnel syndrome. *Arch Iran Med* 2010;13:516-21.
17. Ng AW, Griffith JF, Tong CS, Law EK, Tse WL, Wong CW, *et al.* MRI criteria for diagnosis and predicting severity of carpal tunnel syndrome. *Skeletal Radiol* 2020;49:397-405.
18. Bagga B, Sinha A, Khandelwal N, Modi M, Ahuja CK, Sharma R. Comparison of magnetic resonance imaging and ultrasonography in diagnosing and grading carpal tunnel syndrome: A prospective study. *Curr Probl Diagn Radiol* 2020;49:102-15.
19. Crnković T, Bilić R, Trkulja V, Cesarik M, Gotovac N, Kolundžić R. The effect of epineurotomy on the median nerve volume after the carpal tunnel release: A prospective randomised double-blind controlled trial. *Int Orthop* 2012;36:1885-92.
20. Peters BR, Martin AM, Memauri BF, Bock HW, Turner RB, Murray KA, *et al.* Morphologic analysis of the carpal tunnel and median nerve following open and endoscopic carpal tunnel release. *Hand (N Y)* 2021;16:310-5.
21. Oge HK, Acu B, Gucer T, Yanik T, Savlarlı S, Firat MM. Quantitative MRI analysis of idiopathic carpal tunnel syndrome. *Turk Neurosurg* 2012;22:763-8.
22. Kutlar N, Bayrak AO, Bayrak İK, Canbaz S, Türker H. Diagnosing carpal tunnel syndrome with Doppler ultrasonography: A comparison of ultrasonographic measurements and electrophysiological severity. *Neurol Res* 2017;39:126-32.
23. Rahmani M, Ghasemi Esfe AR, Vaziri-Bozorg SM, Mazloumi M, Khalilzadeh O, Kahnouji H. The ultrasonographic correlates of carpal tunnel syndrome in patients with normal electrodiagnostic tests. *Radiol Med* 2011;116:489-96.
24. Skie M, Zeiss J, Ebraheim NA, Jackson WT. Carpal tunnel changes and median nerve compression during wrist flexion and extension seen by magnetic resonance imaging. *J Hand Surg Am* 1990;15:934-9.
25. Bleecker ML, Bohlman M, Moreland R, Tipton A. Carpal tunnel syndrome: Role of carpal canal size. *Neurology* 1985;35:1599-604.
26. Dekel S, Papaioannou T, Rushworth G, Coates R. Idiopathic carpal tunnel syndrome caused by carpal stenosis. *Br Med J* 1980;280:1297-9.
27. Pacek CA, Tang J, Goitz RJ, Kaufmann RA, Li ZM. Morphological analysis of the carpal tunnel. *Hand (N Y)* 2010;5:77-81.
28. Richman JA, Gelberman RH, Rydevik BL, Gylys-Morin VM, Hajek PC, Sartoris DJ. Carpal tunnel volume determination by magnetic resonance imaging three-dimensional reconstruction. *J Hand Surg Am* 1987;12:712-7.
29. Ablove RH, Peimer CA, Diao E, Oliverio R, Kuhn JP. Morphologic changes following endoscopic and two-portal subcutaneous carpal tunnel release. *J Hand Surg Am* 1994;19:821-6.
30. Pierre-Jerome C, Bekkelund SI, Nordstrøm R. Quantitative MRI analysis of anatomic dimensions of the carpal tunnel in women. *Surg Radiol Anat* 1997;19:31-4.
31. Pierre-Jerome C, Bekkelund SI, Mellgren SI, Nordstrøm R. Quantitative MRI and electrophysiology of preoperative carpal tunnel syndrome in a female population. *Ergonomics* 1997;40:642-9.
32. Sarraf P, Malek M, Ghajarzadeh M, Miri S, Parhizgar E, Emami-Razavi SZ. The best cutoff point for median nerve cross sectional area at the level of carpal tunnel inlet. *Acta Med Iran* 2014;52:613-8.
33. Uchiyama S, Itsubo T, Nakamura K, Kato H, Yasutomi T, Momose T. Current concepts of carpal tunnel syndrome: Pathophysiology, treatment, and evaluation. *J Orthop Sci* 2010;15:1-13.
34. Sahin B, Emirzeoglu M, Uzun A, Incesu L, Bek Y, Bilgic S, *et al.* Unbiased estimation of the liver volume by the Cavalieri principle using magnetic resonance images. *Eur J Radiol* 2003;47:164-70.

Correlation of Cephalo-Facial Parameters with Body Height in Indian and African Students of a University in North India

Abstract

Introduction: In forensic anthropology, body height or stature estimation is important for identification of missing persons. Stature has a proportional relationship with different parts of the human body including cephalo-facial region. The cephalo-facial indices are different for different people. Therefore, they may help in stature reconstruction and identification of a person. The study was conducted to find out if there is any correlation between four cephalo-facial parameters and body height and to derive regression formulae in Indian and African students. **Material and Methods:** The present study was conducted on 170 students of a University in North India belonging to two different races, i.e., Indian (85) and African (85). Stature and four cephalo-facial dimensions, i.e., maximum head length (MHL), horizontal head circumference (HHC), morphological facial length (MFL) and bigonial diameter (BD) were measured. The data were analyzed using SPSS software version 15. **Results:** In both Indian and African students all the four cephalo-facial parameters, i.e., MHL, HHC, MFL, and BD showed a positive correlation with stature ($P < 0.001$). It was found that in Indians the strongest correlation of stature was with MHL and least correlation was with HHC. In Africans, the highest correlation was observed with MHL and lowest with BD. **Discussion and Conclusion:** In this study, it was found that among the cephalo-facial parameters, cephalic parameters are more reliable than facial parameters. Out of the two cephalic parameters HHC was found to be more reliable than MHL in the estimation of stature in both Indian and African students. The regression equations derived turned out to be population/race-specific and therefore, cannot be generalized for all population groups.

Keywords: Anthropography, cephalo-facial measurements, regression equation, stature

Introduction

Stature is a very important anthropometric parameter used in identification of an individual. Height of body in standing position is defined as stature. Every part of the human body has a proportional relationship with stature including cephalo-facial dimensions.^[1] Cranio-facial anthropometry involves measurements of parameters on the skull and face. The dimensions of the head and face are dependent on various factors, such as geography, genetic influence, and nutrition. Cephalo-facial parameters are important and are used in identification of individuals, sex determination, and in classifying of races. Cephalo-facial measurements also help in summarizing the anatomical complexity of the head and face of human being living within a similar geography.

This is an open access journal, and articles are distributed under the terms of the Creative Commons Attribution-NonCommercial-ShareAlike 4.0 License, which allows others to remix, tweak, and build upon the work non-commercially, as long as appropriate credit is given and the new creations are licensed under the identical terms.

For reprints contact: WKHLRPMedknow_reprints@wolterskluwer.com

Various techniques are used to study craniofacial parameters.^[2] Cephalometry is the most commonly used technique because it is simple, acceptable, practical, and valid.^[3] Both radiological and osteological studies on cadaveric skull have been carried out to estimate stature.^[4-7]

Body height or stature can be estimated from bones. Regression analysis is an easy and reliable method. Each race will require its own formula for estimation of stature.^[8] Regression formulae obtained using major long bones are generally considered to be more accurate. However, studies using cephalo-facial parameters to correlate with stature are few.

The present study was conducted to find out the correlation between cephalo-facial parameters and body height and also to assess which of these parameters is more accurate for estimation of stature as this could be of great help in identification of an individual when only craniofacial remains are available.

How to cite this article: Nair SC, Samanta PP, Kharb P. Correlation of cephalo-facial parameters with body height in Indian and African students of a university in North India. *J Anat Soc India* 2022;XX:XX-XX.

Sreekala C. Nair,
Prajna Paramita
Samanta¹,
Poonam Kharb²

Department of Anatomy, School of Allied Health Sciences,

¹Department of Anatomy, School of Medical Sciences and Research, Greater Noida,

²Department of Human Anatomy, ITS Dental College, Ghaziabad, Uttar Pradesh, India

Article Info

Received: 01 January 2021

Revised: 10 February 2022

Accepted: 21 June 2022

Available online: ***

Address for correspondence:

Dr. Prajna Paramita Samanta, Department of Anatomy, School of Medical Sciences and Research, Greater Noida, Uttar Pradesh, India.

E-mail: prajnap.samanta@sharda.ac.in

Access this article online

Website: www.jasi.org.in

DOI:
10.4103/jasi.jasi_1_21

Quick Response Code:



Material and Methods

The present study was conducted on 170 students of a University in North India belonging to two different races (85 students each of Indian and African origin between 18 and 25 years of age) after getting approval from the Institutional Ethics Committee. Informed written consent was obtained from each student before the study.

The height was measured with the subject in standing position and being barefooted with close approximation of both the feet and head kept in Frankfurt's Plane.

The following cephalo-facial parameters were measured:

1. Maximum head length (MHL) was measured as distance between glabella and opisthocranium (the area near the top of occipital bone)
2. Horizontal head circumference (HHC) was measured as the maximum head circumference from just above the glabella area to the opisthocranium
3. Morphological facial length (MFL) was measured as distance from root of nose (nasion) to the lowest point on the lower border of the mandible in the mid-sagittal plane (gnathion)
4. Bigonial diameter (BD) was measured as the maximum breadth of the lower jaw between two gonion points on the angles of mandible.

Measurements were taken at a fixed time between 14.00 and 16.30 h to exclude differences due to diurnal variation. The measurements were taken three times by the same person and the average was taken to minimize the errors in methodology.

Multiple linear regression analyses were done for the estimation of stature using the above parameters. (SPSS Ver 20.0, IBM, USA).

Results

The mean height was found to be 165.20 ± 10.54 cm in Indian students and 169.49 ± 9.44 cm in African students, respectively. The mean values of MHL, HHC, MFL, and BD were found to be 18.19 ± 0.97 cm, 54.74 ± 0.22 cm, 10.77 ± 0.07 cm, and 9.85 ± 0.07 cm in Indians and 18.96 ± 0.09 cm, 57.28 ± 0.2 cm, 11.3 ± 0.08 cm, and 9.64 ± 0.07 cm in Africans, respectively Table 1].

It was observed that the mean height, MHL, HHC, and MFL were higher in Africans than in Indian students whereas BD was higher in Indians. The mean BD of Indian students was found to be 9.85 ± 0.07 cm and in Africans, it was 9.64 ± 0.07 cm. It was observed that all cephalo-facial parameters were higher in males than in females in Indian students However, in African students, the MHL, MFL, and BD were found to be higher in males whereas HHC was found to be higher in females.

Correlation between height and the measured parameters was found out by calculating correlation coefficient. For MFL Carl Pearson correlation coefficient and for MHL,

HHC, and BD Spearman rank correlation coefficient was calculated for both the races. In Indian students, all the cephalo-facial parameters showed a significant correlation with stature. All these values were also found to be statistically highly significant ($P < 0.001$). It was found that in Indians the highest correlation of stature was with MHL and lowest correlation was with HHC. In Africans, all cephalo-facial parameters showed a significant correlation with stature ($P < 0.001$). The highest correlation was observed with MHL and lowest with MFL [Table 2].

After finding a positive correlation between the measured parameters (MHL, HHC, MFL, BD) and stature, regression analysis was done for the estimation of stature in both Indians and Africans. To calculate regression equations the values of constants "a" (regression coefficient of the dependent variable) and "b" (regression coefficient of the independent variable) were calculated. Then, the stature was calculated.

Table 3 shows the standard error of estimate (SEE). The SEE shows the difference in evaluated stature from the actual stature. A low SEE is suggestive of the higher reliableness of prediction from a measurement and high SEE denotes less reliableness of prediction.

Among the cephalo-facial parameters, HHC showed lowest value of SEE in Indians SEE (± 0.47) and in Africans SEE (± 0.52) which explains its higher reliability factor and accuracy in stature estimation as compared to the other three cephalo-facial parameters measured in the study. In

Table 1: Stature (cm) and cephalo-facial measurements (cm) in Indian and African students

Parameters	Mean \pm SD (cm)	
	Indian (n=85)	African (n=85)
Stature (height)	165.2 \pm 10.54	169.49 \pm 9.44
MHL	18.19 \pm 0.97*	18.96 \pm 0.09
HHC	54.74 \pm 0.22*	57.28 \pm 0.2
MFL	10.77 \pm 0.07 [#]	11.3 \pm 0.08
BD	9.85 \pm 0.07*	9.64 \pm 0.07

*Mann-Whitney test, [#]Student *t*-test. MHL: Maximum head length, HHC: Horizontal head circumference, MFL: Morphological facial length, BD: Bigonial diameter, SD: Standard deviation

Table 2: Cephalo-facial correlation with stature in Indians and African students

Parameters	Indians		Africans	
	Correlation coefficient	<i>P</i>	Correlation coefficient	<i>P</i>
MHL	0.62	0.001*	0.62	0.001*
BD	0.59	0.001*	0.51	0.001*
MFL	0.57	0.001 [#]	0.41	0.001*
HHC	0.53	0.001*	0.53	0.001 [#]

*Spearman Correlation coefficient, [#]Pearson correlation coefficient. MHL: Maximum head length, HHC: Horizontal head circumference, MFL: Morphological facial length, BD: Bigonial diameter

Table 3: Regression equation for stature evaluation (cm) from cephalo-facial parameters in Indians and Africans

Parameters	Regression formula		Predicted height (y)		SEE		P	
	Indians	Africans	Indians	Africans	Indians	Africans	Indians	Africans
MHL	Y=42.37+6.75 MHL	Y=73.90+5.04 MHL	165.15	169.45	0.92	1.04	0.001	0.001
HHC	Y=15.78+2.72 HHC	Y=113.73+0.97 HHC	164.6	169.29	0.47	0.52	0.001	0.001
MFL	Y=72.22+8.62 MFL	Y=113.22+4.97 MFL	165.05	169.38	1.35	1.2	0.001	0.001
BD	Y=78.89+8.75 BD	Y=99.46+7.25 BD	165.07	169.35	1.37	1.38	0.001	0.001

A-regression coefficient of the dependent variable (stature), RC (b)-regression coefficient of the independent variable (cephalo-facial or PCTL). CC (r): Correlation coefficient, CD (R²): Coefficient of determination, Y: Estimated height, X: MHL, SEE: Standard error of estimate, MHL: Maximum head length, HHC: Horizontal head circumference, MFL: Morphological facial length, BD: Bigonial diameter, PCTL: Percutaneous tibia length

this study, it was also found that among the cephalo-facial parameters, cephalic parameters are more reliable than facial parameters.

Discussion

The evaluation of stature from skull bones alone can be a difficult task. Nonavailability of body height data along with cephalo-facial measurements is one of the difficulties faced in computing the stature estimation formula.

In the present study, the four cephalo-facial dimensions, i.e., MHL, HHC, MFL, and BD showed a positive correlation with stature in both Indian and African students. The correlation coefficient values of all four cephalo-facial dimensions were more than 0.5 in Indian students which denotes there is a positive correlation between stature and cephalo-facial parameters studied. However, in African students, MHL, HHC, and BD showed correlation coefficient values more than 0.5 whereas MFL had a lower value, i.e., 0.414 which means that MFL is not reliable for the evaluation of stature in African students.

Agnihotri *et al.* observed that in the Indo-Mauritian population the correlation coefficient of cephalo-facial dimensions were <0.5 in all cases.^[9] Since correlation coefficient is significant only above 0.5, they concluded that there was no positive correlation between stature and cephalo-facial parameters. Shah *et al.* found the correlation coefficient of all cephalo-facial dimensions to be <0.5 which indicates stature estimation from cephalo-facial dimensions is not reliable.^[10]

In the present study, among the four cephalo-facial parameters, MHL showed the highest correlation coefficient value (0.62) for both Indian and African students. Similar findings were reported by Ilayperuma who studied the relationship between the cranial dimensions and height of adults in the Sri Lankan population and observed the correlation coefficient of MHL to be 0.72 and therefore MHL is significantly correlated with stature.^[11] However, according to studies by Saxena *et al.* on Agra population, Jadav and Shah on Gujarat population, Sudhir *et al.* on Maharashtra population, Seema and Mahajan (2011) on Punjab population, Santosh *et al.* on Rajasthan population, Ryan and Bidmos on South African population, the range

of correlation coefficients between stature and head length were ranging between 0.34 to 0.44 for females and 0.28 to 0.35 for males.^[12-17]

In the present study, in Indian students, HHC showed the least correlation (0.53) and lowest value of SEE, i.e., 0.47. In African students, the highest correlation was shown by MHL (0.62) and then by HHC but HHC showed lower value of SEE (0.52). This indicates that the regression equation calculated for the HHC gives a higher level of reliability and accuracy in the estimation of stature in both Indian and African students. The findings of the present study are similar to the study conducted by Krishan and Kumar where the HHC showed lowest SEE (standard error of estimate) (3.72) which is higher than the SEE values of the present study (0.47).^[5] Ewunonu and Anibeze observed that HHC exhibits the lowest value of SEE (6.93) than MHL (7.48) in the South-Eastern Nigerian population.^[18] Ekezie *et al.* mentioned that the HHC did not show any positive correlation with stature in Igbos (South Eastern Nigerians).^[19] However, in the present study, HHC showed good correlation (0.53) and lowest SEE (0.52) values in African students.

From the above discussion, it can be concluded that out of the two cephalic parameters HHC was found to be more reliable than MHL in estimation of stature in both Indian and African students.

MFL showed good correlation (0.57) with stature in Indian students, whereas in African students the correlation coefficient was 0.41 since correlation coefficient is considered significant only above 0.5, so it was concluded that MFL is not reliable for estimation of stature in African students. This is also confirmed by high SEE value of MFL (1.20). In studies conducted by Ekezie *et al.* in South-Eastern Nigerians and Kumar and Gopichand in Haryanvi adults, the SEE was found to be 7.34 (for both males and females) and 5.38 (males), respectively, whereas in the present study, the SEE of MFL for Indians was 1.35 and for Africans was 1.20 (for both males and females) which is comparatively lower than the above studies.^[19,20] Similar to the present study, Ekezie *et al.* observed MFL to be reliable for the estimation of stature due to low SEE as compared to other cephalo-facial parameters.^[19] Kumar and

Gopichand concluded that MFL is less reliable as compared to other cephalo-facial parameters.^[20]

Swami *et al.* estimated stature MFL and BD in Haryanvi Baniyas.^[21] Both parameters showed a good correlation with stature, since MFL showed low value of SEE in males (5.3) and (4.3) in females as compared to SEE values of BD, i.e., (5.4) in males and (4.6) in females, so they concluded that among the facial parameters MFL is more reliable in estimating stature than BD. The data of the present study are similar to the above study, even though both MFL and BD showed good correlation but on regression analysis, MFL showed lower SEE value (1.35) in Indian students and (1.2) in African students than the SEE value of BD, i.e., (1.37) in Indians and (1.38) in Africans. Thus, from the above discussion, it can be concluded that among the four facial parameters MFL is more reliable in the estimation of stature in both Indian and African students.

In the present study, the cephalic dimensions proved to be more reliable than facial dimensions for the estimation of stature in both Indian and African students as lower SEE was observed in cephalic dimensions. This observation shows that the calculation of regression formulae from cephalic measurements is more reliable and accurate than facial measurements. The findings were comparable to Krishan and Kumar and Krishan.^[5,22] In the above-mentioned studies, cephalic dimensions proved to be more reliable than facial dimensions.

Conclusion

A significant correlation was found between cephalo-facial measurements with stature. Out of the four cephalo-facial parameters studied, cephalic parameters, i.e., MHL and HHC were found to be better correlated with stature than facial parameters, i.e., MFL and BD in both Indian and African students.

Among the cephalo-facial parameters, HHC has the highest degree of reliability and accuracy in the estimation of stature.

In Indians as well as African students, MHL showed the highest correlation with stature. However, in Indians, the lowest correlation was seen with HHC whereas in Africans lowest correlation was with BD, therefore, it is essential to derive regression equations which are specific for people of a particular race or specific area and they are not applicable to all population groups.

Financial support and sponsorship

Nil.

Conflicts of interest

There are no conflicts of interest.

References

1. Krogman WM, Iscan MY. The Human Skeleton in Forensic Medicine. 2nd ed. Springfield: Thomas CC; 1986. p. 58.
2. McIntyre GT, Mossey PA. Size and shape measurement in contemporary cephalometrics. *Eur J Orthod* 2003;25:231-42.
3. Rexhepi A, Meka V. Cephalofacial morphological characteristics of Albanian Kosova population. *Int J Morphol* 2008;26:935-40.
4. Introna F Jr., Di Vella G, Petrachi S. Determination of height in life using multiple regression of skull parameters. *Boll Soc Ital Biol Sper* 1993;69:153-60.
5. Krishan K, Kumar R. Determination of stature from cephalo-facial dimensions in a North Indian population. *Leg Med (Tokyo)* 2007;9:128-33.
6. Patil KR, Mody RN. Determination of sex by discriminant function analysis and stature by regression analysis: A lateral cephalometric study. *Forensic Sci Int* 2005;147:175-80.
7. Chiba M, Terazawa K. Estimation of stature from somatometry of skull. *Forensic Sci Int* 1998;97:87-92.
8. Trotter M, Gleser GC. Estimation of stature from long bones of American Whites and Negroes. *Am J Phys Anthropol* 1952;10:463-514.
9. Agnihotri AK, Kachhwaha S, Googoolye K, Allock A. Estimation of stature from cephalo-facial dimensions by regression analysis in Indo-Mauritian population. *J Forensic Leg Med* 2011;18:167-72.
10. Shah T, Patel MN, Nath PS, Bhise RS, Menon SK. Estimation of stature from cephalo-facial dimensions by regression analysis in Gujarati population. *J Indian Acad Forensic Med* 2015;37:253-7.
11. Ilayperuma I. On prediction of personal stature from cranial dimensions. *Int J Morphol* 2010;28:1135-40.
12. Saxena SK, Jeyasingh P, Gupta AK, Gupta CD. The estimation of stature from head length. *J Anat Soc Indian* 1981;30:78-9.
13. Jadav HR, Shah GV. Determination of the personal height from the length of the head in Gujarat Region. *J Anat Soc Indian* 2004;5:20-1.
14. Sudhir PE, Zambare BR, Shinde SV, Readdy BB. Determination of personal height from the length of head in Maharashtra region. *Indian J Forensic Med Pathol* 2010;3:55-8.
15. Seema, Mahajan A. Estimation of personal height from the length of head in Punjab Zone. *International Journal of Plant, Animal and Environmental Sciences* 2011;1:205-8.
16. Kumar S, Garg R, Mogra K, Choudhary R. Prediction of stature by the measurement of head length in population of Rajasthan. *J Evol Med Dent Sci* 2013;2:1334-9.
17. Ryan I, Bidmos MA. Skeletal height reconstruction from measurements of the skull in indigenous South Africans. *Forensic Sci Int* 2007;167:16-21.
18. Ewunonu EO, Anibeze CI. Anthropometric study of the facial morphology in South-Eastern Nigerian population. *Hum Biol Rev* 2013;2:314-23.
19. Ekezie J, Anibeze C, Uloneme GC, Anyanwu GE. Height estimation of the Igbos using cephalo-facial anthropometry. *Int J Curr Microbiol Appl Sci* 2015;4:305-16.
20. Kumar M, Gopichand P. Estimation of stature from cephalo-facial anthropometry in 800 Haryanvi adults. *Int J Plant Anim Environ Sci* 2013;3:42-6.
21. Swami S, Kumar M, Patnaik VV. Estimation of stature from facial anthropometric measurements in 800 adult Haryanvi Baniyas. *Indian J Basic Appl Med Res* 2015;5:122-32.
22. Krishan K. Estimation of stature from footprint and foot outline dimensions in Gujjars of North India. *Forensic Sci Int* 2008;175:93-101.

Numerical Chromosomal Aberrations in Acute Lymphoblastic Leukemia in North Indians

Abstract

Introduction: Alterations in chromosome number have a strong impact on outcome in childhood ALL. Genetic findings may predict the prognosis and biologic properties of the leukemia more consistently than does morphology. To see the numerical aberrations in ALL in North Indian population **Material and Methods:** Culture and chromosome banding of bone marrow and blood sample of 51 North Indian patients of ALL (44 males and 7 females) from the age group of 2 to 42 years were done. Only 39 shows good chromosomal spread, so 39 karyograms were prepared and observed for the chromosomal gain or loss and their frequency. **Results:** Numerical abnormalities were observed in 14 patients (35.9%) of the 39 cytogenetically analysed cases. Trisomy 21 was found in 3 cases. Trisomy of chromosome number 13 and 14 were found in 5.12% cases. Trisomy of chromosome number 3, 4, 6, 8, 11, 15, 17 and 18 were present in 2.56% cases (Fig. 21, 30, 31, 34, 35, 42). Gain of chromosome X was seen in 5.12% cases while only in one case (2.56%) gain of chromosome Y was detected. **Discussion and Conclusion:** Numerical chromosomal abnormality in this study was 15.38% which was different from other population described in previous studies. Trisomy 21 is most common in this study. The findings of the present study may be useful for the clinician in predicting outcome, remission, survival and treatment response in ALL.

Keywords: Acute lymphoblastic leukemia, numerical aberrations, trisomy

Introduction

Acute lymphoblastic leukemia (ALL) is a malignant transformation and proliferation of lymphoid progenitor cells in bone marrow, blood, and extramedullary sites. The hallmark of ALL is chromosomal abnormalities and genetic alterations involved in the differentiation and proliferation of lymphoid precursor cells. Over two-thirds of childhood, ALL cases demonstrate numerical gains or losses of chromosomes and/or translocation.^[1] Genetic findings predict the prognosis and biological properties of leukemia. The association of a high hyperdiploid karyotype with a good prognosis is known for more than 20 years. Conversely, the loss of chromosomes in the near-haploid group indicates a poor outcome.^[2]

Material and Methods

The present study was a descriptive type. This study included 51 patients (44 males

and 7 females) of age group 2 years to 42 years (5 adult and 46 pediatric cases). Patients were screened in the Department of Pediatrics and the samples were collected from the Department of Pathology. Bone marrow and peripheral blood of diagnosed cases of ALL were taken with their consent. A culture of bone marrow and blood sample was done; a trypsin-Giemsa technique was used for chromosome banding. Karyograms were prepared and 20–25 metaphases were analyzed in each case for various chromosomal anomalies in the Cytogenetic Laboratory of the Department of Anatomy, King George's Medical University, UP, Lucknow, India.

Observation and Results

This study included 51 patients (44 males and 7 females) of age group 2 years to 42 years (5 adult and 46 pediatric cases). Out of 51 ALL patients under study, only 39 cases (76.47%) could provide good chromosomal spread and karyograms were obtained. Among 39 successful cases, 24 exhibited abnormal karyograms (1 adult and 23

This is an open access journal, and articles are distributed under the terms of the Creative Commons Attribution-NonCommercial-ShareAlike 4.0 License, which allows others to remix, tweak, and build upon the work non-commercially, as long as appropriate credit is given and the new creations are licensed under the identical terms.

For reprints contact: WKHLRPMedknow_reprints@wolterskluwer.com

How to cite this article: Shri I, Verma RK, Rani A, Kumar N. Numerical chromosomal aberrations in acute lymphoblastic leukemia in North Indians. J Anat Soc India 2022;XX:XX-XX.

**Indu Shri,
Rakesh Kumar
Verma¹,
Archana Rani¹,
Navneet Kumar¹**

*Department of Anatomy,
Government Medical College,
Kannauj, ¹Department of
Anatomy, King George's
Medical University, Lucknow,
Uttar Pradesh, India*

Article Info

Received: 22 May 2021
Revised: 16 August 2022
Accepted: 30 September 2022
Available online: ***

Address for correspondence:

*Dr. Rakesh Kumar Verma,
Additional Professor,
Department of Anatomy,
King George's Medical
University, UP, Lucknow,
Uttar Pradesh, India.
E-mail: rakesh_gsvm@yahoo.
co.in*

Access this article online

Website: www.jasi.org.in

DOI:
10.4103/jasi.jasi_97_21

Quick Response Code:



pediatric cases) and 15 (38.46%) cases showed normal karyograms. Along with numerical and structural chromosomal anomalies, complex karyograms were also seen. Out of 39 cases, numerical chromosomal abnormalities were noted in 6 cases (15.38%) and structural chromosomal abnormalities were observed in 10 cases (25.64%) and 8 cases (20.51%) showed complex karyogram [Table 1].

Numerical abnormalities (hyperdiploidy) were observed in 14 patients (35.9%) of the 39 cytogenetically analyzed cases. Trisomy 21 was found in three cases [Figure 1]. Trisomy of chromosome numbers 13 and 14 was found in 5.12% of cases. Trisomy of chromosome numbers 3, 4, 6, 8, 11, 15, 17, and 18 was present in 2.56% of cases. A gain of chromosome X was seen in 5.12% of cases [Figure 2], while only in one case (2.56%), a gain of chromosome Y was detected [Table 2].

Discussion

Ploidy distribution and recurrent translocations are associated with specific morphology and immune-phenotypic pattern in ALL and their prognostic value was confirmed by several studies. The prognostic importance of chromosome findings in ALL concerns demonstration of long-term survival in patients with high hyperdiploid leukemic clones and identification of patients with certain translocations who are at high risk of treatment failure and for whom alternative therapy such as bone marrow transplantation may be desirable.^[3]

Current intensive chemotherapies cure about 70% of the children with ALL. On the other hand a significant number of the children are not cured despite intensive treatment. At the same time some highly curable patients are treated too intensively and suffer from unnecessary side effects of the chemo- and radiotherapy applied. In order to further improve the therapeutic results in this disease, we have to distinguish between the cases with a better and a

worse prognosis. The initial karyotype (both numerical and structural chromosome abnormalities) proved to be one of the most reliable prognostic parameters, leading to the suggestion of developing genotype-specific therapies.^[4]

In a study in West Indian population by Gadhia *et al.* showed 68.57% chromosomal alteration, including numerical and/or structural abnormalities. Hyperploidy was most common numerical abnormality.^[5] Shikano observed 6.45% (8 patients) cases of ALL patients with hyperploidy,^[6] Raimondi *et al.* noted 14.38% cases with hyperploidy,^[7] and Rokaya *et al.* reported that hyperploidy was 24.5%.^[8] In the present study, hyperploidy was present in 35.90%. Our results were in concordance with previous study by Silva *et al.* and Udayakumar *et al.* who reported hyperploidy in 26%–55% of ALL patients, where hyperploidy is the most common abnormality in ALL cases.^[9,10] Comparison with previous studies were shown in Table 3. The difference between previous and current findings may be a result of the different comparison groups employed for analysis.

The most plausible cause of the gain or loss of a whole chromosome is nondisjunction at mitosis.^[11] Hyperdiploidy probably also resulted with the development of tetraploidy that loses of several chromosomes in a stepwise or sequential fashion or undergoes abnormal mitosis or endomitoses to acquire multiple chromosomes.^[12]

Uckun *et al.* previously showed that hyperdiploid leukemic cells had a lower plating efficiency than did pseudodiploid leukemic cells or near diploid leukemic cells with structural chromosome abnormalities, which suggests that hyperdiploid leukemia might be a less aggressive form of leukemia.^[13] Hyperdiploid (DNA index between 1.16 and 1.35) leukemic cells showed a higher sensitivity than nonhyperdiploid cells to 6-mercaptopurine, 6-thioguanine, cytarabine, and L-asparaginase.^[14]

Trisomy 21 was found in three cases (7.69%), which was the most common trisomy in the present study. Trisomy 21 is the most common trisomy in ALL patients reported by Oláh *et al.* and Nordgren *et al.*^[4,15] Jena Rabindra *et al.* saw a gain of chromosome 21 in 40 South Indian patients.^[16] The emerging theory for the role of constitutional trisomy 21 in leukemia predisposition is that genes on this chromosome contribute to the expansion of hematopoietic compartments during early development that results in an increased pool of potential tumor precursor cells.^[17] Gain of chromosome X was seen in two cases (5.13%) in our study which was also reported by Raimondi *et al.* in 3% of cases.^[7] In the present study, trisomy of chromosome 14 was reported in two cases (5.13%). Oláh *et al.* and Nordgren *et al.* found trisomy of chromosome 14 as a frequently occurring chromosomal



Figure 1: Karyogram-47XY, +21, del 6q, t (8;14)

Table 1: Distribution of different types of karyogram in analyzed cases

Karyogram	Normal	Structural chromosomal abnormalities	Numerical chromosomal abnormalities	Complex rearrangement
No. of cases	15	10	6	8
% (n=39)	38.46%	25.64%	15.38%	20.51%

Table 2: Various numerical anomalies and their distribution in analyzed cases

Numerical chromosomal abnormalities	Number of patients	% out of total karyogram obtained cases (n=39)	% out of total abnormal cases (n=24)
+21	3	7.69%	13.63%
+X	2	5.12%	9.09%
+14	2	5.12%	9.09%
+13	2	5.12%	9.09%
+11	1	2.56%	4.55%
+4	1	2.56%	4.55%
+8	1	2.56%	4.55%
+15	1	2.56%	4.55%
+17	1	2.56%	4.55%
+18	1	2.56%	4.55%
+3	1	2.56%	4.55%
+6	1	2.56%	4.55%
+Y	1	2.56%	4.55%

Table 3 : Comparision with previous studies

Author & Year	Population	Percentage of hyperploidy
Shikano <i>et al</i> (1989)	Japanese	6.45%
Raimondi <i>et al</i> (1992)	Memphis	14.38%
Silva <i>et al</i> (2002)	Brazilian	26-55%
Rokaya <i>et al</i> (2010)	Egyptian	24.5%
Gadhia <i>et al</i> (2018)	West Indian	11.43%
Present Study	North Indian	35.90%

aberration.^[4,15] In our study, trisomy 13 was present in two cases (5.13%). This trisomy was also seen by Oláh *et al.* and Heerema *et al.* as a less frequently occurring chromosomal anomaly.^[4,18] Trisomy 13 occurring as a single cytogenetic abnormality has been associated with undifferentiated or biphenotypic acute leukemias and with an adverse prognostic outcome. Trisomies of chromosomes 3, 4, 6, 8, 11, 15, 17, and 18 were noted in this study, each with one case. This was also noted by Oláh *et al.*, and Heerema *et al.* in ALL patients.^[4,18] Reddy *et al* observed most common numerical abnormalities involving chromosomes 4, 9, 10, 11, 16, 22 and X.^[19]

Jena Rabintra *et al.* documented trisomy 11 as a frequently occurring chromosomal anomaly in the South Indian population.^[16] Jha *et al* found trisomy in 21.42% cases and polyploidy in 7.1% cases.^[20] Trisomy of chromosome 4 was also documented by Raimondi *et al.* and Nordgren *et al.*^[15,21] Trisomy 8 was also reported previously by Hrusák *et al.* and Bakshi *et al.*^[22,23] Genes

**Figure 2: Karyogram-47XXX, del 9p**

with possible significance in leukemogenesis located on chromosome 8 includes c-myc,^[24] on 8q24, c-mos,^[25] on 8q22, MOZ,^[26] on 8p11, and ETO on 8q22.^[27] Trisomy 8 could represent an alternative mechanism for increasing C-MYC gene dosage to achieve amplification of C-MYC oncogene.^[28] Stephen and Rowe reported trisomy 15 and according to them, it appears to occur most frequently in myelodysplasia.^[29] The combination of trisomy of chromosome 10 and trisomy of chromosome 17 predicted improved outcomes compared with either trisomy alone and particularly compared with the outcome of patients lacking both trisomies.^[18] Trisomy 18 was also reported in many previous studies such as Raimondi *et al.*, Malekasgar *et al.*,^[21,30] and Jackson *et al.* suggested that trisomy of chromosome 6 was a favorable risk factor for childhood ALL.^[31] A single case of gain of chromosome Y was noted in the present study, which was reported in past by Gibbons *et al.*^[32]

Conclusion

Numerical chromosomal abnormality in this study was 15.38% which was different from other populations described in previous studies. Hyperdiploidy was present in 35.90% of cases in the present study. Trisomy 21 is the most common (7.69% cases) trisomy in the present study. Gain of chromosome X and trisomy of chromosome 13.14 were observed in the present study, each with two cases. Gain of chromosome Y and trisomies of chromosomes 3, 4, 6, 8, 11, 15, 17, and 18 were noted in this study, each with one case. There was a random distribution of various chromosomal anomalies in different age groups and sex in the present study. The findings of the present study may be useful to pediatricians and physicians in predicting outcome, remission, survival, and treatment response in ALL.

Acknowledgments

Name	Role
Prof.A. K. Srivastava, Head of the Department of Anatomy	Inspiration and providing the necessary facilities during my study
Lt. Col Sandeep Kumar	My husband for giving me constant Support and encouragement
Mr. Arun Kumar	Laboratory technician of Genetic Laboratory

Financial support and sponsorship

Nil.

Conflicts of interest

There are no conflicts of interest.

References

- Vardiman JW, Harris NL, Brunning RD. The World Health Organization (WHO) classification of the myeloid neoplasms. *Blood* 2002;100:2292-302.
- Harrison CJ. The detection and significance of chromosomal abnormalities in childhood acute lymphoblastic leukaemia. *Blood Rev* 2001;15:49-59.
- Secker-Walker LM. Prognostic and biological importance of chromosome findings in acute lymphoblastic leukemia. *Cancer Genet Cytogenet* 1990;49:1-13.
- Oláh E, Balogh E, Kajtár P, Pajor L, Jakab Z, Kiss C. Diagnostic and prognostic significance of chromosome abnormalities in childhood acute lymphoblastic leukemia. *Ann N Y Acad Sci* 1997;824:8-27.
- Gadhia P, Parekh N, Chavda P, Bhatia G, Vaniawala S. Cytogenetics Findings Of Patients With Acute Lymphoblastic Leukemia In West Indian Region. *Int J Adv Res* 2018;6:63-570.
- Shikano T. Correlation of karyotype with clinical features in childhood acute lymphoblastic leukemia. *Hokkaido Igaku Zasshi* 1989;64:727-37.
- Raimondi SC, Pui CH, Head D, Behm F, Privitera E, Roberson PK, *et al.* Trisomy 21 as the sole acquired chromosomal abnormality in children with acute lymphoblastic leukemia. *Leukemia* 1992;6:171-5.
- Shalaby RH, Ashaat NA, El Wahab NA, El-Hamid MA, El Wakeel SH. Bcl-2 expression and chromosomal abnormalities in childhood acute lymphoblastic leukemia. *Acad J Cancer Res* 2010;3:34-43.
- Silva ML, Ornellas de Souza MH, Ribeiro RC, Land MG, Boulhosa de Azevedo AM, Vasconcelos F, *et al.* Cytogenetic analysis of 100 consecutive newly diagnosed cases of acute lymphoblastic leukemia in Rio de Janeiro. *Cancer Genet Cytogenet* 2002;137:85-90.
- Udayakumar AM, Bashir WA, Pathare AV, Wali YA, Zacharia M, Khan AA, *et al.* Cytogenetic profile of childhood acute lymphoblastic leukemia in Oman. *Arch Med Res* 2007;38:305-12.
- Pedersen-Bjergaard J, Rowley JD. The balanced and the unbalanced chromosome aberrations of acute myeloid leukemia may develop in different ways and may contribute differently to malignant transformation. *Blood* 1994;83:2780-6.
- Sato Y, Rowley JD. Chromosomal abnormalities in childhood haematologic malignant disease. In: Nathan DG, Orkin SH. (Eds), "Nathan and Oski's Haematology and Oncology of infancy and Childhood", 5th edition, Philadelphia:W.B. Saunders; 1998.
- Uckun FM, Kersey JH, Gajl-Peczalska KJ, Heerema NA, Provisor AJ, Haag D, *et al.* Heterogeneity of cultured leukemic lymphoid progenitor cells from B cell precursor acute lymphoblastic leukemia (ALL) patients. *J Clin Invest* 1987;80:639-46.
- Kaspers GJ, Smets LA, Pieters R, Van Zantwijk CH, Van Wering ER, Veerman AJ. Favorable prognosis of hyperdiploid common acute lymphoblastic leukemia may be explained by sensitivity to antimetabolites and other drugs: Results of an *in vitro* study. *Blood* 1995;85:751-6.
- Nordgren A, Farnebo F, Johansson B, Holmgren G, Forestier E, Larsson C, *et al.* Identification of numerical and structural chromosome aberrations in 15 high hyperdiploid childhood acute lymphoblastic leukemias using spectral karyotyping. *Eur J Haematol* 2001;66:297-304.
- Jena Rabindra K, Suresh Ch P, Sahu GR, Ray B, Swain K. Secondary chromosomal abnormalities in acute lymphoblastic leukemia. *Caryologia* 2002;55:349-55.
- Lo KC, Chalker J, Strehl S, Neat M, Smith O, Dastugue N, *et al.* Array comparative genome hybridization analysis of acute lymphoblastic leukaemia and acute megakaryoblastic leukaemia in patients with down syndrome. *Br J Haematol* 2008;142:934-45.
- Heerema NA, Sather HN, Sensel MG, Zhang T, Hutchinson RJ, Nachman JB, *et al.* Prognostic impact of trisomies of chromosomes 10, 17, and 5 among children with acute lymphoblastic leukemia and high hyperdiploidy (>50 chromosomes). *J Clin Oncol* 2000;18:1876-87.
- Reddy P, Shankar R, Koshy T, Radhakrishnan V, Ganesan P, Jayachandran PK, *et al.* Evaluation of cytogenetic abnormalities in patients with acute lymphoblastic leukemia. *Indian J Hematol Blood Transfus* 2019;35:640-8.
- Jha S, Kumar D, Kaul JM, Singh T, Dubey AP. Cytogenetic pattern profiling in cases of Acute Lymphoblastic Leukemia in pediatric age group. *Journal of the Anatomical Society of India* 2017;66:48-53.
- Raimondi SC, Pui CH, Hancock ML, Behm FG, Filatov L, Rivera GK. Heterogeneity of hyperdiploid (51-67) childhood acute lymphoblastic leukemia. *Leukemia* 1996;10:213-24.
- Hrusák O, Porwit-MacDonald A. Antigen expression patterns reflecting genotype of acute leukemias. *Leukemia* 2002;16:1233-58.
- Bakshi SR, Brahmabhatt MM, Trivedi PJ, Dalal EN, Patel DM, Purani SS, *et al.* Trisomy 8 in leukemia: A GCRI experience. *Indian J Hum Genet* 2012;18:106-8.
- Koskinen PJ, Alitalo K. Role of myc amplification and overexpression in cell growth, differentiation and death. *Semin Cancer Biol* 1993;4:3-12.
- Diaz MO, Le Beau MM, Rowley JD, Drabkin HA, Patterson D. The role of the c-mos gene in the 8:21 translocation in human acute myeloblastic leukemia. *Science* 1985;229:767-9.
- Borrow J, Stanton VP Jr., Andresen JM, Becher R, Behm FG, Chaganti RS, *et al.* The translocation t (8;16)(p11;p13) of acute myeloid leukaemia fuses a putative acetyltransferase to the CREB-binding protein. *Nat Genet* 1996;14:33-41.
- Wang J, Wang M, Liu JM. Transformation properties of the ETO gene, fusion partner in t (8:21) leukemias. *Cancer Res* 1997;57:2951-5.
- Jennings BA, Mills KI. c-myc locus amplification and the acquisition of trisomy 8 in the evolution of chronic myeloid leukaemia. *Leuk Res* 1998;22:899-903.
- Smith SR, Rowe D. Trisomy 15 in hematological malignancies: Six cases and review of the literature. *Cancer Genet Cytogenet*

- 1996;89:27-30.
30. Malekasgar AH, Pedram M, Eshaghousaini SK. Numerical chromosomal abnormalities in patients with acute lymphoblastic and myeloid leukemia in Iran. *Clin Med Diag* 2012;2:45-50.
 31. Jackson JF, Boyett J, Pullen J, Brock B, Patterson R, Land V, *et al.* Favorable prognosis associated with hyperdiploidy in children with acute lymphocytic leukemia correlates with extra chromosome 6. A pediatric oncology group study. *Cancer* 1990;66:1183-9.
 32. Gibbons B, MacCallum P, Watts E, Rohatiner AZ, Webb D, Katz FE, *et al.* Near haploid acute lymphoblastic leukemia: Seven new cases and a review of the literature. *Leukemia* 1991;5:738-43.

Anthropometric Parameters of Idiopathic Familial Short Stature Females and its Correlation with Height and Comparison with the Control Group

Abstract

Introduction: Familial Short stature is considered one of the most common causes of Short Stature along with the constitutional delay in growth and puberty (CDGP) from which it can easily be distinguish. The core parameters of anthropometry represent diagnostic criteria for obesity and other non-communicable diseases. To measure the anthropometric parameters in the patients with idiopathic clinically non-syndromic familial short-stature and to correlate those parameters with their height and compare them with the control group. **Material and Methods:** A cross-sectional study was conducted among Familial Short Stature females of 5-18 years age group referred from Paediatric and Genetic OPD of AIIMS, Rishkesh. Non-parametric tests were applied for comparing the variables and correlation coefficients were obtained. **Results:** There was a significant difference between the groups in terms of Standing Height (cm) ($W = 376.000, P = <0.001$), BMI (Kg/m²) ($W = 1128.500, P = 0.002$), with the median BMI (Kg/m²) and Waist/Height Ratio ($W = 1164.500, P = <0.001$), with the median Waist/Height Ratio being highest in the Short-Stature group. There was moderate to strong positive correlation between standing height and other anthropometric parameters. The mean waist to height ratio of 0.6 among short stature and 0.5 among the control group, with short stature having more odds of getting overweight and also shows a greater predilection of short-stature group for developing Cardio-vascular diseases. **Discussion and Conclusion:** Familial short stature though being a manifestation of some underlying cause, can fall in a non-syndromic group until further studies including karyotyping, next-generation sequencing etc. Extensive research for appropriate categorization and how this can effectively help combat the burden of malnutrition and non-communicable diseases should be done.

Keywords: Anthropometry, familial short stature, idiopathic short stature, standing height

Karishma Sharma¹,
Rishita Chandra^{2,3},
Brijendra Singh¹,
Shashi Ranjan
Mani Yadav⁴,
Manisha Naithani⁴,
Surekha Kishore⁵,
Vivek Mishra⁶,
Kriti Mohan⁷,
Prashant Kumar
Verma⁸

Departments of ¹Anatomy,
²MPH, ⁴Biochemistry,
³Paediatrics, All India Institute
of Medical Sciences, Rishikesh,
Departments ⁵Community and
Family Medicine, ⁶Anatomy,
⁷Paediatrics, AIIMS, Gorakhpur,
Uttarakhand, ³Project Manager-
MIS, PHRS Department
of Community and Family
Medicine, Odisha, India

Introduction

Short stature (SS) is defined as “a condition in which the height of an individual is 2 standard deviations (SDs) below the corresponding mean height of a given age, sex, and population group.”^[1] It can be a manifestation of some underlying conditions related to genetic or familial predisposition, endocrine disorders, skeletal dysplasia, malnutrition, and some chronic diseases.

Familial SS (FSS) is a condition in which the final adult height achieved is less than the third percentile for the patient’s age, gender, and population. It is considered one of the most common causes of SS along with the constitutional delay in growth and puberty (CDGP) from which it can easily be distinguished. A child presenting with SS two or more SDs below the mean

for age, gender, and population where no other causes can be found is deemed to have idiopathic SS (ISS). By adopting this definition, some authorities have included cases of FSS and CDGP as part of ISS. Hence, a category of familial ISS is distinguished from the nonfamilial ISS. On the other hand, others have listed it as a separate entity.

As per a study, about 5.6% of study participants were found to be of SS according to the Indian standard, i.e., below the fifth percentile of growth.^[2] Another study reported that 555 of 79,495 (0.7%) had SS, 75% of cases were FSS and CDGP, underlying organic disease 14%, while only 5% had endocrine causes.^[3]

A study from South India reported a prevalence rate of 2.86% in school-going children. The major reasons behind SS were genetics and constitutional delay in

Article Info

Received: 09 November 2021
Revised: 20 January 2022
Accepted: 31 July 2022
Available online: ***

Address for correspondence:

Dr. Prashant Kumar Verma,
Department of Paediatrics,
All India Institute of Medical
Sciences, Rishikesh - 249 203,
Uttarakhand, India.
E-mail: 2004pkv@gmail.com

Access this article online

Website: www.jasi.org.in

DOI:
10.4103/jasi.jasi_182_21

Quick Response Code:



How to cite this article: Sharma K, Chandra R, Singh B, Yadav SR, Naithani M, Kishore S, *et al.* Anthropometric parameters of idiopathic familial short stature females and its correlation with height and comparison with the control group. J Anat Soc India 2022;XX:XX-XX.

This is an open access journal, and articles are distributed under the terms of the Creative Commons Attribution-NonCommercial-ShareAlike 4.0 License, which allows others to remix, tweak, and build upon the work non-commercially, as long as appropriate credit is given and the new creations are licensed under the identical terms.

For reprints contact: WKHLRPMedknow_reprints@wolterskluwer.com

growth; only 6.69% of children were reported to have SS caused by malnutrition.^[4]

SS can appear as an isolated physical trait in an otherwise normal and healthy child, which we call “ISS.” Human height is a polygenic trait that can be inherited which is regulated by multilocus genes. FSS which is also known as genetic SS is the most common type of SS and needs to be explored more.

The core parameters of anthropometry are important because they represent diagnostic criteria for obesity, which significantly increases the risk for conditions such as cardiovascular disease, hypertension, diabetes mellitus, and many more. By measuring the height for age, weight for age, and weight for height, it can be determined if children are stunted, underweight, or wasted. Another anthropometric measurement useful to assess nutritional status in children is mid-upper arm circumference, which can be used to define the severity of malnutrition.^[5]

SS is one of the most common causes of referral to the department of pediatric endocrinology. SS not only affects the physique and appearance of an individual but is reported to have a psychological impact on children and their parents. A survey suggested that impaired height has a significant impact on the emotional and mental well-being of a child.^[6]

The accurate assessment of physical growth and development in children has attracted much attention from health-care providers and pediatricians. There is a lack of information in this domain. The topic is highly important, but the area is still unexplored, and more research need to be done. Hence, the current study aims to establish the correlation of height with arm span, waist circumference (WC), and waist-to-height ratio of females with FSS. There has not been any such study conducted as best of our knowledge. Hence, the result and inferences obtained would be helpful to find out mild dysmorphic syndrome for defining it as a variation or anomaly and can be a guiding light for many researchers in the same field.

Objectives

The objectives of this study were to measure the anthropometric parameters, e.g., height, arm span, WC, and waist-to-height ratio in patients with idiopathic clinically nonsyndromic familial SS and to correlate all the mentioned parameters with their height and to compare them with the control group.

Material and Methods

Study design

A cross-sectional study was conducted at All India Institute of Medical Sciences, Rishikesh, Uttarakhand, from February 2019 to May 2021.

Study participants

A total of 40 patients with FSS of the age group 5–18 years, referred from the Paediatric and Genetic Outpatient Department (OPD) of AIIMS, Rishikesh, were consecutively recruited in the study. Forty healthy females of the normal height of the same age group were enrolled in the study as controls. After a brief session of providing information related to the study, informed consent was obtained from both the groups.

Inclusion criteria for short stature

1. Females height below third centile according to WHO, comes in OPD from Uttarakhand.
2. FSS after checking midparental height/one of the parents identified as FSS.

Exclusion criteria for short stature

1. Height more than 2 SDs below the median (>3rd percentile) and age below 5 years above 18 years
2. External genitalia like male or ambiguous
3. Chronic protein energy malnutrition
4. Chronic disease (congenital heart disease and malabsorption)
5. Chronic steroid therapy (nephrotic syndrome, asthma, and atopic disease)
6. Skeletal dysplasia
7. Acquired causes of SS such as spine fracture, spinal tuberculosis, and limb fracture
8. Clinically diagnosed well-known syndrome with growth failure
9. SS well defined clinically isolated medical condition and responded with therapy (growth hormone and hypothyroidism)
10. Bone age mismatch to chronological age
11. Participants not willing to be part of the study

Data collection and analysis

The midparental height of the participants was taken to estimate their stature. Anthropometric parameters were recorded for each participant using digital weight machine, stadiometer, and flexible measuring tape.

The data were analyzed using SPSS v23 (IBM Corp) software. The Chi-square test was applied to find the association between variables. For the data that were not distributed normally, nonparametric tests were applied for comparing the variables of the SS and control groups. To establish the relation between standing height and other anthropometric parameters, correlation coefficients were obtained.

Results

A total of 40 females with idiopathic FSS and 40 healthy females as control of the age group 5–18 years were recruited for the study. The average age of the SS group

was reported to be 13.20 ± 3.88 and the control group was 12.35 ± 3.67 . The association between group and age was estimated for both the SS group and the control group. After applying the Chi-square test, it was estimated that there was no significant association between various age groups in terms of age ($\chi^2 = 0.258, P = 0.879$). In the SS group, 22.5% of the participants belonged to 5–9 years of age group with 35.0% from 10 to 14 years of age group,

and 42.5% belonged to 15–18 years. In Control group 22.5% of the participants were of age 5-9 years, 40.0% of 10-14 years and, 37.5% belonged to the age group of 15-18 years.

In Figure 1, the association between standing height and the age group is depicted for the SS and control groups. As the variable standing height (cm) was not distributed normally, nonparametric tests (Kruskal–Wallis test) were used to

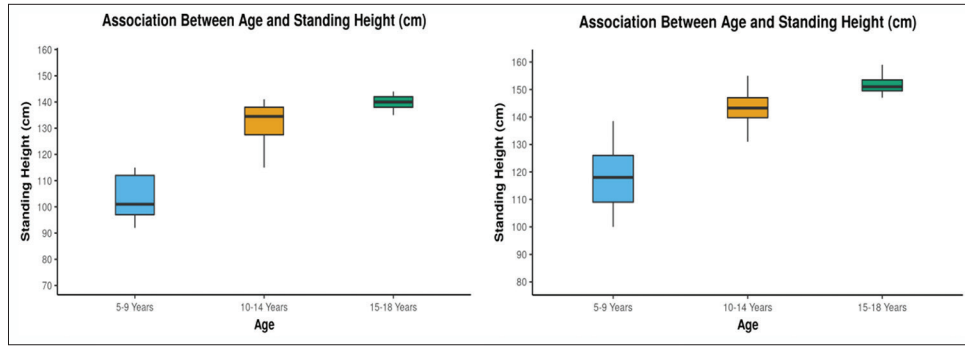


Figure 1: Association between age and standing height

Table 1: Comparison between standing height and other anthropometric measures among the short stature and control groups

Standing height (cm)	Group		Wilcoxon-Mann-Whitney <i>U</i> -test	
	Short stature	Control	<i>W</i>	<i>P</i>
Mean±SD	129.07±15.46	141.10±15.18	376.000	<0.001
Median (IQR)	135 (118.75-140)	145 (138.38-151.25)		
Range	92-144	100-159		
Weight (kg)	Group		<i>t</i> -test	
	Short stature	Control	<i>t</i>	<i>P</i>
Mean±SD	34.83±11.81	36.21±9.61	-0.575	0.567
Median (IQR)	35.5 (27.25-43.25)	38 (30-41.65)		
Range	12-63	15-60.9		
BMI (kg/m ²)	Group		Wilcoxon-Mann-Whitney <i>U</i> -test	
	Short stature	Control	<i>W</i>	<i>P</i>
Mean±SD	20.17±3.73	17.79±2.01	1128.500	0.002
Median (IQR)	19.2 (17.8-22.67)	17.63 (16.59-18.64)		
Range	14.18-30.81	14.49-24.09		
Arm span (cm)	Group		Wilcoxon-Mann-Whitney <i>U</i> -test	
	Short stature	Control	<i>W</i>	<i>P</i>
Mean±SD	132.90±16.68	138.70±14.34	615.000	0.076
Median (IQR)	138.5 (122.25-144.25)	143.5 (135-148.25)		
Range	90-153	104-154		
WC (cm)	Group		Wilcoxon-Mann-Whitney <i>U</i> -test	
	Short stature	Control	<i>W</i>	<i>P</i>
Mean±SD	74.12±15.29	74.40±12.74	830.000	0.776
Median (IQR)	80 (64-85)	75.5 (67.5-82.25)		
Range	19-100	23-98		
Waist/height ratio	Group		Wilcoxon-Mann-Whitney <i>U</i> -test	
	Short stature	Control	<i>W</i>	<i>P</i>
Mean±SD	0.57±0.08	0.53±0.07	1164.500	<0.001
Median (IQR)	0.58 (0.54-0.61)	0.53 (0.49-0.56)		
Range	0.21-0.7	0.2-0.7		

SD: Standard deviation, IQR: Interquartile range, BMI: Body mass index, WC: Waist circumference

make group comparisons. There was a significant difference between the groups in terms of standing height (cm) among the SS group ($\chi^2 = 27.033, P \leq 0.001$) and the control group ($\chi^2 = 25.645, P \leq 0.001$), with the median standing height (cm) being highest in 15–18 years of age group.

The comparison was established between the SS group and the control group for other anthropometric measures, e.g., standing height, weight, body mass index (BMI), arm span, WC, and waist/height ratio, as described in Table 1. For the variables that were not distributed normally, nonparametric test (Wilcoxon–Mann–Whitney *U*-test), and for normally distributed variables, parametric test (*t*-test) was used to make group comparisons. There was a significant difference between the two groups in terms of standing height (cm) ($W = 376.000, P \leq 0.001$), with the median standing height (cm) being highest in the control group; BMI (kg/m^2) ($W = 1128.500, P = 0.002$), with the median BMI (kg/m^2) being highest in the SS group; and waist/height ratio ($W = 1164.500, P \leq 0.001$), with the median waist/height ratio being highest in the SS group.

The BMI interpretation, as shown by the graph in Figure 2, suggested a significant difference as well ($\chi^2 = 4.021, P = 0.045$). Participants in the control group had a larger proportion of acceptable BMI as compared to the SS group that reflected a larger proportion of overweight BMI. The females of the SS group reported an odds of 3.41 to be overweight as compared to 0.29 odds of the control group to be overweight.

The correlation coefficients for both the groups, i.e., the SS group and the control group for the anthropometric measures of age, weight, BMI, arm span, WC, and waist-to-hip ratio with the standing height, were estimated and are depicted in Figure 3. Among the SS group and the control group, there was a strong positive correlation between age (years) and standing height (cm). This correlation was statistically significant for the SS group ($\rho = 0.85, P \leq 0.001$) and for the control group ($\rho = 0.82, P \leq 0.001$). For every 1 unit increase in age (years), the standing height (cm) increases by 3.71 units in the SS group, and in the control group, for every 1 unit increase in age (years),

the standing height (cm) increases by 3.65 units. There was a strong positive correlation between weight (kg) and standing height (cm), and this correlation was statistically significant ($\rho = 0.75, P \leq 0.001$) among the SS group, and for every 1 unit increase in weight (kg), the standing height (cm) increases by 1.13 units. Among the control group, there was a very strong positive correlation between weight (kg) and standing height (cm), and this correlation was statistically significant ($\rho = 0.9, P \leq 0.001$), and for every 1 unit increase in weight (kg), the standing height (cm) increases by 1.43 units.

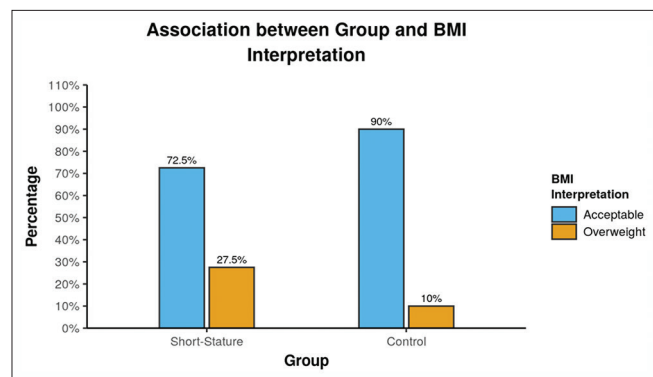


Figure 2: BMI interpretation among the short stature and control groups. BMI: Body index mass

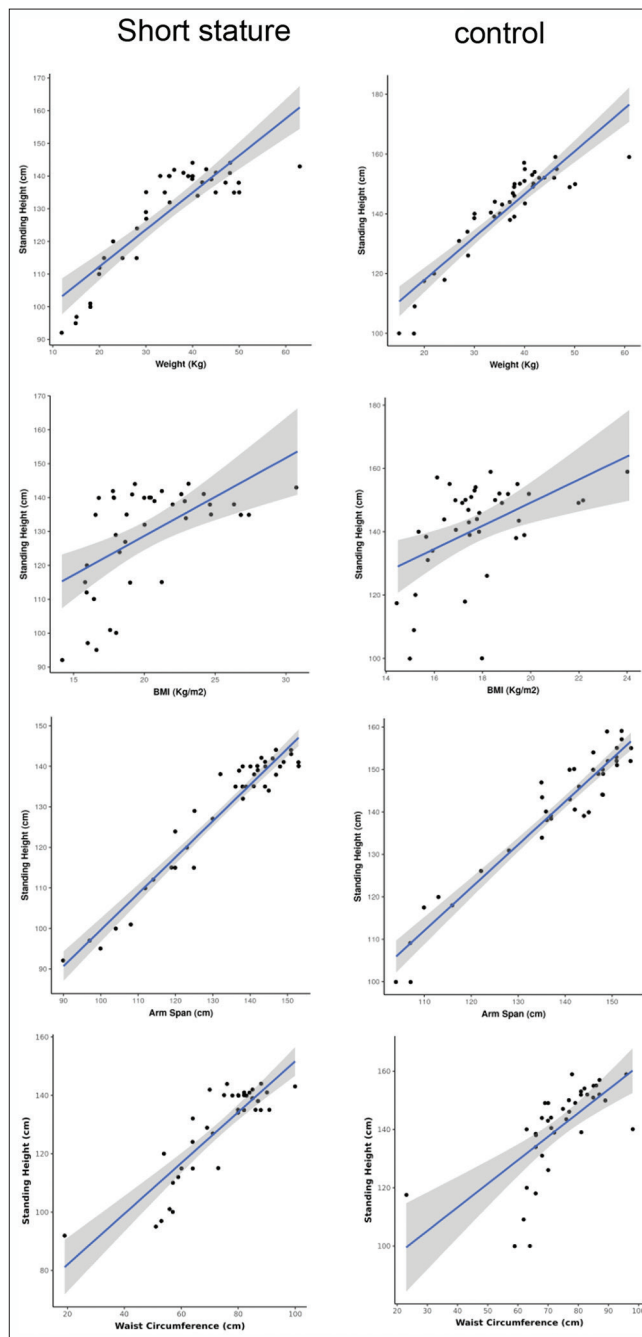


Figure 3: Correlation of anthropometric parameters with standing height among the SS and control groups. SS: Short stature, BMI: Body index mass

Short stature control

Among the SS group as well as the control group, there was a moderate positive correlation between BMI (kg/m²) and standing height (cm). This correlation was statistically significant ($\rho = 0.52$, $P \leq 0.001$), and for every 1 unit increase in BMI (kg/m²), the standing height (cm) increases by 2.30 units in the SS group, and among the control group ($\rho = 0.44$, $P = 0.004$), for every 1 unit increase in BMI (kg/m²), the standing height (cm) increases by 3.66 units.

There was a strong positive correlation between arm span (cm) and standing height (cm), among both the groups. Among the short-stature group, $\rho = 0.89$, $P = <0.001$ and among the control group $\rho = 0.9$, $P = <0.001$.

There was a strong positive correlation recorded between WC (cm) and standing height (cm) in both the groups. Among the SS group ($\rho = 0.71$, $P \leq 0.001$), for every 1 unit increase in WC (cm), the standing height (cm) increases by 0.87 units, and in the control group ($\rho = 0.81$, $P \leq 0.001$), for every 1 unit increase in WC (cm), the standing height (cm) increases by 0.81 units. There was a significant difference between the two groups in terms of waist/height ratio ($W = 1164.500$, $P \leq 0.001$), with the median waist/height ratio being highest in the SS group.

Discussion

Several studies have been conducted to estimate the growth pattern among children. The anthropometric parameters have been stated as one of the significant measures to assess the nutritional status of the children, with arm span being quoted by many studies. The standing height was correlated with sitting height, leg length, and arm wingspan,^[7] while other studies used knee height to estimate height.^[8] However, in all these studies, the variable that proved to be consistently reliable was the arm wing span. Similarly, in the present study, the correlation between arm wing span and height with $r = 0.89$ for SS and 0.9 for control, respectively, agreed with the study among biracial populations, where a correlation of 0.852 was recorded for Black population.^[9] However, the estimation equations obtained from this study differ from the one obtained for the present study, thereby justifying that the association between anthropometric measures differs in ethnic and racial groups. Even though several studies of this nature are available on Western populations, very limited data are available on Indian subjects.

The effectiveness of using various anthropometric parameters to predict an individual's height has been reported. The arm span was reported to be the most reliable parameter for predicting height.^[10,11]

However, exact height cannot be measured directly in the cases with deformities in lower limb, in individuals who

have undergone amputation of lower limbs or shortening due to fractures and bone decomposition. In these circumstances, an estimation of the height has to be done with the help of other anthropometric body parameters.^[12] The current study advocates that the diagnosis of FSS can also be done by estimating their anthropometric parameters to predict height.

BMI is an index for assessing under- or overnutrition in children, adolescents as well as adults. It is an indicator to evaluate general adiposity. Obesity in children is associated with chronic diseases in adulthood, such as heart disease, hyperlipidemia, hyperinsulinemia, hypertension, and atherosclerosis. However, the WC, which is a measure of central/abdominal obesity, has been found to have more risk related to cardiovascular diseases as compared to BMI.

To the best of our knowledge, this is one of the pioneer studies in the field of addressing familial SS female children and their comparison with healthy female children of the same age. The correlation between BMI and standing height in the present study was found to have a moderate positive relationship with $r = 0.52$ and 0.44, respectively, for the SS group and the control group. The moderate association of BMI with height as found in the present study is in alignment to the results found in several studies.^[13-15] The current study reported a larger proportion of overweight individuals among the SS group that justifies the positive correlation between BMI and height. The comparison made between the SS group and the control group for BMI and waist-to-height ratio reflected a significant difference in both the groups as per this current study similar to a study^[16] that reported a significant correlation between height and BMI.

Association of WC with risk factors such as diastolic blood pressure and insulin resistance has been reported.^[17] Waist-to-height ratio has been reported to be an alternative tool for assessing obesity in children.^[18,19]

The current study reported a strong positive relation between standing height and waist-to-height ratio in both the groups. Due to the role of the visceral fat depot in health risks associated with obesity, WC is also the preferred measurement in the context of population studies.^[20,21]

The Waist-to-height ratio (WHtR) is a newly developed index, proposed to be superior to the BMI, because of its relationship to cardiovascular risks, as a consequence of abdominal obesity. A study reported a 0.5 WHtR cutoff in both men and women and proposed a health initiative that WC does not exceed one-half of the height. Our study reflected a mean waist-to-height ratio of 0.6 among the SS group and 0.5 among the control group and shows a greater predilection of the SS group for developing cardiovascular diseases.^[22]

The current study reported that the females of the SS group reported an odds of 3.41 to be overweight as compared

to 0.29 odds of the control group to be overweight. Due to the unavailability of significant literature, as there have been minimal or no studies where an issue like FSS has been addressed extensively, many of the findings in the current study are one of a kind. The correlation coefficients between standing height and other anthropometric parameters showed a positive correlation in both the SS and control groups with a minor difference between their correlation coefficient, r . This might indicate that although the SS group is showing a strong prediction for obesity/overweight as reflected by BMI and waist-to-height ratio comparisons, the SS group may have other anthropometric measures as normal as the control group of the same age. To derive the more significant associations and patterns of relationship among the anthropometric parameters of SS individuals, more investigation and research are required. As FSS has a predilection toward getting cardiovascular diseases, so detailed knowledge of nutrition had to be given and parents should be educated about the risk of diseases associated with obesity and the importance to seek proper health care.

The current study advocates that genetic analysis plays a vital role in providing information on an individual's genotyping. There are many methods such as Barr body estimation, karyotyping, and *polymerase chain reaction* (PCR) to assess and evaluate the genomic cause of SS, developmental delay, genetic disorders, and intellectual disability. Therefore, extensive research for appropriate categorization of genetically syndromic and nonsyndromic FSS, importance of nutrition, and how this can effectively help combat the burden of malnutrition and noncommunicable diseases should be done.

Conclusion

The study is one of its kind in the domain of health that has not been extensively researched. FSS is a condition that is considered to have a genetic predisposition and might also curve into an idiopathic, nonsyndromic group. The study reported that SS female children have more odds of getting overweight/obese than the control group of healthy females of the same age. The anthropometric measures showed a positive correlation with standing height in both the groups with a significant difference in BMI and waist-to-height ratio. FSS, though being a manifestation of some underlying cause, can fall into a nonsyndromic group until further studies including karyotyping and next-generation sequencing.

Limitation of the study

The current study used a smaller sample size and is one of the novel research in the field, and the findings need to be validated by more research.

Recommendations

For assessing the cause of FSS and to curve it in the domain of genetic predisposition, more techniques need to be used, e.g., Sanger's sequencing and reverse transcription-quantitative PCR next-generation sequencing.

Financial support and sponsorship

Nil.

Conflicts of interest

There are no conflicts of interest.

References

1. Ranke MB. Towards a consensus on the definition of idiopathic short stature. *Horm Res* 1996;45 Suppl 2:64-6.
2. Colaco P, Desai M, Choksi CS. Short stature in Indian children: The extent of the problem. *Indian J Pediatr* 1991;58 Suppl 1:57-8.
3. Lindsay R, Feldkamp M, Harris D, Robertson J, Rallison M. Utah Growth Study: Growth standards and the prevalence of growth hormone deficiency. *J Pediatr* 1994;125:29-35.
4. Velayutham K, Selvan SS, Jeyabalaji RV, Balaji S. Prevalence and etiological profile of short stature among school children in a south Indian population. *Indian J Endocrinol Metab* 2017;21:820-2.
5. Casadei K, Kiel J. Anthropometric measurement. In: *StatPearls*. Treasure Island (FL): StatPearls Publishing; 2021. Available from: <https://pubmed.ncbi.nlm.nih.gov/30726000/>. [Last updated on 2021 Apr 25].
6. Cuttler L, Silvers JB, Singh J, Marrero U, Finkelstein B, Tannin G, *et al.* Short stature and growth hormone therapy. A national study of physician recommendation patterns. *JAMA* 1996;276:531-7.
7. Mitchell CO, Lipschitz DA. Arm length measurement as an alternative to height in nutritional assessment of elderly. *J Parenter Enteral Nutr* 2001;22:443-58.
8. Chumlea WC, Roche AE, Steinberg ML. Estimating stature from Knee – Height for persons 60 to 90 years of age. *J Am Geriatr Soc* 1985;33:116-20.
9. Steel MF, Chenier TC. Arm span, height and age in black and white women. *Ann Hum Biol* 1990;14:541-53.
10. Yun DJ, Yun DK, Chang YY, Lim SW, Lee MK, Kim SY. Correlation among height and arm span in growing Korean children. *Ann Hum Biol* 1995;22:443-58.
11. Jarzem PF, Gledhill RB. Predicting height from arm measurements. *J Pediatr Orthop* 1993;13:761-5.
12. Sarma A, Barman B, Das GC, Saikia H, Momin AD. Correlation between the arm-span and the standing height among males and females of the Khasi tribal population of Meghalaya state of North-Eastern India. *J Family Med Prim Care* 2020;9:6125-9.
13. Fung KP, Lee J, Lau SP, Chow OK, Wong TW, Davis DP. Properties and clinical implications of body mass indices. *Arch Dis Child* 1990;65:516-9.
14. Frankiln MF. Comparison of weight and height relations in boys from 4 countries. *Am J Clin Nutr* 1999;70:157S-62S.
15. Freedman DS, Thonton JC, Mei Z, Wang J, Dietz WH, Pierson RN Jr., *et al.* Height and adiposity among children. *Obes Res* 2004;12:846-53.
16. Santomauro F, Lorini C, Pieralli F, Niccolai G, Piccioli P, Vezzosi S, *et al.* Waist-to-height ratio and its associations with body mass index in a sample of Tuscan children in primary

- school. *Ital J Pediatr* 2017;43:53.
17. Maffeis C, Pietrobelli A, Grezzani A, Provera S, Tatò L. Waist circumference and cardiovascular risk factors in prepubertal children. *Obes Res* 2001;9:179-87.
 18. Sijtsma A, Bocca G, L'abée C, Liem ET, Sauer PJ, Corpeleijn E. Waist-to-height ratio, waist circumference and BMI as indicators of percentage fat mass and cardiometabolic risk factors in children aged 3-7 years. *Clin Nutr* 2014;33:311-5.
 19. Bacopoulou F, Efthymiou V, Landis G, Rentoumis A, Chrousos GP. Waist circumference, waist-to-hip ratio and waist-to-height ratio reference percentiles for abdominal obesity among Greek adolescents. *BMC Pediatr* 2015;15:50.
 20. Després JP, Lemieux S, Lamarche B, Prud'homme D, Moorjani S, Brun LD, *et al.* The insulin resistance-dyslipidemic syndrome: Contribution of visceral obesity and therapeutic implications. *Int J Obes Relat Metab Disord* 1995;19 Suppl 1:S76-86.
 21. Seidell JC, Bouchard C. Visceral fat in relation to health: Is it a major culprit or simply an innocent bystander? *Int J Obes Relat Metab Disord* 1997;21:626-31.
 22. Ashwell M, Browning L. The increasing importance of waist-to-height ratio to assess cardiometabolic risk: A plea for consistent terminology. *Open Obes J* 2011;3:70-7.

Evaluation of the Brain Indexes of Subjects with and without Brain Atrophy Using Computed Tomography

Abstract

Introduction: This study was undertaken to determine the values of brain indexes using computed tomography (CT) in our population. **Material and Methods:** This study was carried out on the 520 senior subjects (196 subjects having brain atrophy and 324 subjects having no brain atrophy) aged 60–90 years. Measurements of the brain indexes were taken from subjects having axial brain CT image in the radiology department. Furthermore, the data were analyzed according to age and gender. **Results:** The means and standard deviations of the measurements were as follows: the maximum distance between anterior horns, 37.35 ± 3.76 mm; minimum bicaudate nuclei distance, 20.76 ± 3.78 mm; maximum internal skull diameter, 135.66 ± 6.51 mm; maximum internal diameter of the frontal bone, 103.23 ± 6.23 ; internal skull diameter measured along the same line, 116.28 ± 6.60 mm; maximum external diameter of the skull, 144.08 ± 5.93 mm; and cella media width, 35.88 ± 6.93 mm; and the indices were calculated and found as follows: Huckman number, 58.11 ± 6.99 mm; bifrontal index, 0.36 ± 0.03 ; bicaudate frontal index, 0.55 ± 0.07 ; bicaudate index, 0.18 ± 0.03 ; bicaudate temporal index, 0.15 ± 0.03 ; and Schiersmann's index (SI), 4.22 ± 1.16 in subjects having brain atrophy. The same values were measured as 32.28 ± 3.19 mm; 15.32 ± 3.05 mm; 133.67 ± 6.71 mm; 102.05 ± 6.13 mm; 113.12 ± 6.04 mm; 141.14 ± 6.12 mm; 28.92 ± 5.79 mm; 47.59 ± 5.63 mm; 0.32 ± 0.03 ; 0.47 ± 0.08 ; 0.14 ± 0.03 ; 0.11 ± 0.02 ; and 5.09 ± 1.13 in healthy elderly subjects, respectively. There was a significant difference in all measurements (except SI) ($P < 0.05$). **Discussion and Conclusion:** The brain index dimensions of Turkish population provide important and useful knowledge for the clinicians in terms of comparison of abnormalities and atrophy of the brain.

Keywords: Brain atrophy, brain indexes, computed tomography, effects of aging on brain, morphometry

**Mahmut Öksüzler,
Sema Polat¹,
Mahmut Tunç¹,
Duygu Vurallı¹,
Pinar Göker¹**

Department of Radiology, Adana Medline Hospital, ¹Department of Anatomy, Faculty of Medicine, Cukurova University, Adana, Turkey

Introduction

As subjects get older, their brain gradually declines and some changes that are associated with normal aging could be seen at all levels from molecules to morphology. It is generally observed that normal brain aging defines the changes in the structure and function of the brain without clinically important impairments. Aging leads to reduction in brain size or volume, weight vasculature, cognition, enlargement of the brain ventricles, hormones, and neurotransmitters. Moreover, cognitive impairment is one of the typical finding for aging in the structure and function of the brain. Furthermore, the reason of the changes may show as nerve cell loss that is loss of synapses and dendritic pruning in the brain with increasing age in certain brain regions.^[1-3] The hippocampus and

frontal lobes are most vulnerable brain regions. Especially, in subjects over the age of 60 years, there is a reduction in brain volume and the weight. The increase in ventricular volume and cerebrospinal fluid spaces follow loss in the brain volume. In addition, according to 90 years, compared to last 30 years, the volume losses are 14% in the cerebral cortex, 35% in the hippocampus, and 26% cerebral white matter.^[1,4,5] However, there is a decrease with age at a rate of around 5%/decade after the age of 40 years with the actual rate of decline possibly increasing with age, particularly over the age of 70 years.^[3]

The number of subjects aged 60 years and above is expected to more than double by 2050 and 3.1 billion in 2100 (962 million in 2017, 2.1 billion in 2050, and 3.1 billion in 2100). Furthermore, the number of people aged 80 years or over was 137

This is an open access journal, and articles are distributed under the terms of the Creative Commons Attribution-NonCommercial-ShareAlike 4.0 License, which allows others to remix, tweak, and build upon the work non-commercially, as long as appropriate credit is given and the new creations are licensed under the identical terms.

For reprints contact: WKHLRPMedknow_reprints@wolterskluwer.com

How to cite this article: Öksüzler M, Polat S, Tunç M, Vurallı D, Göker P. Evaluation of the brain indexes of subjects with and without brain atrophy using computed tomography. J Anat Soc India 2022;XX:XX-XX.

Article Info

Received: 26 January 2022

Accepted: 16 August 2022

Available online: ***

Address for correspondence:

Dr. Mahmut Tunç,
Department of Anatomy,
Faculty of Medicine, Cukurova
University, Adana 01330,
Turkey.
E-mail: fzt.mtunc@gmail.com

Access this article online

Website: www.jasi.org.in

DOI:
10.4103/jasi.jasi_20_22

Quick Response Code:



million and this is estimated to be rising from 425 million in 2050 to 909 million in 2100. Furthermore, the number of subjects aged 100 years or over is expected to reach more than 25 million.^[2]

Imaging techniques such as computed tomography (CT) and magnetic resonance imaging (MRI) provide an assessment opportunity of intracranial structures.^[6-9] These different imaging modalities show the brain anatomy and pathological changes. Some studies have reported that MRI is more suitable for examination and has become possible to achieve reliable and accurate neuroanatomical views and critical detailed knowledge about brain related with normal brain aging or in neuromuscular diseases,^[7,10-15] whereas some studies have declared that CT scan is useful for the evaluation of brain morphology such as the size and shape of the ventricular system and affordable method for brain imaging.^[15,16] The CT is able to visualize changes in size and shape of the intracranial fluid spaces and the linear ratio measurements can also be studied on CT easily.^[15-20]

To our knowledge, this is the first study considering the indexes of the brain using CT in detail to investigate age and gender differences in Turkish healthy subjects and subjects having brain atrophy aged 60 years and above. Therefore, the purpose of this study was to document the mean values of brain indexes in healthy and brain atrophy subjects in our 60–90 years people and to present the reference values for our population.

Material and Methods

This study was carried out on 520 subjects (333 males and 287 females; 196 subjects having brain atrophy and 324 healthy subjects) aged 60–90 years. This study was a retrospective observational study performed in the department of radiology. All CT scans were obtained using a 64 × 2-slice multidetector CT (Siemens Somatom Definition AS, Siemens Healthcare). The axial brain CT image was used. Exclusion criteria were as follows: genetic disorders, intraventricular or subarachnoid hemorrhage, a history of head trauma, or central nervous system infection. Healthy adult subjects with optimal health criteria and subjects with brain atrophy according to presence of atrophy in CT images were included in this study group. The assessment of the brain CT images were determined by the experienced radiologist (MO) and the brain atrophy according to normal aging was determined as the presence of dilatations in all cortical sulcus, cisterna, fissura, and ventricular system that included the subarachnoid space. This study was approved by the Institutional Review Ethics Committee at Çukurova University (2020/105-36).

The measurements were made on the computer screen with an electronic caliper and estimations were expressed as millimeters and some specified linear measurements on the selected transverse sections were performed as following: the maximum distance between anterior horns (AH),

minimum bicaudate nuclei distance (BCN), maximum internal skull diameter (MISD), maximum internal diameter of frontal bone (FBMID), internal skull diameter along the same line (MISD_{SL}), maximum external diameter of the skull (MESD), and cella media width (CMW).^[2,15,21,22] From these measurements, the brain indexes were calculated as follows:

- Huckman number (HN): Sum of the maximum distance between AH and minimum BCN distance^[2,15]
- Bifrontal index (BFI): Maximum distance between AH divided by FBMID^[15]
- Bicaudate frontal index (BCFI-ventricular index): Minimum BCN distance divided by maximum distance between AH^[15]
- Bicaudate index (BCI): Minimum BCN distance divided by MISD_{SL}^[15]
- Bicaudate temporal index (BCTI): Minimum BCN distance divided by MISD^[15,21]
- Schiersmann's index (SI): MESD divided by CMW.^[2,15,21]

All the measurements are shown in Figures 1 and 2.

The data were divided into two groups as healthy elderly subjects without brain atrophy and elderly subjects having brain atrophy, and the data were also analyzed according to gender in both the groups [Tables 1 and 2]. Furthermore, the subjects were divided into five age groups to establish reference values of both healthy adult subjects and subjects with brain atrophy and the decade method was used. The age groups were as follows: Subjects aged between 60

Table 1: Evaluation of the brain indexes' parameters in all subjects

Measurements	P	Mean±SD	
		Subjects with brain atrophy (196)	Healthy adult subjects (324)
AH	<0.001	37.35±3.76	32.28±3.19
BCN	<0.001	20.76±3.78	15.32±3.05
MISD	0.001	135.66±6.51	133.67±6.71
FBMID	0.036	103.23±6.23	102.05±6.13
MISD _{SL}	<0.001	116.28±6.60	113.12±6.04
MESD	<0.001	144.08±5.93	141.14±6.12
CMW	<0.001	35.88±6.93	28.92±5.79
HN	<0.001	58.11±6.99	47.59±5.63
BFI	<0.001	0.3624±0.0353	0.3166±0.0283
BCFI	<0.001	0.5540±0.0724	0.4737±0.0767
BCI	<0.001	0.1787±0.0315	0.1353±0.0253
BCTI	<0.001	0.1530±0.0266	0.1146±0.0224
SI	<0.001	4.2187±1.1587	5.0910±1.1273

AH: The maximum distance between anterior horns, BCN: Minimum bicaudate nuclei distance, MISD: Maximum internal skull diameter, FBMID: Maximum internal diameter of frontal bone, MISD_{SL}: Internal skull diameter measured along the same line, MESD: Maximum external skull diameter, CMW: Cella media width, BCFI: Bicaudate frontal index, BCTI: Bicaudate temporal index, SI: Schiersmann's index, BCI: Bicaudate index, BFI: Bifrontal index, HN: Huckman number, SD: Standard deviation (In linear measurements: mm)

and 64 years determined as decade 1, 65 and 69 years determined as decade 2, 70 and 74 years determined as decade 3, 75 and 79 years determined as decade 4, and 80 and over years determined as decade 5 [Tables 3 and 4].

Statistical analysis

The statistical analysis was done using IBM SPSS Statistics for Windows, Version 21.0. Armonk, NY: IBM Corp. (2012) (SPSS version 21.0) was used for statistical analysis of the measurement results. From these measurements, means, standard deviations (SD), minimum (min.), and maximum (max.) values were calculated. In all statistical analyses, *P* value under 0.05 was considered statistically significant. In addition, Kolmogorov–Smirnov test to analyze the sample with a reference probability distribution was used. For normal distribution and variance homogeneity among the age groups, the parametric ANOVA test was used. For nonnormal distribution, the nonparametric Mann–Whitney *U*-test was used.

Results

The linear measurements of brain indexes in coronal CT images were shown in Figures 1 and 2. In addition, CT images of subjects with brain atrophy and those not having atrophy are given in Figure 3. The evaluation of the brain indexes' parameters in both groups is shown in Table 1. The means and SDs of the AH, BCN, MISD, FBMID, MISD_{SL}, MESD, CMW, HN, BFI, BCFI, BCI, BCTI, and SI were as 37.35 ± 3.76 mm, 20.76 ± 3.78 mm, 135.66 ± 6.51 mm, 103.23 ± 6.23 mm, 116.28 ± 6.60 mm, 144.08 ± 5.93 mm, 35.88 ± 6.93 mm, 58.11 ± 6.99 mm, 0.36 ± 0.03 , 0.55 ± 0.07 , 0.18 ± 0.03 , 0.15 ± 0.03 , and 4.22 ± 1.16 in subjects having brain atrophy, respectively. The same values were measured as 32.28 ± 3.19 mm, 15.32 ± 3.05 mm, 133.67 ± 6.71 mm, 102.05 ± 6.13 mm, 113.12 ± 6.04 mm, 141.14 ± 6.12 mm, 28.92 ± 5.79 mm, 47.59 ± 5.63 mm, 0.32 ± 0.03 , 0.47 ± 0.08 , 0.14 ± 0.03 , 0.11 ± 0.02 , and 5.09 ± 1.13 in healthy elderly subjects, respectively [Table 1]. There were significant differences in all measurements and these parameters were higher in subjects having brain atrophy than healthy elderly subjects (except SI).

The data according to gender in both groups are given in Table 2. In addition, there was a significant difference in AH, BCN, MISD, FBMID, MISD_{SL}, MESD, CMW, and HN, whereas BFI, BCI, BCTI, and SI showed no difference in subjects having brain atrophy. Moreover, the significant difference was found in all parameters according to the gender [Table 2]. Age-related changes of the brain index parameters from decade 1 to decades 5 in both the groups are shown in Tables 3-6.

Discussion

There are number of reasons for measuring the dimensions of the brain and one of that is brain atrophy. For analyzing the brain atrophy, few imaging methods are used such as

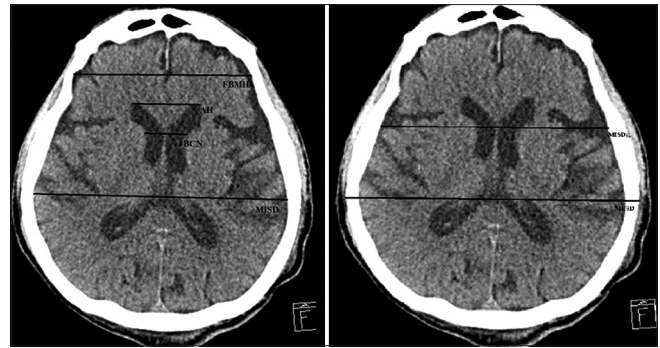


Figure 1: Evaluation of linear measurements on CT images. AH: Anterior horns, BCN: Bicaudate nuclei distance, MISD: Maximum internal skull diameter, FBMID: Maximum internal diameter of frontal bone, MISD_{SL}: Maximum internal skull diameter along the same line, MESD: Maximum external skull diameter, CT: Computed tomography



Figure 2: Evaluation of linear measurements on CT images. CT: Computed tomography, CMW: Cella media width

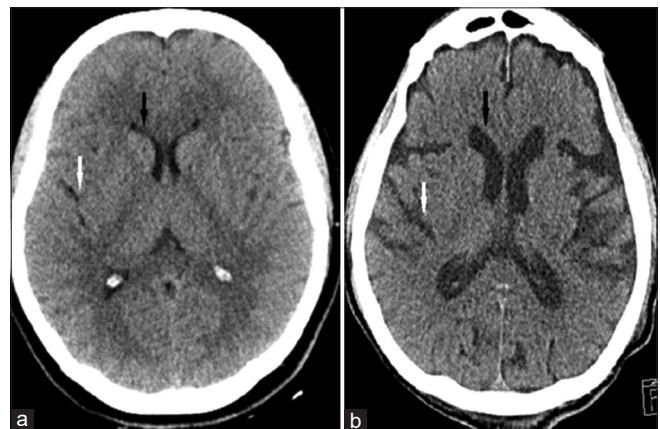


Figure 3: CT images of subjects with brain atrophy and those not having atrophy. (a) The lateral ventricles (black arrow) and cerebral sulci (white arrow) are observed in normal width in healthy adult subjects. (b) The lateral ventricles (black arrow) and cerebral sulci (white arrow) are enlarged in subjects with brain atrophy. CT: Computed tomography

CT, MRI, and ultrasonography. CT is especially useful for the evaluation of brain morphology, including the size and shape of the ventricular system.^[15,22] In the present study,

Table 2: The mean values of the brain index measurements in two groups according to gender (n=520; 333 males, 287 females)

Measurements	Gender	Subjects with brain atrophy (196)			Healthy adult subjects (324)			P (significant level P between groups)
		Mean±SD	Minimum	Maximum	Mean±SD	Minimum	Maximum	
AH	Males	38.18±3.73	30.50	47.00	33.67±3.15	25.80	44.90	<0.001
	Females	36.11±3.47	31.30	45.30	31.51±2.96	20.40	39.30	<0.001
P value for gender		<0.001			<0.001			-
BCN	Males	21.40±3.64	11.80	29.10	16.45±3.08	8.20	29.60	<0.001
	Females	19.78±3.79	12.00	29.60	14.69±2.86	8.00	29.60	<0.001
P value for gender		0.030			<0.001			-
MISD	Males	137.90±5.51	113.50	155.70	137.22±6.89	110.30	151.00	0.478
	Females	132.27±6.48	107.00	147.00	131.71±5.74	116.00	149.70	0.406
P value for gender		<0.001			<0.001			-
FBMID	Males	105.08±5.41	90.00	124.40	104.90±5.50	93.00	119.40	0.931
	Females	100.42±6.38	89.40	120.00	100.49±5.90	75.00	136.50	0.802
P value for gender		<0.001			<0.001			-
MISD _{SL}	Males	118.49±5.73	100.60	134.20	116.20±5.63	103.30	131.00	0.054
	Females	112.92±6.43	101.00	128.30	111.43±5.58	96.00	141.60	0.002
P value for gender		<0.001			<0.001			-
MESD	Males	145.35±5.38	133.10	159.50	143.36±6.90	115.40	159.40	0.002
	Females	142.17±6.24	131.00	154.10	139.92±5.27	122.00	159.60	0.015
P value for gender		<0.001			<0.001			-
CMW	Males	36.75±6.68	19.70	47.50	30.57±5.55	18.00	45.00	<0.001
	Females	34.55±7.12	11.30	48.50	28.02±5.72	14.20	48.70	<0.001
P value for gender		0.029			<0.001			-
HN	Males	59.58±6.88	46.20	76.10	50.12±5.65	37.80	68.40	<0.001
	Females	55.90±6.59	44.00	71.00	46.21±5.12	34.70	63.00	<0.001
P value for gender		<0.001			<0.001			-
BFI	Males	0.3641±0.039	0.27	0.47	0.3210±0.025	0.26	0.40	<0.001
	Females	0.3600±0.0298	0.30	0.42	0.3141±0.030	0.20	0.39	<0.001
P value for gender		0.425			0.037			-
BCFI	Males	0.5591±0.0667	0.34	0.74	0.4874±0.071	0.28	0.76	<0.001
	Females	0.5464±0.0800	0.32	0.74	0.4662±0.079	0.30	0.75	<0.001
P value for gender		0.230			0.017			-
BCI	Males	0.1811±0.0320	0.09	0.26	0.1414±0.024	0.07	0.23	<0.001
	Females	0.1750±0.0306	0.11	0.25	0.1319±0.025	0.07	0.23	<0.001
P value for gender		0.189			0.001			-
BCTI	Males	0.1553±0.0260	0.08	0.22	0.1200±0.0218	0.06	0.21	<0.001
	Females	0.1495±0.0274	0.09	0.23	0.1117±0.0222	0.07	0.19	<0.001
P value for gender		0.137			0.001			-
SI	Males	4.1242±0.9972	3.01	7.68	4.853±0.9663	3.10	8.06	<0.001
	Females	4.3618±1.3619	2.77	12.48	5.222±1.1886	2.78	9.73	<0.001
P value for gender		0.160			0.005			-

AH: The maximum distance between anterior horns, BCN: Minimum bicaudate nuclei distance, MISD: Maximum internal skull diameter, FBMID: Maximum internal diameter of frontal bone, MISD_{SL}: Internal skull diameter measured along the same line, MESD: Maximum external skull diameter, CMW: Cella media width, HN: Huckman number, BFI: Bifrontal index, BCFI: Bicaudate frontal index, BCI: Bicaudate index, BCTI: Bicaudate temporal index, SI: Schiersmann's index, SD: Standard deviation (In linear measurements: mm)

the brain indexes were estimated for determining the reference data of these indexes in our elderly population who had brain atrophy and not have atrophy using CT. Furthermore, we demonstrated that in both the groups (who had atrophy or no atrophy), the mean values of Huckman number, BFI, bicaudate frontal index, and BCI were found as increased due to age. Conversely, SI values

were decreased. In addition, these values were clearly shown that there were significant differences by gender. All the values were found greater in males than females except SI' values in our population.

In autopsy and MR studies, it was reported that at a gross level, there was a decrease in brain volume and weight in individuals over the age of 60 years.^[22] Furthermore, it was

Table 3: Age related changes of the brain index parameters in healthy elderly subjects

Measurements	P	Decade 1 (60-64 years; n=136)	Decade 2 (65-69 years; n=162)	Decade 3 (70-74 years; n=102)	Decade 4 (75-79 years; n=80)	Decade 5 (80 years or over; n=40)
AH	0.068	32.08±3.39 (20.40-40.90)	32.15±2.91 (25.20-39.40)	33.54±3.63 (27.00-44.90)	31.66±2.75 (26.10-36.10)	32.49±2.48 (29.90-36.90)
BCN	0.196	14.92±3.10 (8.20-25.00)	15.29±2.98 (9.70-29.60)	16.06±3.14 (8.00-22.60)	15.97±2.53 (12.20-21.20)	15.15±3.95 (11.00-21.00)
MISD	0.004	134.25±6.40 (116.00-151.00)	134.70±6.92 (110.30-150.00)	131.44±6.91 (118.20-145.10)	132.15±5.10 (122.70-142.40)	129.23±7.16 (118.00-137.80)
FBMID	0.019	102.50±5.54 (90.00-119.40)	102.57±5.72 (85.90-116.00)	100.88±6.77 (75.00-117.10)	101.93±8.45 (88.70-136.50)	96.63±3.81 (92.50-102.00)
MISD _{SL}	0.034	113.54±5.75 (99.30-127.30)	113.76±6.08 (101.00-131.00)	112.20±6.20 (96.00-123.80)	111.92±6.87 (105.10-141.60)	108.59±3.02 (105.30-113.80)
MESD	0.599	141.18±6.13 (122.00-159.00)	141.66±6.49 (115.40-159.40)	140.07±7.14 (127.00-156.30)	140.33±4.26 (132.70-149.90)	141.45±3.40 (137.00-147.50)
CMW	0.001	27.70±6.52 (14.20-45.00)	28.72±5.29 (16.70-41.70)	31.97±4.40 (23.80-43.50)	30.06±5.17 (20.80-48.70)	29.04±4.89 (24.00-36.90)
HN	0.135	46.99±5.80 (34.70-63.00)	47.44±5.32 (37.60-68.40)	49.60±6.36 (35.00-67.30)	47.63±4.36 (40.00-54.40)	47.65±6.14 (42.00-59.50)
BFI	<0.001	0.3129±0.0284 (0.20-0.38)	0.3137±0.0252 (0.24-0.39)	0.3326±0.0293 (0.28-0.40)	0.3116±0.0290 (0.25-0.37)	0.3367±0.0277 (0.30-0.39)
BCFI	0.130	0.4649±0.826 (0.28-0.75)	0.4745±0.072 (0.30-0.76)	0.4765±0.067 (0.30-0.61)	0.5057±0.073 (0.35-0.65)	0.4622±0.093 (0.35-0.62)
BCI	0.032	0.1312±0.026 (0.07-0.23)	0.1342±0.023 (0.09- 0.23)	0.1430±0.026 (0.07-0.20)	0.1429±0.022 (0.11-0.19)	0.1398±0.037 (0.10-0.20)
BCTI	0.030	0.1112±0.023 (0.06-0.19)	0.1135±0.021 (0.07-0.21)	0.1221±0.023 (0.07-0.17)	0.1210±0.020 (0.09-0.16)	0.1178±0.032 (0.08-0.17)
SI	<0.001	5.3977±1.375 (3.23-9.73)	5.1049±0.994 (3.10-8.34)	4.4547±0.584 (3.36-5.81)	4.7869±0.750 (2.78-6.53)	4.9967±0.834 (3.91-6.04)

AH: The maximum distance between anterior horns, BCN: Minimum bicaudate nuclei distance, MISD: Maximum internal skull diameter, FBMID: Maximum internal diameter of frontal bone, MISD_{SL}: Internal skull diameter measured along the same line, MESD: Maximum external skull diameter, CMW: Cella media width, HN: Huckman number, BFI: Bifrontal index, BCFI: Bicaudate frontal index, BCI: Bicaudate index, BCTI: Bicaudate temporal index, SI: Schiersmann's index (In linear measurements: mm)

established that there was a 10% loss of neurons in the human cerebral cortex with improved stereology method.^[23]

Huckman index known as sum of the maximum distance between AH and minimum BCN distance is a most important parameter to evaluate the diameter of the anterior ventricular horn.^[15] In a study performed by Wilk *et al.* including 507 subjects the HN were calculated as 4.001 ± 0.750 cm in subjects aged between 0 and 12 months, whereas the same parameter was 4.389 ± 0.438 cm in subjects aged between 15 and 18 years.^[15] Furthermore, this value was reported as 57.9 ± 9.64 mm in 70–79 years old and as 60.69 ± 8.53 mm in 70 and 99 years old Polish population with brain atrophy.^[2] Whereas, this value was established 54.60 ± 6.90 mm in over 65 years aged healthy Swedish population and 58.75 ± 8.04 mm patients with Alzheimer's disease in Swedish population.^[24] When we analyzed our Huckman value, it was found between 46.99 and 47.65 mm in 60 and 90 years aged healthy people and between 54.39 and 59.40 mm in subjects with brain atrophy in the same ages. Our results show similarity to Polish population than Swedish population.

BCI is a well-established method and used to assess the size of the intracranial ventricular system.^[25-27] This method

is reliable This method is both reliable about determining the normal pattern of enlargement from rostral to occipital horns of the lateral ventricles and according to a rostral-caudal sequence of ventricular dilatation and practical marker of ventricular volume. Also, this parameter is used to evaluation of ventriculomegaly, Huntington's chorea, cerebral atrophy, and multiple sclerosis.^[16,27] A study performed by Kukuljan *et al.* evaluated the BCI; it was reported that age was positively correlated with BCI.^[27] Some researchers using CT have documented a progressive increase in ventricular size and subarachnoid space volume with normal aging. Furthermore, it was found that from seventh to the ninth decade ventricular size increases.^[17,28] In a study including Indian healthy population, it was reported that the mean value of BCI was between 0.14–0.16 and 60–90 years age. The same index was found to be 0.13 in healthy and 0.14 in brain atrophy group in Swedish population.^[16,24] Our values of healthy group are closer to Swedens in healthy group but our values of subjects with brain atrophy values are higher than both Indians and Swedens.^[16,24]

For analyzing the ventricular size, in this paper, the mean SI was found to be 4.97 in subjects aged 60 years with brain

Table 4: Age related changes of brain index measurements in subjects with brain atrophy

Measurements	P	Decade 1 (60-64 years; n=17)	Decade 2 (65-69 years; n=42)	Decade 3 (70-74 years; n=58)	Decade 4 (75-79 years; n=50)	Decade 5 (80 years or over; n=29)
AH	0.038	35.87±3.43 (20.40-43.00)	36.79±3.87 (25.20-45.30)	38.52±3.64 (27.00-44.90)	36.89±3.51 (26.10-47.00)	37.51±3.99 (29.90-45.60)
BCN	0.022	18.52±3.67 (8.20-25.00)	20.05±4.35 (9.70-29.60)	21.31±3.44 (8.00-28.70)	20.82±3.00 (12.20-29.10)	21.89±4.29 (11.00-29.60)
MISD	0.267	137.80±8.62 (113.50-155.70)	136.03±7.31 (107.00-150.00)	136.34±6.17 (118.20-145.60)	134.30±5.74 (122.70-144.00)	134.88±5.65 (118.00-148.20)
FBMID	0.002	106.25±6.31 (90.00-124.40)	105.24±6.46 (85.90-120.00)	103.60±6.02 (75.00-117.10)	101.34±5.41 (88.70-136.50)	101.05±6.22 (91.00-115.00)
MISD _{SL}	<0.001	120.66±5.46 (99.30-134.20)	116.93±6.60 (100.60-131.00)	117.79±6.15 (96.00-131.20)	113.56±6.42 (101.00-141.60)	114.40±6.24 (105.00-122.80)
MESD	0.005	147.11±5.75 (122.00-159.00)	143.81±5.19 (115.40-159.50)	145.62±6.60 (127.00-156.30)	142.20±4.97 (132.70-155.00)	142.86±6.00 (131.00-153.30)
CMW	0.002	32.01±8.33 (19.70-43.00)	33.58±8.52 (19.20-48.20)	38.07±5.60 (22.00-48.50)	36.48±5.83 (11.30-47.00)	36.05±6.09 (25.20-47.50)
HN	0.026	54.39±6.57 (46.20-66.00)	56.84±7.39 (44.00-71.00)	59.83±6.62 (46.40-73.10)	57.71±6.16 (50.20-76.10)	59.40±7.79 (49.00-74.40)
BFI	<0.001	0.3381±0.0321 (0.28-0.41)	0.3504±0.0383 (0.27-0.47)	0.3721±0.0311 (0.30-0.43)	0.3643±0.0319 (0.29-0.45)	0.3716±0.0365 (0.32-0.46)
BCFI	0.025	0.5141±0.0778 (0.34-0.62)	0.5433±0.0940 (0.32-0.74)	0.5518±0.0607 (0.45-0.68)	0.5637±0.0506 (0.44-0.69)	0.5807±0.0778 (0.48-0.74)
BCI	0.001	0.1540±0.0317 (0.09-0.19)	0.1715±0.0372 (0.11-0.26)	0.1812±0.029 (0.13-0.24)	0.1833±0.0235 (0.16-0.25)	0.1905±0.0313 (0.15-0.25)
BCTI	0.006	0.1355±0.0309 (0.08-0.19)	0.1469±0.0279 (0.09-0.20)	0.1563±0.0238 (0.11-0.21)	0.1548±0.0196 (0.13-0.22)	0.1623±0.0317 (0.12-0.23)
SI	0.002	4.9719±1.5645 (3.58-7.68)	4.6010±1.3312 (2.99-7.45)	3.9171±0.7094 (2.77-6.87)	4.0772±1.3176 (3.04-8.48)	4.0707±0.6962 (3.01-5.82)

AH: The maximum distance between anterior horns, BCN: Minimum bicaudate nuclei distance, MISD: Maximum internal skull diameter, FBMID: Maximum internal diameter of frontal bone, MISD_{SL}: Internal skull diameter measured along the same line, MESD: Maximum external skull diameter, CMW: Cella media width, HN: Huckman number, BFI: Bifrontal index, BCFI: Bicaudate frontal index, BCI: Bicaudate index, BCTI: Bicaudate temporal index, SI: Schiersmann's index (In linear measurements: mm)

Table 5: The *post hoc* test results by age groups in healthy elderly subjects

Measurements	AH	BCN	MISD	FBMID	MISD _{SL}	MESD	CMW	HN	BFI	BCFI	BCI	BCTI	SI
Decade 1-Decade 2	0.855	0.342	0.602	0.924	0.774	0.546	0.164	0.535	0.842	0.331	0.361	0.413	0.039
Decade 1-Decade 3	0.009	0.035	0.016	0.131	0.205	0.306	<0.001	0.009	<0.001	0.388	0.008	0.006	<0.001
Decade 1-Decade 4	0.520	0.091	0.120	0.649	0.186	0.495	<0.042	0.578	0.816	0.009	0.023	0.031	0.006
Decade 1-Decade 5	0.677	0.806	0.016	0.002	0.009	0.891	0.454	0.712	0.006	0.911	0.277	0.344	0.244
Decade 2-Decade 3	0.014	0.155	0.005	0.113	0.139	0.142	0.001	0.030	0.001	0.881	0.046	0.029	0.001
Decade 2-Decade 4	0.447	0.275	0.060	0.606	0.132	0.287	0.247	0.870	0.719	0.046	0.088	0.099	0.154
Decade 2-Decade 5	0.732	0.884	0.009	0.002	0.006	0.911	0.859	0.909	0.008	0.609	0.476	0.541	0.753
Decade 3-Decade 4	0.013	0.905	0.647	0.462	0.844	0.861	0.155	0.139	0.001	0.107	0.986	0.837	0.199
Decade 3-Decade 5	0.328	0.379	0.320	0.038	0.074	0.507	0.125	0.302	0.661	0.578	0.703	0.566	0.141
Decade 4-Decade 5	0.456	0.446	0.209	0.013	0.115	0.605	0.608	0.994	0.010	0.107	0.724	0.681	0.585

AH: The maximum distance between anterior horns, BCN: Minimum bicaudate nuclei distance, MISD: Maximum internal skull diameter, FBMID: Maximum internal diameter of frontal bone, MISD_{SL}: Internal skull diameter measured along the same line, MESD: Maximum external skull diameter, CMW: Cella media width, HN: Huckman number, BFI: Bifrontal index, BCFI: Bicaudate frontal index, BCI: Bicaudate index, BCTI: Bicaudate temporal index, SI: Schiersmann's index (In linear measurements: mm)

atrophy subjects whereas the same index was found lower in subjects aged 80 years of the same group. According to findings in the literature, this index was reported as 5.32 in 70 years and 4.23 in 80 years aged Poland people.^[2] Moreover, Goldstein *et al.* found this value as 0.259 in centerians and 0.255 in subjects aged between 61 and 77

years, respectively. Meanwhile, Chrzan *et al.* presented the new data with using the Goldstein's value: 1/0.259 (3.86) and 1/0.255 (3.92).^[2,17] In addition, the ventricular index values of the present study were from 0.51–0.58 to 60–90 years aged people with brain atrophy. Based on the results of our study, there was a significant difference

Table 6: The *post hoc* test results by age groups in subjects with brain atrophy

Measurements	AH	BCN	MISD	FBMID	MISD _{sl}	MESD	CMW	HN	BFI	BCFI	BCI	BCTI	SI
Decade 1-Decade 2	0.389	0.151	0.345	0.560	0.040	0.048	0.414	0.215	0.210	0.154	0.046	0.129	0.250
Decade 1-Decade 3	0.010	0.007	0.416	0.112	0.099	0.351	0.001	0.004	0.002	0.056	0.001	0.004	0.001
Decade 1-Decade 4	0.329	0.028	0.056	0.004	<0.001	0.003	0.018	0.086	0.051	0.014	0.001	0.009	0.005
Decade 1-Decade 5	0.148	0.003	0.142	0.005	0.001	0.017	0.050	0.018	0.010	0.002	<0.001	0.001	0.009
Decade 2-Decade 3	0.022	0.095	0.814	0.181	0.499	0.122	0.001	0.033	0.002	0.558	0.117	0.076	0.003
Decade 2-Decade 4	0.889	0.322	0.203	0.002	0.011	0.185	0.040	0.546	0.051	0.173	0.066	0.145	0.026
Decade 2-Decade 5	0.419	0.042	0.462	0.004	0.096	0.496	0.129	0.124	0.010	0.031	0.010	0.015	0.051
Decade 3-Decade 4	0.023	0.495	0.104	0.54	0.001	0.002	0.220	0.110	0.235	0.387	0.724	0.306	0.459
Decade 3-Decade 5	0.230	0.495	0.322	0.064	0.018	0.036	0.186	0.780	0.941	0.076	0.179	0.772	0.547
Decade 4-Decade 5	0.470	0.220	0.702	0.836	0.569	0.627	0.784	0.293	0.362	0.307	0.308	0.217	0.980

AH: The maximum distance between anterior horns, BCN: Minimum bicaudate nuclei distance, MISD: Maximum internal skull diameter, FBMID: Maximum internal diameter of frontal bone, MISD_{sl}: Internal skull diameter measured along the same line, MESD: Maximum external skull diameter, CMW: Cella media width, HN: Huckman number, BFI: Bifrontal index, BCFI: Bicaudate frontal index, BCI: Bicaudate index, BCTI: Bicaudate temporal index, SI: Schiersmann's index (In linear measurements: mm)

in all measurements and these parameters were higher in subjects having brain atrophy than healthy elderly subjects (except SI).

As a result, when we analyzed the observations obtained in this study, most of the mean brain index values are shown an increase due to age, (except SI values). The SI values are shown to decrease due to age. Moreover, according to gender, in all data means (except SI), it is seen that male's values are greater than females'. Finally, the mean values of all measurements are found higher in subjects with brain atrophy than healthy elderly group.

Conclusion

We think that the data presented in this study have provided the mean values of brain indices to evaluate the brain atrophy due to age and gender and they can be used both in terms of comparison of abnormalities and brain atrophy and, as reference values of brain indexes for our elderly population.

Financial support and sponsorship

Nil.

Conflicts of interest

There are no conflicts of interest.

References

- Anderton BH. Ageing of the brain. *Mech Ageing Dev* 2002;123:811-7.
- Chrzan R, Gleń A, Bryll A, Urbanik A. Computed tomography assessment of brain atrophy in centenarians. *Int J Environ Res Public Health* 2019;16:3659.
- Peters R. Ageing and the brain. *Postgrad Med J* 2006;82:84-8.
- Esiri MM, Hyman BT, Beyreuther K, Masters CL. Ageing and dementia. In: Graham D, Lantos PL, editors. *Greenfield's Neuropathology*. London: Arnold; 1997. p. 153-233.
- Jernigan TL, Archibald SL, Fennema-Notestine C, Gamst AC, Stout JC, Bonner J, *et al.* Effects of age on tissues and regions of the cerebrum and cerebellum. *Neurobiol Aging* 2001;22:581-94.
- Alper F, Kantarci M, Altunkaynak E, Varoglu AO, Karaman A, Oral E, *et al.* Quantitative magnetic resonance imaging of brainstem volumes, plaques, and surface area in the occipital regions of patients with multiple sclerosis. *Acta Radiol* 2006;47:413-8.
- Antar V, Turk O, Katar S, Ozden M, Sahin B, Yuceli S, *et al.* Morphometric assesment of the external anatomy of fourth ventricle and dorsal brainstem in fresh cadavers. *Turk Neurosurg* 2019;29:445-50.
- Blatter DD, Bigler ED, Gale SD, Johnson SC, Anderson CV, Burnett BM, *et al.* MR-based brain and cerebrospinal fluid measurement after traumatic brain injury: Correlation with neuropsychological outcome. *AJNR Am J Neuroradiol* 1997;18:1-10.
- Polat SÖ, Öksüzler FY, Öksüzler M, Yücel AH. The morphometric measurement of the brain stem in Turkish healthy subjects according to age and sex. *Folia Morphol (Warsz)* 2020;79:36-45.
- Doraiswamy PM, Patterson L, Na C, Husain MM, Boyko O, McDonald WM, *et al.* Bicaudate index on magnetic resonance imaging: Effects of normal aging. *J Geriatr Psychiatry Neurol* 1994;7:13-7.
- Gama RL, Távora DF, Bomfim RC, Silva CE, Bruin VM, Bruin PF. Morphometry MRI in the differential diagnosis of parkinsonian syndromes. *Arq Neuropsiquiatr* 2010;68:333-8.
- Lee NJ, Park IS, Koh I, Jung TW, Rhyu IJ. No volume difference of medulla oblongata between young and old Korean people. *Brain Res* 2009;1276:77-82.
- Raininko R, Autti T, Vanhanen SL, Ylikoski A, Erkinjuntti T, Santavuori P. The normal brain stem from infancy to old age. A morphometric MRI study. *Neuroradiology* 1994;36:364-8.
- Raz N, Gunning-Dixon F, Head D, Williamson A, Acker JD. Age and sex differences in the cerebellum and the ventral pons: A prospective MR study of healthy adults. *AJNR Am J Neuroradiol* 2001;22:1161-7.
- Wilk R, Kluczevska E, Syc B, Bajor G. Normative values for selected linear indices of the intracranial fluid spaces based on CT images of the head in children. *Pol J Radiol* 2011;76:16-25.
- Dhok A, Gupta P, Shaikh ST. Evaluation of the Evan's and Bicaudate Index for rural population in central India using computed tomography. *Asian J Neurosurg* 2020;15:94-7.
- Goldstein SJ, Wekstein DR, Kirkpatrick C, Lee C, Markesbery WR. Imaging the centenarian brain. A computed tomographic study. *J Am Geriatr Soc* 1985;33:579-84.

18. Naidich TP, Epstein F, Lin JP, Kricheff II, Hochwald GM. Evaluation of pediatric hydrocephalus by computed tomography. *Radiology* 1976;119:337-45.
19. Prassopoulos P, Cavouras D. CT evaluation of normal CSF spaces in children: Relationship to age, gender and cranial size. *Eur J Radiol* 1994;18:22-5.
20. Silverwood RJ, Cole TJ. Statistical methods for constructing gestational age-related reference intervals and centile charts for fetal size. *Ultrasound Obstet Gynecol* 2007;29:6-13.
21. Meese W, Kluge W, Grumme T, Hopfenmüller W. CT evaluation of the CSF spaces of healthy persons. *Neuroradiology* 1980;19:131-6.
22. Ragan L, Waczulikova I, Guller L, Bilicky J, Benuska J. Cella media distance in human brain in relation to age and gender. *Biomed Pap Med Fac Univ Palacky Olomouc Czech Repub* 2009;153:307-13.
23. Pakkenberg B, Boesen J, Albeck M, Gjerris F. Unbiased and efficient estimation of total ventricular volume of the brain obtained from CT-scans by a stereological method. *Neuroradiology* 1989;31:413-7.
24. Zhang Y, Londos E, Minthon L, Wattmo C, Liu H, Aspelin P, *et al.* Usefulness of computed tomography linear measurements in diagnosing Alzheimer's disease. *Acta Radiol* 2008;49:91-7.
25. van Gijn J, Hijdra A, Wijdicks EF, Vermeulen M, van Crevel H. Acute hydrocephalus after aneurysmal subarachnoid hemorrhage. *J Neurosurg* 1985;63:355-62.
26. Vassilouthis J, Richardson AE. Ventricular dilatation and communicating hydrocephalus following spontaneous subarachnoid hemorrhage. *J Neurosurg* 1979;51:341-51.
27. Kukuljan M, Kolic Z, Bonifacic D, Vukas D, Miletic D. Normal bicaudate index by aging. *Curr Med Imaging Rev* 2009;5:72-4.
28. Barron SA, Jacobs L, Kinkel WR. Changes in size of normal lateral ventricles during aging determined by computerized tomography. *Neurology* 1976;26:1011-3.

Ambiguity of the Radiographs around the Elbow Joint: Anatomical Variant versus Degenerative Changes

Abstract

Introduction: Interpretation of traumatological radiographs of the region of the elbow joint may come with many challenges. Aside from traumatological avulsions and fractures, we can also identify other entities such as persistent epiphysis, aseptic necrosis, osteochondritis dissecans, calcific bursitis, synovial chondromatosis, and other degenerative changes. It is also necessary for all these pathological conditions to be differentiated from the anatomical variants. **Material and Methods:** We performed a retrospective analysis of patients admitted to our clinic between 2010 and 2020 for arthroscopic treatment of chronic elbow joint stiffness. We evaluated the radiographs of their elbow joints for the presence of accessory ossification. If present, these cases were then sorted by previously defined criteria into groups according to the kind of anatomical variant and degenerative changes. On the basis of these data, we performed a statistical analysis. **Results:** We analyzed 39 limbs in 39 patients (12 women and 27 men). The average age was 40.9 years (span 16–74). The exclusion criteria did not exclude any patient. Accessory ossifications were present in 78.4% (29/37) of patients, and all three criteria for accessory bone were fulfilled by two patients. **Discussion and Conclusion:** This sample of patients suffering from joint stiffness due to degenerative changes around the elbow joint enabled us to prove the usefulness of the criteria for differentiating degenerative changes from accessory bones. We were also able to validate the hypothesis that in a sample of patients suffering from elbow stiffness, the dominant cause of the stiffness should be the degenerative changes, while the accessory bones prevalence should not differ significantly from their prevalence in the healthy population. Our analysis showed that the seemingly ovoid intra-articular loose bodies do not appear on the radiographs as regularly shaped and can be differentiated from accessory bones. In order to avoid the wrong interpretation of elbow radiographs, it is necessary to be aware of this issue. Our study validates the three previously defined criteria as means to diagnose accessory bones with a high specificity. The intra-articular loose bodies macroscopically seemed ovoid and regular. Nevertheless, they do not appear as regularly shaped on radiographs and do not, therefore, fulfill the criteria of accessory bones.

Keywords: *Accessory ossicles, degenerative changes, Elbow joint*

Introduction

To interpret elbow joint radiographs is a challenging task. We must be able to determine whether the patient suffers from skeletal trauma or other pathological disorders such as persistent epiphysis, aseptic necrosis, osteochondritis dissecans, calcifying bursitis, and synovial chondromatosis or whether the issue is caused by the degenerative changes that may be present. Several anatomical variants, especially accessory bones, might be misinterpreted as pathological or traumatic conditions. As those variants are usually presented unilaterally, the contralateral X-ray is not helpful, which

makes the correct diagnosis potentially challenging for many clinicians.^[1] Some of the accessory bones might be symptomatic and need surgical treatment.^[2]

Accessory bones around the elbow joint are a rare entity compared to the accessory bones of the hand and foot, and the literature on this topic is scarce with issues still unsolved.^[1,3-5] Contrary to the term pathological ossification, the term “accessory (variable, variant, and supernumerary) bone (ossicle)” is reserved for a congenital anatomical structure. In our previous study, we proposed a nomenclature based on the older classifications of Wood and Campbell,^[6] Obermann and Loose,^[7] and Schwarz.^[8] This terminological classification based on 2413 radiographs of

This is an open access journal, and articles are distributed under the terms of the Creative Commons Attribution-NonCommercial-ShareAlike 4.0 License, which allows others to remix, tweak, and build upon the work non-commercially, as long as appropriate credit is given and the new creations are licensed under the identical terms.

For reprints contact: WKHLRPMedknow_reprints@wolterskluwer.com

How to cite this article: Kunc V, Kunc V, Kuncova K, Kachlik D, Kopp L. Ambiguity of the radiographs around the elbow joint: Anatomical variant versus degenerative changes. *J Anat Soc India* 2022;XX:XX-XX.

Vojtech Kunc^{1,2},
Vladimir Kunc³,
Katerina Kuncova²,
David Kachlik²,
Lubomir Kopp^{1,2}

¹Clinic of Traumatology, Masaryk Hospital, Ústí Nad Labem, ²Department of Anatomy, Second Faculty of Medicine, Charles University, Prague 5, ³Department of Computer Science, Faculty of Electrical Engineering, Czech Technical University, Prague 2, Czech Republic

Article Info

Received: 24 April 2021
Revised: 06 April 2022
Accepted: 16 August 2022
Available online: ***

Address for correspondence:

Dr. Vojtech Kunc,
Department of Anatomy, Second Faculty of Medicine, Charles University, V Úvalu 84, 150 06, Prague 5, Czech Republic.
E-mail: vjpkunc@gmail.com

Access this article online

Website: www.jasi.org.in

DOI:
10.4103/jasi.jasi_80_21

Quick Response Code:



elbow joints distinguishes six types of accessory bones of the elbow [Figure 1].^[1]

This study aimed to verify the efficiency of the previously described criteria for the radiographic evaluation of the accessory bones on a sample of patients with chronic elbow disorders caused by assumed ossification of a pathologic origin. For the confirmation of the previously defined criteria, we presume that the prevalence of accessory bones in our current sample will be similar to the prevalence in the healthy sample used for our previous work. Therefore, if the previously defined criteria enable the differentiation of the degenerative changes (pathological ossification) from the variable accessory bones, the latter would occur with similar prevalence in patients with chronic elbow disorders as in healthy patients. All elbows were visualized arthroscopically (as a part of the treatment of elbow joint stiffness).

Material and Methods

We carried out a retrospective analysis of patients admitted to our department for the arthroscopic treatment of elbow joint stiffness from 2010 to 2021. All patients fulfilled our indication criteria for the arthroscopic visualization of the elbow joint (posttraumatic mild-to-severe intrinsic elbow joint stiffness without any improvement on receiving physiotherapy treatment). Exclusion criteria were defined as: (1) incomplete radiographs (only single projection), (2) radiographs in the cast or (3) radiographs containing osteosynthesis material, (4) incomplete surgical protocol, (5) patient's disagreement with his/her inclusion in this study, and (6) degenerative changes of Grade 3 or 4 according to Kellgren–Lawrence classification: an example

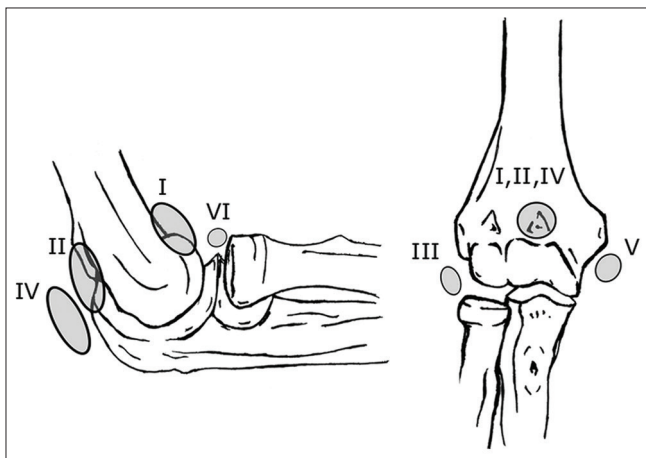


Figure 1: Type I and II refer to intra-articular bones. Type I is situated ventrally in the coronoid fossa (*os supratrochleare anterius*), type II is situated dorsally in the olecranon fossa (*os supratrochleare posterius*). Type III and V (*os subepicondylare mediale* and *subepicondylare laterale*) are sesamoid bones in the common origin of flexor muscles under the medial epicondyle and in the common origin of extensor muscles under the lateral condyle, respectively. Type IV and VI (*os sesamoideum tricipitale* and *os sesamoideum brachiale*) are also sesamoid bones in the tendons of corresponding muscles. Existence of so-called “*patella cubiti*” is still not clear and this entity is considered the synonym to the *os sesamoideum tricipitale* in this classification^[1]

shown in Figure 2.^[9] This study was done in accordance with the ethical standards stated by the Helsinki Declaration of 1975, as revised in 2000.

Overall, we analyzed 39 limbs in 39 patients of central European origin, from which 30.8% (12/39) were women and 69.2% were men. There were more procedures performed on the right extremity (59% – 23/39) than on the left (41% – 16/39). Two patients with severe degenerative changes met our exclusion criteria. Patients' age ranged from 16 to 74 years (average 40.9, median 39, and standard deviation 14.87).

We collected the following data from the documentation: the age of the patient during the procedure, side, date of the procedure, description of the accessory body in the joint (if present), and previous surgeries performed on the analyzed elbow that had taken place before the arthroscopic procedure. Subsequently, we analyzed the elbow X-ray in anteroposterior and lateral projections on the Phillips 227E monitor with a resolution of 1920 × 1080 px in the basic settings.

We used the criteria defined in our previous study for the identification of accessory bones: (I) a regular ovoid shape, (II) smooth margins, and (III) a regular ratio of cortical to cancellous bone along its circumference. If all the criteria were fulfilled and therefore the finding was considered an accessory bone, we used the previously defined classification based on the position of the bone to identify which category it belongs [Figure 1].

We used the Fisher's exact test to compare the observed prevalence of accessory bones with the prevalence described in our previous study. The same test was used to check if the fulfillment of criteria I-III had any connection to sex or the side of the procedure. To assess the relationship between the presence of an accessory bone in our sample and the patient's age, we used logistic regression and Kendall's correlation (variant b). The



Figure 2: Pathological ossification do not fulfill the criteria for accessory bones

presence of an accessory bone was coded as value 1 and its absence as value 0. In the case of logistic regression, we tested if the presented coefficient differed significantly from zero in a model with a constant term included. In the case of Kendall's correlation, we tested if the correlation coefficient differed significantly from zero. The statistical analysis was concluded in the Python 3.8 language with the use of SciPy version 1.2.1 library.^[10]

Results

Accessory ossification (before the application of any exclusion criterion) was present in 78.4% of the (29/37) cases. Of these cases, criterion I was fulfilled by 27.6% (8/29), criterion II by 17.2% (5/29), and criterion III by 6.9% (2/29). Overall, 10.3% (3/29) of the ossification cases met one of the criteria, 10.3% (3/29) of the cases fulfilled two of the criteria, and 6.9% (2/29) of the cases fulfilled all the three criteria. According to the mentioned criteria, the congenital accessory bones were present in two out of 29 patients.

As the first step, we analyzed if there was a statistically significant difference between the prevalence of the accessory bones in the current sample compared to the previous study. In the current sample, 2 out of 29 patients (6.9%) had accessory bones, whereas in the previous study, it was 15 out of 1940 (0.77%). The difference was shown to be statistically significant by Fisher's exact test ($P = 0.025$). However, one *os supratrochleare anterius* was present in this sample, while the previous study has not reported any case in this category of the accessory bone. The patient in question came to us due to the symptoms resulting from the presence of this bone, making our sample biased by its occurrence as it was no coincidence. The observation of the *os supratrochleare anterius*, therefore, did not come from a random sample of the population, and we cannot include it when assessing its prevalence in the overall population. After the exclusion of this finding, the Fisher's exact test did not show a statistically significant difference among the studies ($P = 0.21$).

The presence of accessory ossification (both congenital and pathological) did not have any statistically significant relationship to the patient's age. The coefficient for age neither significantly differ from zero in logistic regression ($P = 0.182$), nor does Kendall's correlation significantly differ from zero ($P = 0.184$).

As a sanity check, we analyzed if any criterion showed any correlation with age, gender, or the side of the procedure. This analysis did not show any significant relationship [Table 1].

Discussion

All the three criteria for accessory bone identification were fulfilled in 6.9% (2/29) of patients, and those cases were,

therefore, considered congenital or due to the trauma in early childhood. Pathological posttraumatic degenerative accessory ossifications were distributed equally in the sample (78.4%) without any relation to gender or side. The criteria for accessory bone identification were not in relation to any of the collected parameters (age, gender, and side). If they were of a degenerative or posttraumatic origin, it would be more probable that there would be such a relation.

Two of the observed accessory bones were classified as *os subepicondylare mediale* (type V) and *os supratrochleare anterius* (type I). The first is the most commonly occurring accessory bone of the elbow in the Central European population (0.46%) [Figure 3]. The latter is an interesting case, as it was not present in the sample of 2413 elbows in our previous study.^[1] The previous literature describes only rare cases of it.^[2] It is very probable that its' presence was symptomatic and had brought the patient to the hospital.

Os sesamoideum tricipitale and *os supratrochleare posterius* are also rare symptomatic accessory bones. They were not present in our sample, and 18 cases^[2,8,11,12] and 36 cases^[1,13,14] were described in the previous literature, respectively.

If we did not exclude patients with severe degenerative changes, we would incorrectly add one *os sesamoideum*



Figure 3: *Os subepicondylare mediale* is the most common accessory bone around the elbow joint

Table 1: P value of each test used for a statistical significance analysis of relation between the criteria and each of the followed parameters in our sample

	Criteria I	Criteria II	Criteria III	Method
Gender	1	0.62	1	Fisher's exact test
Side of the procedure	0.25	0.63	1	Fisher's exact test
Age	0.6	0.69	0.85	Logistic regression
Age	0.58	0.69	0.92	Kendall's correlation

brachiale and one accessory bone around the tip of the olecranon (no such bone is described in our previous classification). Therefore, we conclude that our criteria for accessory bones differentiation are not helpful in degenerative elbows of higher than grade 3 severity according to Kellgren–Lawrence classification. For such differentiation, a fourth criterion based on the length-to-width ratio might be helpful, as no other accessory bone in the human body is extensively long and narrow. Unfortunately, it is impossible to define such a criterion based merely on two cases.

Even though the comparison of 6.9% prevalence in this study to 0.77% in the previous study might seem like a reason to question the previous criteria, we conclude that these data for reasons stated above do not contradict our previous work. The symptoms are usually described as pain and stiffness.^[2,15] Cases of an accessory bone fracture have also been described in the literature.^[7,16]

It is incredibly difficult to diagnose the accessory bones in children, as there is not enough information in the previous literature about such cases, except for “*patella cubiti*” (type VI).^[17-19] In a detailed analysis of ossification centers presented by Silberstein et al., there is neither a description of the accessory ossification centers nor a description of the accessory bones.^[20-24] It is, therefore, reasonable to hypothesize that the ossification of the accessory bones occurs at a later age.

Our arthroscopic examination showed that pathological ossifications are visually also ovoid-shaped and regularly shaped. Nevertheless, this shape is made up of tissues other than bone as the X-ray image is irregular. Therefore, arthroscopic differentiation of these entities is not possible, and imaging (or histology) is the golden diagnostic standard.

Conclusion

This study showed that all the three diagnostic criteria for accessory bone differentiation can be used in the elbow region with a high specificity in all cases except for the joints suffering from severe degenerative changes.

Financial support and sponsorship

Nil.

Conflicts of interest

There are no conflicts of interest.

References

- Kunc V, Kunc V, Černý V, Polovinčák M, Kachlík D. Accessory bones of the elbow: Prevalence, localization and modified classification. *J Anat* 2020;237:618-22.
- Mittal R, Sampath Kumar V, Gupta T. Patella cubiti: A case report and literature review. *Arch Orthop Trauma Surg* 2014;134:467-71.
- Amar E, Rozenblat Y, Chechik O. Sesamoid and accessory bones of the hand – An epidemiologic survey in a Mediterranean population. *Clin Anat* 2011;24:183-7.
- Coskun N, Yuksel M, Cevener M, Arican RY, Ozdemir H, Bircan O, et al. Incidence of accessory ossicles and sesamoid bones in the feet: A radiographic study of the Turkish subjects. *Surg Radiol Anat* 2009;31:19-24.
- Koo BS, Song Y, Lee S, Sung YK, Sung IH, Jun JB. Prevalence and distribution of sesamoid bones and accessory ossicles of the foot as determined by digital tomosynthesis. *Clin Anat* 2017;30:1072-6.
- Wood VE, Campbell GS. The supratrochleare dorsale accessory ossicle in the elbow. *J Shoulder Elbow Surg* 1994;3:395-8.
- Obermann WR, Loose HW. The os supratrochleare dorsale: A normal variant that may cause symptoms. *AJR Am J Roentgenol* 1983;141:123-7.
- Schwarz GS. Bilateral antecubital ossicles (fabellae cubiti) and other rare accessory bones of the elbow. *Radiology* 1957;69:730-4.
- Kellgren JH, Lawrence JS. Radiological assessment of osteo-arthritis. *Ann Rheum Dis* 1957;16:494-502.
- Virtanen P, Gommers R, Oliphant TE, Haberland M, Reddy T, Cournapeau D, et al. SciPy 1.0: Fundamental algorithms for scientific computing in Python. *Nat Methods* 2020;17:261-72.
- Habbe JB. Patella cubiti: A report of four cases. *Am J Roentgenol* 1942;48:513-26.
- Kjelland PM. A rare anomaly in the elbow; patella cubiti. *Acta Radiol* 1945;26:491-6.
- Canamero B, Ángeles M, Giraldo S, Alberto W, Rivera G, Ignacio J, et al. Os supratrochleare dorsale del codo. *Acta Rheumatol* 2014;1:25-8.
- Gudmundsen TE, Ostensen H. Accessory ossicles in the elbow. *Acta Orthop Scand* 1987;58:130-2.
- Ahlgren SA, Rydholm A. Patella cubiti. Report of an operated case. *Acta Orthop Scand* 1975;46:931-3.
- Behnke E, Home K. Fractured os supratrochleare dorsale: A case report of elbow pain in a young person with a history of remote trauma. *Am J Roentgenol* 2011;196:A58-52.
- Burge P, Benson M. Bilateral congenital pseudarthrosis of the olecranon. *J Bone Joint Surg Br* 1987;69:460-2.
- Kattan KR, Babcock DS. Case report 105. Bilateral patella cubiti. *Skeletal Radiol* 1979;4:249-50.
- Thijn CJ, van Ouwerkerk WP, Scheele PM, de Jongh HJ. Unilateral patella cubiti: A probable posttraumatic disorder. *Eur J Radiol* 1992;14:60-2.
- Silberstein MJ, Brodeur AE, Graviss ER. Some vagaries of the capitellum. *J Bone Joint Surg Am* 1979;61:244-7.
- Silberstein MJ, Brodeur AE, Graviss ER, Luisiri A. Some vagaries of the medial epicondyle. *J Bone Joint Surg Am* 1981;63:524-8.
- Silberstein MJ, Brodeur AE, Graviss ER, Luisiri A. Some vagaries of the olecranon. *J Bone Joint Surg Am* 1981;63:722-5.
- Silberstein MJ, Brodeur AE, Graviss ER. Some vagaries of the lateral epicondyle. *J Bone Joint Surg Am* 1982;64:444-8.
- Silberstein MJ, Brodeur AE, Graviss ER. Some vagaries of the radial head and neck. *J Bone Joint Surg Am* 1982;64:1153-7.

Effect of Different Doses of Aluminum Chloride on Neurodegeneration in Hippocampus Region of the Rat Brain

Abstract

Introduction: Aluminum (AL) compounds are widely used as food additives, cosmetics, antacids, and buffered aspirins. Chronic consumption of AL may lead to its accumulation in tissues causing AL toxicity. The study aims to investigate the toxic effect of $AlCl_3$ on hippocampus region of rat brain by qualitative and quantitative analysis of neurons. **Material and Methods:** Adult male albino Wistar rats were divided into three groups with six rats in each group. Group 1 was the control, Group 2 rats received 100 mg/kg b. w, and Group 3 received 300 mg/kg b. w of $AlCl_3$ orally for 30 days. The neuronal count was done at the CA1, CA2, CA3, and CA4 regions of hippocampus by staining with cresyl violet stain. Neuronal damage in the $AlCl_3$ groups was compared with the control group. **Results:** A significant damage was observed in all the regions of hippocampus both in Groups 2 and 3 compared to the control group ($P < 0.00001$). Further higher dose of AL caused marked neuronal damage in CA1 ($P < 0.03$) and CA3 ($P < 0.05$) regions compared to the lower dose of AL. The neurons in the CA3 and CA1 regions were most vulnerable to AL toxicity and the CA2 region of the hippocampus had a maximum number of viable neurons indicative of resistance to AL toxicosis. **Discussion and Conclusion:** Consumption of higher dose of AL even for a short term could have variable degrees of deleterious effects on different regions of the rat brain. This study sets a background for an in-depth exploration on toxicology of AL compounds on human participants which could be of public health importance.

Keywords: Aluminum toxicity, CA2 region, CA3 region, hippocampus, neuronal degeneration

Introduction

Human beings are overexposed to aluminum (AL) these days as this metal exists as a component of food additives, cosmetics, antiperspirants, cooking utensils, paints, and buffered aspirin. According to the WHO, the tolerable intake is 1 mg/kg body weight/day.^[1] Chronic consumption of AL may lead to its accumulation in the bones, kidneys, and brain causing AL toxicity. Several researchers have detected elevated content of AL in the brains of patients with Alzheimer's disease (AD), pointing at its role in the pathogenesis of neurological disease. Since the hippocampus region of the brain is critical for learning and memory, it is most vulnerable to damage in AD.^[2] Al can cross blood-brain barrier and cause inflammation in the brain which may lead to loss of memory. Several neurodegenerative disorders such as Parkinson's disease and multiple sclerosis is attributed to AL accumulation

in hippocampus and frontal cortex of the cerebrum.^[3,4] Intestinal absorption of AL salts in rats is rapid through the oral route, and the bioavailability may go up to 0.21%.^[5] Administration in high dose leads to its accumulation in the brain, especially to a greater extent in cortex and hippocampus.^[6] Hence, more research is warranted to confirm the direct correlation between concentration and duration of exposure to AL with neurotoxicity. This study was undertaken to evaluate neurotoxicity of two different doses of AL chloride (100 and 300 mg/Kg body weight/day for 30 days) on four areas of hippocampus region of the rat brain by qualitative and quantitative analysis of neurons.

Material and Methods

The present study was carried out on in-house bred male albino Wistar rats aged about 3–4 months, weighing between 200 and 250 gm. Rats were given *ad libitum* access to laboratory food and drinking

This is an open access journal, and articles are distributed under the terms of the Creative Commons Attribution-NonCommercial-ShareAlike 4.0 License, which allows others to remix, tweak, and build upon the work non-commercially, as long as appropriate credit is given and the new creations are licensed under the identical terms.

For reprints contact: WKHLRPMedknow_reprints@wolterskluwer.com

How to cite this article: Massand A, Basera M, Grace S, Reshma K, Sudha K, Rai R, et al. Effect of different doses of aluminum chloride on neurodegeneration in hippocampus region of rat brain. J Anat Soc India 2022;XX:XX-XX.

Amit Massand,
Mallika Basera¹,
Sonal Grace¹,
Reshma
Kumarachandra¹,
K. Sudha¹,
Rajalakshmi Rai,
Murlimanju BV,
K. Sowndarya¹

Departments of Anatomy, and
¹Biochemistry, Kasturba Medical
College Mangalore, Manipal
Academy of Higher Education,
Manipal, India

Article Info

Received: 03 March 2022
Revised: 30 July 2022
Accepted: 13 September 2022
Available online: ***

Address for correspondence:

Dr. K. Sudha,
Department of Biochemistry,
Kasturba Medical College
Mangaluru, Manipal Academy
of Higher Education,
Mangaluru - 575 004,
Karnataka, India.
E-mail: sudha.k@manipal.edu

Access this article online

Website: www.jasi.org.in

DOI:
10.4103/jasi.jasi_39_22

Quick Response Code:



water. The animals were housed in a polypropylene cage with a paddy husk bedding in controlled temperature, light and dark cycle (12:12 h), humidity (50% ±10%), and pathogen-free environment. The study was approved by the Institutional Animal Ethics Committee (KMC/MNG/IAEC/05-2019 on February 15, 2019). All procedures performed in the study were in accordance with the guidelines provided by the Indian government for the usage of laboratory animals.^[7]

The albino Wistar rats were divided into three groups with six rats in each group. The grouping details are as follows:

- Group 1: Rats were given food and water for 30 days. This served as a control group
- Group 2 (Al 100): Rats orally received 100 mg/kg body weight/day of AlCl₃ for 30 days
- Group 3 (Al 300): Rats orally received 300 mg/kg body weight/day of AlCl₃ for 30 days.

AlCl₃ was procured from Sigma-Aldrich, USA, of the highest analytical grade. The solubility of AlCl₃ is 458 g/L at 20°C. The AlCl₃ was dissolved in distilled water at a final concentration of 300 mg/Kg b. w (1/10 LD50). Stock solution was prepared by dissolving 2 g of AlCl₃ in 20 ml of distilled water. This was administered orally at a dose of 0.5 ml/100 g b. w using gavage in one bolus.

Histological study

After 30 days of AlCl₃ administration, all the animals were sacrificed and the brain was perfused with cold phosphate buffer saline and 10% formalin and then stored in 10% formalin. Subsequently, paraffin blocks were prepared, 6–7 µm thick sections of the tissue were taken using a microtome, and the sections were processed with different grades of alcohol and xylene, and stained with 0.1% cresyl violet acetate solution. A minimum of six histological sections were taken from each region of each rat. The different regions of hippocampus were demarcated based on the topographical location of the dentate gyrus. The viable neurons were identified in CA1, CA2, CA3, and CA4 regions of both sides of the hippocampus by VUE software and counted using the imaging software NIS-Elements (Br version 4.30).^[8,9] The cell count was expressed as the number of cells per unit length of the cell field (cells/300 µm length). A single person was involved in the counting of neurons at three different 300 µm areas of the same region to avoid interobserver bias. The average of the three

readings was considered to prevent intraobserver bias. The neuronal cell count was compared between the three groups. The histopathological changes were examined using Nikon trinocular microscope (H600 L) under ×20 to evaluate the neuromorphological changes in the hippocampus. The percentage of neuronal loss was calculated as mean number of neurons in control sections minus the mean number of neurons in the treated section divided by the mean number of neurons in the control section multiplied by 100.^[10]

All the groups were statistically analyzed using the one-way analysis of variance followed by Tukey’s *post hoc* test to compare between the different groups. The experimental data were represented as mean ± standard deviation with six rats in each group. The *P* < 0.05 was considered to be statistically significant.

Results

A significant decrease in healthy neurons was observed in rats fed with AL chloride compared to controls (*P* < 0.00001). The neurons in which the cell membrane was disrupted and those showing peripherally placed pyknotic nuclei or without nuclei were considered as degenerated neurons. Neuronal counts in four regions of hippocampus revealed a significant decline in healthy neurons in the CA3 followed by CA1, CA4, and CA2 in both Group 2 and Group 3 rats compared to the normal group [Table 1]. The histological study also depicts significant neurodegeneration in the CA3 and CA1 regions of hippocampus among all regions (CA1, CA2, CA3, and CA4) of the rat brains in the AL groups [Figures 1-5].

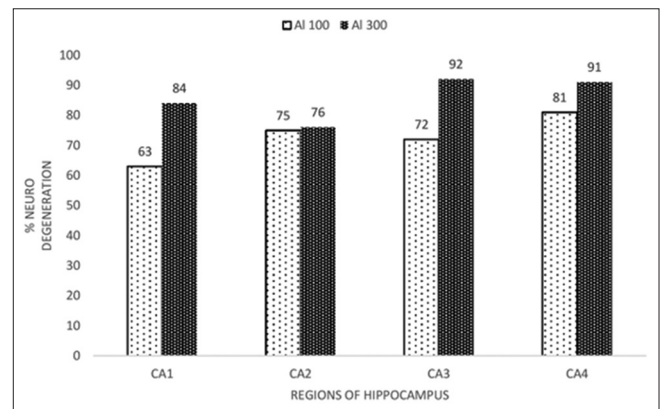


Figure 1: Comparison of neurodegeneration in different regions of hippocampus with the two doses of aluminum

Table 1: Comparison of neuronal count at 300 µm area of different regions of hippocampus at the same topography between control and aluminum-treated groups

	Regions of hippocampus			
	CA1	CA2	CA3	CA4
Group 1 (Control)	19.28±4.60	20.85±3.93	15.571±4.27	20.43±2.78
Group 2 (Al 100)	7.0±3.958*	5.28±1.38*	4.285±3.35*	3.85±3.53*
Group 3 (Al 300)	3.0±1.914* ^a	5.0±2.88*	1.285±0.95* ^b	1.85±1.21*

Values are mean±SD. **P*<0.00001 different from controls, ^a*P*<0.03, ^b*P*<0.05 different from Group 2. SD: Standard deviation

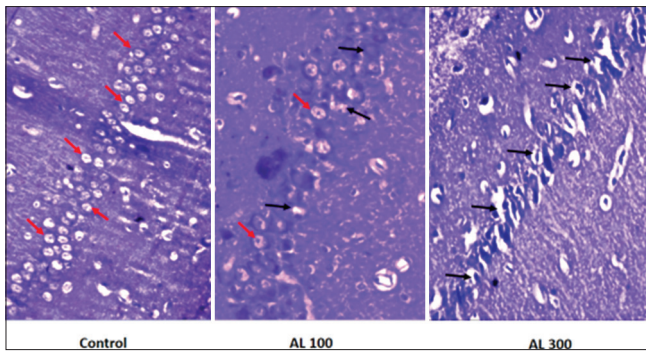


Figure 2: The photomicrographs of CA1 subfield of hippocampus stained with cresyl violet. (Red arrows indicate normal neurons and black arrows indicate degenerated neurons)

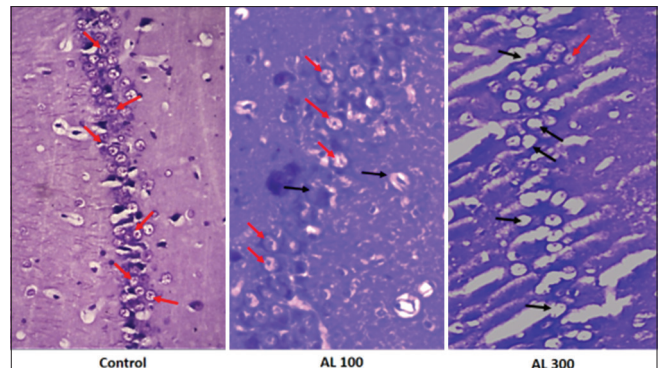


Figure 3: The photomicrographs of CA2 subfield of hippocampus stained with cresyl violet. (Red arrows indicate normal neurons and black arrows indicate degenerated neurons)

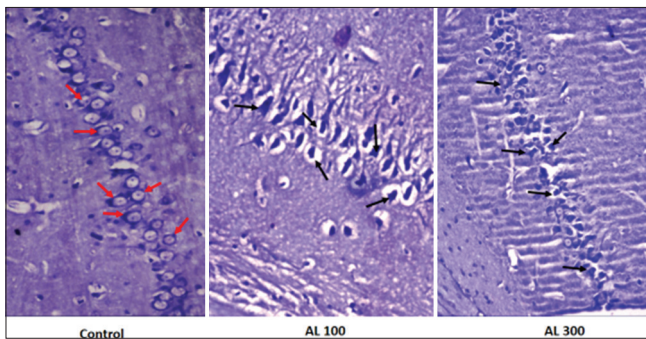


Figure 4: The photomicrographs of CA3 subfield of hippocampus stained with cresyl violet. (Red arrows indicate normal neurons and black arrows indicate degenerated neurons)

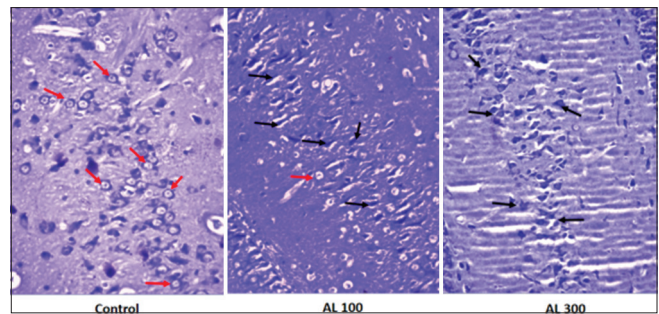


Figure 5: The photomicrographs of CA4 subfield of hippocampus stained with cresyl violet. (Red arrows indicate normal neurons and black arrows indicate degenerated neurons)

Neurodegeneration was almost double in CA1 and CA4 regions while it was four times higher in the CA3 region of hippocampus in rats fed with 300 mg/kg b. w of AL chloride compared to those fed with 100 mg/kg b. w. However, neurodegeneration was at the same level in these two groups in the CA2 region [Figure 1]. The CA3 region was most vulnerable to AL toxicity and a higher dose of AL was more effective in the induction of neurodegeneration. Compared to the control group, CA1 and CA3 regions were more sensitive to AL toxicity compared to other regions of the hippocampus.

Discussion

AL toxicity has multidimensional effects such as generation of free radicals, reduction in antioxidant defense, prevention of DNA repair, change in protein conformation, and inhibition of enzymes such as Na, K-ATPase, and inflammatory reactions.^[11] There is growing evidence to suggest that intraneuronal accumulation of metal ions such as AL, arsenic, lead, and nickel also leads to mitochondrial changes decreasing ATP production and cell death.^[12] In humans, the accumulation of AL in the brain has been associated with neurodegenerative diseases such as AD, Parkinson's disease, and multiple sclerosis.^[3,4] AL intake promotes oxidative stress and amyloid deposition in nervous tissue which leads to

neuronal necrosis and dysregulated neurogenesis.^[13] The memory loss in neurodegenerative disorder is attributed to the apoptosis of cortical neurons due to the accumulation of AL in the hippocampus and frontal cortex of the cerebrum.^[10] AL chloride administered in male Wistar rats for 1 month was found to increase the rate of protein and lipid damage in the brain.^[14] The histological changes observed in the present study prove that AL induces neuronal damage in the hippocampus region of the rat brain. Rats administered with AL (both doses) showed prominent morphological alterations in all four regions of hippocampus when compared to controls. The neurons in the CA3 subfield were most vulnerable to AL toxicity and a higher dose of AL was more effective in the induction of neurodegeneration. Compared to the control group, CA1 and CA3 regions were more sensitive to AL toxicity with the highest percentage of neurodegeneration compared to other regions of the hippocampus. Earlier studies have revealed that chronic administration of low dose of AL mimics natural aging process in rats.^[15] Chiroma *et al.*^[16] confirmed neurodegenerative changes in CA1 and CA3 subregions of hippocampus in rats administered with 200 mg/Kg/day of $AlCl_3$ for 70 days which is in agreement with the findings of our study. Morphologically, administration of 300 mg of caused major structural changes in the cytoarchitecture such as an increase in number of pyknotic cells and alteration

of pyramidal cell arrangements. By the way of cresyl violet staining, a significant number of degenerative cells were observed in the CA3 region of hippocampus in rats administered with higher dose of AL compared to a lower dose (100 mg/kg/day), which only highlights the vulnerability of neurons of this region of the brain to AL toxicity which is consistent with previously published data. Kumar *et al.*^[17] reported that rats fed with 100 mg/kg/day of AlCl₃ for 60 days showed neuronal damage only in the CA3 region, whereas the same result was observed in our study within 30 days. Enas and Khalil^[18] demonstrated dementia in rats when (300 mg/kg/day) was administered for a month, which supports our study.

Conclusion

In the current investigation, animals exposed to 300 mg of AL have displayed a higher degree of neuronal necrosis in hippocampus which is the site for memory formation. Hence, the research outcome suggests that rats fed with 300 mg of AL/kg/day for 1 month could be the best choice for the study of AD-related pathologies. These findings set a background for an in-depth exploration on toxicology of AL compounds as it is of public health importance.

The limitation of the study is that the tissue penetration of AlCl₃ could not be demonstrated due to the lack of facility involving fluorescein-based fluorescence detection.

Acknowledgment

The author would like to thank technical staff for their support.

Financial support and sponsorship

Nil.

Conflicts of interest

There are no conflicts of interest.

References

1. Tietz T, Lenzner A, Kolbaum AE, Zellmer S, Riebeling C, Gürtler R, *et al.* Aggregated aluminium exposure: Risk assessment for the general population. *Arch Toxicol* 2019;93:3503-21.
2. Gupta VB, Anitha S, Hegde ML, Zecca L, Garruto RM, Ravid R, *et al.* Aluminium in Alzheimer's disease: Are we still at a crossroad? *Cell Mol Life Sci* 2005;62:143-58.
3. Nampoothiri M, John J, Kumar N, Mudgal J, Nampurath GK, Chamallamudi MR. Modulatory role of simvastatin against aluminium chloride-induced behavioural and biochemical changes in rats. *Behav Neurol* 2015;2015:210169.
4. Abu-Taweel GM, Ajarem JS, Ahmad M. Neurobehavioral toxic effects of perinatal oral exposure to aluminum on the developmental motor reflexes, learning, memory and brain neurotransmitters of mice offspring. *Pharmacol Biochem Behav* 2012;101:49-56.
5. European Food Safety Authority. Statement of EFSA on the evaluation of a new study related to the bioavailability of aluminium in food. *EFSA J* 2011;9:2157.
6. Baydar T, Papp A, Aydin A, Nagymajtenyi L, Schulz H, Isimer A, *et al.* Accumulation of aluminum in rat brain: Does it lead to behavioral and electrophysiological changes? *Biol Trace Elem Res* 2003;92:231-44.
7. Singh AP. Government of India notifies the rules for breeding of and conducting animal experiments. *Indian J Pharmacol* 1999;31:92-5.
8. Joy T, Rao MS, Madhyastha S. N-Acetyl cysteine supplement minimize tau expression and neuronal loss in animal model of Alzheimer's disease. *Brain Sci* 2018;8:185.
9. Standring S. Cerebral cortex. In: Gray's Anatomy. 39th ed., Ch. 22. Spain: Elsevier, Churchill Livingstone; 2006. p. 407.
10. Chiroma SM, Mohd Moklas MA, Mat Taib CN, Baharuldin MT, Amon Z. D-galactose and aluminium chloride induced rat model with cognitive impairments. *Biomed Pharmacother* 2018;103:1602-8.
11. Maya S, Prakash T, Madhu KD, Goli D. Multifaceted effects of aluminium in neurodegenerative diseases: A review. *Biomed Pharmacother* 2016;83:746-54.
12. Alasfar RH, Isaifan RJ. Aluminum environmental pollution: The silent killer. *Environ Sci Pollut Res Int* 2021;28:44587-97.
13. Igbokwe IO, Igwenagu E, Igbokwe NA. Aluminium toxicosis: A review of toxic actions and effects. *Interdiscip Toxicol* 2019;12:45-70.
14. Jyoti A, Sethi P, Sharma D. *Bacopa monniera* prevents from aluminium neurotoxicity in the cerebral cortex of rat brain. *J Ethnopharmacol* 2007;111:56-62.
15. Roig JL, Fuentes S, Teresa Colomina M, Vicens P, Domingo JL. Aluminum, restraint stress and aging: Behavioral effects in rats after 1 and 2 years of aluminum exposure. *Toxicology* 2006;218:112-24.
16. Chiroma SM, Hidayat Baharuldin MT, Mat Taib CN, Amom Z, Jagadeesan S, Adenan MI, *et al.* Protective effect of *Centella asiatica* against D-galactose and aluminium chloride induced rats: Behavioral and ultrastructural approaches. *Biomed Pharmacother* 2019;109:853-64.
17. Kumar P, Bairy KL, Nayak V, Reddy SK, Kiran A, Ballal A. Amelioration of aluminium chloride (AlCl₃) induced neurotoxicity by combination of Rivastigmine and Memantine with artesunate in albino wistar rats. *Biomed Pharmacol J* 2019;12:703-11.
18. Enas KA. Study of possible protective and therapeutic influence of coriander (*Coriandrum sativum* L.) against neurodegenerative disorders and Alzheimer's disease induced by aluminum chloride in cerebral cortex of male albino rats. *Nat Sci* 2010;8:202-13.

The Relationship between Isolated Unilateral Concha Bullosa and Mastoid Air Cell Volumes

Abstract

Introduction: The purpose of this study was to investigate the relationship between the pneumatization of mastoid air cells (MACs) and isolated unilateral concha bullosa (CB) using computed tomography (CT) scans of the paranasal sinuses (PNS). **Material and Methods:** A retrospective review of PNS CT scans from 53 patients was performed. Cases with nasal septum angulation $>5^\circ$ were excluded from the study. CT evaluations were made with a 128-slice multislice CT scanner in two projections, axial and coronal. Slice thickness was taken as 1 mm for volumetric analysis. Volume measurements were calculated using the syngo.via software program by selecting the relevant anatomical region and using step-by-step addition and expansion processes. Volumes of the MACs (right and left) and isolated unilateral CB (right and left) were obtained and compared using statistical analysis. **Results:** The volume of MACs and isolated unilateral CB did not change with age; however, the volumes of male participants were larger than that of women. It was observed that the pneumatization of MACs on the side with isolated unilateral CB was significantly greater than for opposing MACs. **Discussion and Conclusion:** In our study, it was concluded that the isolated unilateral CB caused a significant increase in the MACs volume on the same side of CB.

Keywords: Computed tomography, concha bullosa, mastoid air cells, volumetric analysis

Fatih Yüksel,
Mehmet Erkan
Kahraman,
Isa Deniz¹

Departments of
Otorhinolaryngology and
¹Radiology, Konya City
Hospital, Karatay, Konya,
Turkey

Introduction

Concha bullosa (CB) is the most common anatomical variation of the osteomeatal region.^[1,2] It is usually seen in the middle turbinate, rarely in the superior and inferior turbinates. CB can be unilateral or bilateral, and its incidence ranges from 13% to 53.6%.^[3-6] The mechanism of CB formation remains unclear. CB has been reported to originate from anterior or posterior ethmoid cells extending to the middle turbinate.^[7] It is also thought that the imbalance in nasal airflow due to nasal septum deviation (NSD) plays a role in CB formation.^[8] However, there are cases with unilateral or bilateral CB without NSD. CB is thought to play a stabilizing role in airflow on both sides of the nasal passage.^[9] Unless the CB is large and does not obstruct the nasal airway or sinus ostium, it usually does not cause symptoms or require any treatment.^[1]

Another important air structure in skull bones is the mastoid air cells (MACs). Although the function of the MAC is not

fully known, it is thought to function as a gas reserve to balance middle ear pressure.^[10] Pneumatization of mastoid cells begins at 33 weeks of gestation and continues until puberty.^[11] Radiographically, MACs become visible after birth. The mastoid antrum is present at birth. The development of other cells takes place in three stages: the childhood period from birth to 2 years of age, the transitional period between 2 and 5 years, and the adult period.^[11-13] It has been suggested that nasal airflow and positive pressure in the nasopharynx affect the development of mastoid cells through the eustachian tube.^[14] It has also been shown that conditions affecting nasal airflow, such as septal deviation, cause changes in nasopharyngeal pressure.^[15] There are several theories pointing to the importance of available nasal airflow and normal oxygen pressure for paranasal sinus development.^[16,17] In addition, long-term or recurrent infections in childhood are thought to affect the development of MAC.^[18-20]

Although there are studies investigating the relationship between NSD and CB and between NSD and mastoid pneumatization, we could not find any study in the literature

Article Info

Received: 14 September 2021
Revised: 04 July 2022
Accepted: 25 July 2022
Available online: ***

Address for correspondence:

Dr. Fatih Yüksel,
Department of Otolaryngology,
Konya City Hospital, Akabe,
Karatay 42020, Konya, Turkey.
E-mail: kbbfatih@yahoo.com

Access this article online

Website: www.jasi.org.in

DOI:
10.4103/jasi.jasi_164_21

Quick Response Code:



How to cite this article: Yüksel F, Kahraman ME, Deniz I. The relationship between isolated unilateral concha bullosa and mastoid air cell volumes. J Anat Soc India 2022;XX:XX-XX.

This is an open access journal, and articles are distributed under the terms of the Creative Commons Attribution-NonCommercial-ShareAlike 4.0 License, which allows others to remix, tweak, and build upon the work non-commercially, as long as appropriate credit is given and the new creations are licensed under the identical terms.

For reprints contact: WKHLRPMedknow_reprints@wolterskluwer.com

investigating the relationship between CB (isolated concha bullosa) and mastoid pneumatization in patients without NSD. The aim of this study was to evaluate whether the volumes of MACs are affected in patients with isolated concha bullosa (ICB).

Material and Methods

The images of patients who underwent paranasal sinus computed tomography (CT) examination for any reason between August 15, 2020, and February 15, 2021, at Konya City hospital were retrospectively analyzed. Patients under the age of 18, patients with NSD, history of surgery to the sinonasal and mastoid region, maxillofacial and temporal trauma, sinonasal tumor, radiotherapy, granulomatous disease, middle ear infection, and diffuse sinonasal polyposis were excluded from the study. After applying the exclusion criteria, 53 patients (24 (45.3%) female and 29 (54.7%) male) with unilateral CB on paranasal sinus CT were included in the study. Patient consent was not obtained, because this study was conducted from the records. This study complied with the Helsinki Declaration principles. This study was approved by the Necmettin Erbakan University Faculty of Medicine Ethics Committee (Date: February 04, 2021, No: 2021/3171).

Elimination method of patients with septum deviation

Nasal septal deviation evaluated in coronal CT studies was defined as the curvature of the nasal septal contour in any direction. Septal deviation angle was obtained by measuring the angle between a line drawn from the level of crista galli to the level of the maxillary crest and another line drawn from the level of crista galli to the most prominent point of the septal angulation with a protractor. Septal deviation, when the angle was $<5^\circ$, was considered normal.^[8] Cases with an angle $>5^\circ$ were evaluated for the presence of septum deviation and were excluded from the study [Figure 1].

Computed tomography examination method

Images of all patients were reviewed simultaneously by a radiologist and an otolaryngologist. Paranasal CT evaluations were performed with a 128-slice multislice CT scanner in two projections, axial and coronal (Siemens, Germany). CB was considered present, when more than 50% of the vertical height of the middle turbinate became pneumatic (measured from the top of the coronal plane down). The presence of CB on CT scan was defined as unilateral or bilateral. Patients with bilateral CB were excluded from the study.

Slice thickness was taken as 1 mm for volumetric analysis. Volume measurements were calculated using the syngo.via software program by selecting the relevant anatomical region, using step-by-step addition and expansion processes, and finally displayed as colored areas for analysis. The volume of ICB [Figure 2a and b] and

MACs [Figure 3a and b] was automatically calculated in the three-dimensional reconstruction, 140 kV and 120 mA. The imaging data were stored in a Digital Imaging and Communications in Medicine and then imported to a personal computer running syngo.via software (Germany). When performing reconstruction using a volume-rendering algorithm, the selection of the window thresholds was 1,030 to 300 Hounsfield units.

Statistical analysis

SPSS 26.0 (IBM Corporation, Armonk, New York, United States) program was used in the analysis of the variables. Univariate data were evaluated with the Kolmogorov–Smirnov test and Shapiro–Wilk–Francia test, while the homogeneity of variance was evaluated with the Levene’s test. In the comparison of two independent groups

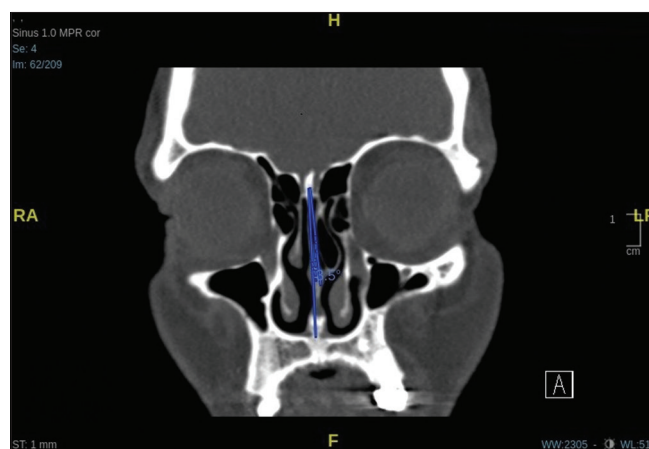


Figure 1: The measurement of the angle of septal deviations

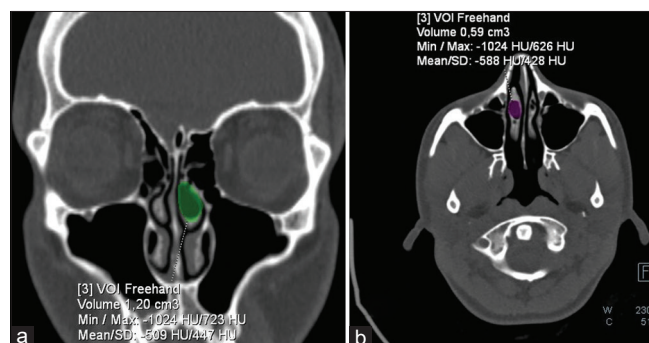


Figure 2: (a and b) These figures show the program used to measure the volume of the concha bullosa at the workstation. (a: coronal view; b: axial view)

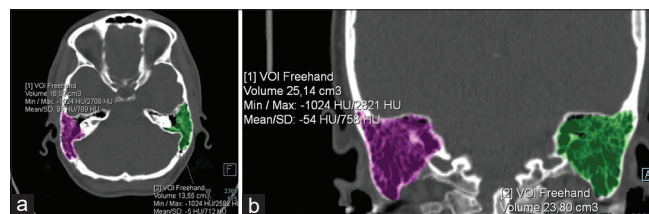


Figure 3: (a and b) These figures show the program used to measure the volume of mastoid air cells at the workstation. (a: coronal view; b: axial view)

according to quantitative data, the independent samples *t*-test was used together with the bootstrap results, while the Mann–Whitney *U* test was used together with the Monte Carlo results. Paired samples *t*-test was used with bootstrap results to compare two replicate measures of dependent quantitative variables with each other. Pearson correlation and Kendall's tau-b tests were used to examine the correlations of the variables with each other. Pearson's Chi-square Monte Carlo Simulation technique was used to compare categorical variables with each other. Quantitative variables were expressed as mean (standard deviation) and median (Percentile 25/Percentile 75) in the tables, while categorical variables were shown as *n* (%). Variables were analyzed at 95% confidence level, and $P < 0.05$ was considered statistically significant.

Results

The mean age of the patients was 30.68 ± 10.78 years. Twenty-four (45.3%) patients were female and 29 (54.7%) were male. There was no statistically significant difference in terms of age and gender in patients with right and left ICB ($P = 0.112$ and $P = 0.783$, respectively). Right ICB was detected in 24 (45.3%) patients and left ICB in 29 (54.7%) patients. Right ICB volume was $0.87 (0.53/1.28) \text{ cm}^3$, and left ICB volume was $0.77 (0.50/1.23) \text{ cm}^3$, and there was no statistically significant difference between right and left ICB volumes ($P = 0.884$). The ipsilateral (right) MAC volume was $14.87 \pm 5.67 \text{ cm}^3$ in patients with right ICB, ipsilateral (left) MAC volume was $10.29 \pm 5.62 \text{ cm}^3$ in patients with left ICB, and there was a significant difference between ipsilateral MAC cell volumes in patients ($P = 0.007$) [Table 1].

Right MAC volumes were $14.87 \pm 5.67 \text{ cm}^3$ and left MAC volumes were $13.37 \pm 5.99 \text{ cm}^3$ in patients with right ICB; the difference was statistically significant ($P = 0.004$). While left MAC volumes were $10.29 \pm 5.62 \text{ cm}^3$ in left ICB patients, right MAC volumes were $9.19 \pm 5.58 \text{ cm}^3$; the difference was statistically significant ($P = 0.001$). It

was determined that the MAC volumes on the ipsilateral side of the ICB were larger than the MAC volumes on the contralateral side [Table 2].

ICB volumes and right and left MAC volumes were found to be significantly larger in male than in female participants (P values 0.005, 0.026, and 0.022, respectively) [Table 3].

Discussion

The size and shape of the paranasal sinuses (PNS) and MAC vary from person to person and can differ between two halves of the body in the same person. This difference is thought to be related to the developmental processes. It has been reported that environmental factors such as trauma and infection, as well as genetic factors, contribute in the difference between individuals.^[21-23] The formation of air spaces within the bone occurs through opportunistic expansion of the epithelium and the formation of bone that counteracts it.^[14] Bone formation and factors affecting the epithelium also play a role in the development of air spaces.

The turbinates are important structures arising from the lateral wall of the nasal cavity. The middle turbinate is formed by the medial part of the ethmoid bone. In the 5th and 6th months of the embryonic period, ethmoid air cell groups are formed by the extension of the nasal epithelium to the lateral nasal wall. CB occurs as an extension of the normal pneumatization of ethmoid air cells.^[3,7] Pneumatization of the middle turbinate is mostly mediated by anterior ethmoid cells. Pneumatization through posterior air cells or both have also been reported.^[3,24] Therefore, CB can also be considered a part of the PNS system. CB becomes evident after 7–8 years and continues to develop even after puberty.^[25]

MAC differs in size and shape from person to person, is one of the important air structures in the skull bones. MAC development begins with the formation of the mastoid antrum, which can first be recognized at 21–22 weeks

Table 1: Comparison of demographic data, isolated concha bullosa, and mastoid air cells volumes by direction of isolated concha bullosa

	Total (<i>n</i> =53)	ICB direction		<i>P</i>
		Right (<i>n</i> =24)	Left (<i>n</i> =29)	
Gender, <i>n</i> (%)				
Female	24 (45.3)	10 (41.7)	14 (48.3)	0.783 ^c
Male	29 (54.7)	14 (58.3)	15 (51.7)	
Age (year), mean±SD	30.68±10.78	28.13±8.75	32.79±11.94	0.112 ^t
ICB volume (cm ³), median (q1/q ³)	0.77 (0.52/1.27)	0.87 (0.53/1.28)	0.77 (0.50/1.23)	0.884 ^u
Contralateral MAC Volume (cm ³), mean±SD	11.68±5.94	13.37±5.99	9.19±5.58	0.075 ^t
Ipsilateral MAC Volume (cm ³), mean±SD	12.37±6.04	14.87±5.67	10.29±5.62	0.007 ^{*t}

Descriptions: MAC, ICB, *n*. ^cPearson's Chi-square test (Monte Carlo), ^tIndependent samples *t*-test (bootstrap), ^uMann-Whitney *U*-test (monte carlo), * $P < 0.05$. SD: Standard deviation, q1: Percentile 25, q3: Percentile 75, MAC: Mastoid air cells, ICB: Isolated concha bullosa, *n*: Number of patients

Table 2: Comparison of right and left mastoid air cells volumes according to the direction of the isolated concha bullosa

ICB direction	Right MAC volume (cm ³), mean±SD	Left MAC volume (cm ³), mean±SD	P
Right (n=24)	14.87±5.67	13.37±5.99	0.004* ^{Pt}
Left (n=29)	9.19±5.58	10.29±5.62	0.001* ^{Pt}

Descriptions: MAC, ICB, n. *P<0.05, ^{Pt}Paired samples t-test (Bootstrap). SD: Standard deviation, MAC: Mastoid air cells, ICB: Isolated concha bullosa, n: Number of patients

Table 3: Analysis of isolated concha bullosa and mastoid air cells volumes by gender

	Gender		P
	Female (n=24)	Male (n=29)	
ICB volume (cm ³), median (q1/q3)	0.53 (0.23/0.86)	0.97 (0.60/1.32)	0.005* ^u
Right MAC volume (cm ³), mean±SD	9.49±5.83	13.64±6.06	0.026* ^t
Left MAC volume (cm ³), mean±SD	9.52±4.76	13.47±6.29	0.022* ^t
Contralateral MAC volume (cm ³), mean±SD	9.52±4.76	13.47±6.29	0.022* ^t
Ipsilateral MAC volume (cm ³), mean±SD	10.27±5.37	14.10±6.10	0.034* ^t

Descriptions: MAC, ICB, n. *P<0.05, ^tIndependent samples t-test (bootstrap), ^uMann-Whitney U-test (Monte Carlo). SD: Standard deviation, q1: Percentile 25, q3: Percentile 75, MAC: Mastoid air cells, ICB: Isolated concha bullosa, n: Number of patients

of gestation.^[11] The mastoid antrum is fully organized at 34 weeks, and there are usually no additional air cells at birth. During the growth and expansion of MACs, mesenchymal tissue is cleared by absorption and/or redistribution.^[12,26] MAC formation continues until puberty with the development of air cells at the petrous apex.^[11-13]

Both airspace systems, consisting of the PNS and the MAC, are formed by resorption of the epithelium in the mastoid bone and PNS. Considering the similar developmental process of both structures, it can be thought that besides genetic factors, CB in the nasal airway may have an effect on MAC. We could not find any study investigating the volumetric relationship of these two structures. We consider this study to be the first.

There are various studies on the relationship between PNS and MAC. MAC pneumatization has been shown to be positively associated with sphenoid sinus pneumatization, but not with maxillary sinuses.^[14] Karakas and Kavakli^[27] reported that PNS and MAC volumes increase with age, mean volume is lower in women, and there is a positive correlation between right-left and ipsilateral PNS and MACs. Lee *et al.*^[19] reported that there was no interaction in the pneumatization of the PNS and MACs in the pediatric

population, and that the growth of both was affected by age. In our study, both mastoid cells and CB volumes were greater in men than in women.

Nasal airflow and positive pressure in the nasopharynx are thought to be factors that affect MAC and PNS pneumatization. The total amount of nasal air space affects nasal airflow, affecting the amount of positive pressure on the mucosa of the nasal cavity and the mastoid cell mucosa through the eustachian nasopharynx.^[28] There are studies showing the possible effects of factors affecting nasal airflow, such as NSD, on PNS and MAC, and reporting different findings. Impairment of airflow due to NSD may result in decreased pneumatization of the MAC.^[20,29,30] Firat *et al.*^[29] reported that as the degree of NSD increased, the total ethmoid cell volume on the NSD side decreased compared to the opposite side. Karataş *et al.*^[31] showed that moderate septum deviation significantly affects the maxillary sinus volume. Kapusuz Gencer *et al.*^[30] reported that maxillary sinus volume tended to be larger on the opposite side of severe NSD in adults. Lee and Jin^[32] showed that the MAC and maxillary sinus volumes on the deviated side were smaller than on the opposite side in a clinical study in children, suggesting that NSD may affect both ventilations. However, there are also studies reporting that NSD does not affect sinus and MAC volumes.^[33,34]

CB is usually asymptomatic and diagnosed incidentally by CT. Swollen or hypertrophic nasal turbinates can cause obstruction of nasal airflow.^[35] The ventilated middle turbinate may completely fill the entire space between the septum and the lateral nasal wall, followed by blockage of the osteomeatal complex, predisposing to paranasal sinus infection.^[35,36] Li *et al.*^[9] reported that CB on the undeviated side of patients with NSD makes the airflow more balanced between the bilateral nasal cavities, which may be a compensatory action for nasal physiology from aerodynamic point of view. However, the presence of CB narrows the ipsilateral nasal cavity. Karataş *et al.*^[37] found a moderately positive correlation between CB and maxillary sinus volume, and a low positive correlation between frontal sinus volume. Özkiriş *et al.*^[36] reported that there is a possible relationship between CB and ipsilateral decreased olfactory bulb volume; however, the exact mechanism remains unclear. According to the authors, decreased nasal airflow on the CB side may be attributed to the pathophysiological mechanism of this finding. Septal deviation and unilateral/dominant CB did not affect the asymmetry in the maxillary sinus volumes.^[38] However, bilateral CB was associated with larger volumes of maxillary sinuses. In our study, MAC volumes were found to be larger on the side with CB than on the opposite side. This finding suggests that the CB affects MAC volumes positively, unlike NSD. Accordingly, it can be said that the MACs are larger on the side with genetically CB.

The limitations of our study are that the number of patients is small and it is single center. In addition, the patients included in our study were those who underwent paranasal sinus CT for suspected sinonasal disease. Therefore, statistical interpretations of the results of our study are valid only for the symptomatic population.

Conclusion

In our study, it was concluded that the ICB caused a significant increase in the MAC volumes on the side where they were located. According to our results, it was thought that ICB increases MAC aerations.

Financial support and sponsorship

Nil.

Conflicts of interest

There are no conflicts of interest.

References

- Demir UL, Akca ME, Ozpar R, Albayrak C, Hakyemez B. Anatomical correlation between existence of concha bullosa and maxillary sinus volume. *Surg Radiol Anat* 2015;37:1093-8.
- Hatipoğlu HG, Cetin MA, Yüksel E. Concha bullosa types: Their relationship with sinusitis, ostiomeatal and frontal recess disease. *Diagn Interv Radiol* 2005;11:145-9.
- Unlü HH, Akyar S, Caylan R, Naçça Y. Concha bullosa. *J Otolaryngol* 1994;23:23-7.
- Doğru H, Döner F, Uygur K, Gedikli O, Cetin M. Pneumatized inferior turbinate. *Am J Otolaryngol* 1999;20:139-41.
- Joe JK, Ho SY, Yanagisawa E. Documentation of variations in sinonasal anatomy by intraoperative nasal endoscopy. *Laryngoscope* 2000;110:229-35.
- Uygur K, Tüz M, Doğru H. The correlation between septal deviation and concha bullosa. *Otolaryngol Head Neck Surg* 2003;129:33-6.
- Bolger WE, Butzin CA, Parsons DS. Paranasal sinus bony anatomic variations and mucosal abnormalities: CT analysis for endoscopic sinus surgery. *Laryngoscope* 1991;101:56-64.
- Yiğit O, Acioglu E, Cakir ZA, Sişman AS, Barut AY. Concha bullosa and septal deviation. *Eur Arch Otorhinolaryngol* 2010;267:1397-401.
- Li L, Zang H, Han D, Ramanathan M Jr., Carrau RL, London NR Jr. Impact of a concha bullosa on nasal airflow characteristics in the setting of nasal septal deviation: A computational fluid dynamics analysis. *Am J Rhinol Allergy* 2020;34:456-62.
- Doyle WJ. The mastoid as a functional rate-limiter of middle ear pressure change. *Int J Pediatr Otorhinolaryngol* 2007;71:393-402.
- Allam AF. Pneumatization of the temporal bone. *Ann Otol Rhinol Laryngol* 1969;78:49-64.
- Cinamon U. The growth rate and size of the mastoid air cell system and mastoid bone: A review and reference. *Eur Arch Otorhinolaryngol* 2009;266:781-6.
- Rubensohn G. Mastoid pneumatization in children at various ages. *Acta Otolaryngol* 1965;60:11-4.
- Kim J, Song SW, Cho JH, Chang KH, Jun BC. Comparative study of the pneumatization of the mastoid air cells and paranasal sinuses using three-dimensional reconstruction of computed tomography scans. *Surg Radiol Anat* 2010;32:593-9.
- Maier W, Krebs A. Is surgery of the inner nose indicated before tympanoplasty? Effects of nasal obstruction and reconstruction on the eustachian tube. *Laryngorhinootologie* 1998;77:682-8.
- Kossowska E, Gasik C. Results of surgical treatment of choanal atresia. *Rhinology* 1979;17:155-60.
- Parsons DS, Wald ER. Otitis media and sinusitis: Similar diseases. *Otolaryngol Clin North Am* 1996;29:11-25.
- Tos M. Mastoid pneumatization. A critical analysis of the hereditary theory. *Acta Otolaryngol* 1982;94:73-80.
- Lee DH, Shin JH, Lee DC. Three-dimensional morphometric analysis of paranasal sinuses and mastoid air cell system using computed tomography in pediatric population. *Int J Pediatr Otorhinolaryngol* 2012;76:1642-6.
- Gencer ZK, Özkiriş M, Okur A, Karaçavuş S, Saydam L. The possible associations of septal deviation on mastoid pneumatization and chronic otitis. *Otol Neurotol* 2013;34:1052-7.
- Austin DF. On the function of the mastoid. *Otolaryngol Clin North Am* 1977;10:541-7.
- Tos M, Stangerup SE. The causes of asymmetry of the mastoid air cell system. *Acta Otolaryngol* 1985;99:564-70.
- Virapongse C, Sarwar M, Bhimani S, Sasaki C, Shapiro R. Computed tomography of temporal bone pneumatization: 1. Normal pattern and morphology. *AJR Am J Roentgenol* 1985;145:473-81.
- Zinreich SJ, Mattox DE, Kennedy DW, Chisholm HL, Diffley DM, Rosenbaum AE. Concha bullosa: CT evaluation. *J Comput Assist Tomogr* 1988;12:778-84.
- Cohen SD, Matthews BL. Large concha bullosa mucopyocele replacing the anterior ethmoid sinuses and contiguous with the frontal sinus. *Ann Otol Rhinol Laryngol* 2008;117:15-7.
- Piza J, Northrop C, Eavey RD. Embryonic middle ear mesenchyme disappears by redistribution. *Laryngoscope* 1998;108:1378-81.
- Karakas S, Kavakli A. Morphometric examination of the paranasal sinuses and mastoid air cells using computed tomography. *Ann Saudi Med* 2005;25:41-5.
- Thomas A, Raman R. A comparative study of the pneumatization of the mastoid air cells and the frontal and maxillary sinuses. *AJNR Am J Neuroradiol* 1989;10:S88.
- Firat AK, Miman MC, Firat Y, Karakas HM, Ozturan O, Altinok T. Effect of nasal septal deviation on total ethmoid cell volume. *J Laryngol Otol* 2006;120:200-4.
- Kapusuz Gencer Z, Ozkiriş M, Okur A, Karaçavuş S, Saydam L. The effect of nasal septal deviation on maxillary sinus volumes and development of maxillary sinusitis. *Eur Arch Otorhinolaryngol* 2013;270:3069-73.
- Karataş D, Koç A, Yüksel F, Doğan M, Bayram A, Cihan MC. The effect of nasal septal deviation on frontal and maxillary sinus volumes and development of sinusitis. *J Craniofac Surg* 2015;26:1508-12.
- Lee DH, Jin KS. Effect of nasal septal deviation on pneumatization of the mastoid air cell system: 3D morphometric analysis of computed tomographic images in a pediatric population. *Int Adv Otol* 2015;10:251-5.
- Şentürk M, Azgın İ, Öcal R, Sakarya EU, Güler İ, Övet G, *et al.* Volumetric analysis of the maxillary sinus in pediatric patients with nasal septal deviation. *ENT Updates* 2015;5:107-12.
- Çelik M, Yegin Y, Olgun B, Altıntaş A, Kayhan FT. Impact of the angles of the septal deviation on the degree of the mastoid pneumatization. *Iran J Otorhinolaryngol* 2020;32:163-8.
- Ozkiriş M, Karaçavuş S, Kapusuz Z, Saydam L. The impact of

- unilateral concha bullosa on mucociliary activity: An assessment by rhinoscintigraphy. *Am J Rhinol Allergy* 2013;27:54-7.
36. Özkiriş M, Gencer ZK, Saydam L. The effect of unilateral concha bullosa on olfactory bulb volume: An assessment by magnetic resonance imaging. *J Craniofac Surg* 2018;29:400-2.
37. Karataş D, Yüksel F, Koç A. Volumetric correlation between concha bullosa and paranasal sinuses. *J Anat Soc India* 2017;2:131-4.
38. Kucybała I, Janik KA, Ciuk S, Storman D, Urbanik A. Nasal septal deviation and concha bullosa – Do they have an impact on maxillary sinus volumes and prevalence of maxillary sinusitis? *Pol J Radiol* 2017;82:126-33.

Unusual Multiple Arterial Variations of the Upper Limb

Abstract

During routine dissection of a 64-year-old male cadaver, multiple variations were observed in the arteries of the upper extremities. The first part of the axillary artery did not give any branches. The second part, after giving superior thoracic and thoracoacromial arteries divided into deep and superficial brachial arteries. Superficial brachial artery gave lateral thoracic artery and continued into the arm. After giving anterior circumflex humeral artery, the deep brachial artery trifurcated into the subscapular artery, posterior circumflex humeral artery, and profunda brachii artery. Understanding upper limb arterial variations are important for performing safer clinical procedures.

Keywords: Arterial variations, axillary artery, deep brachial artery, superficial brachial artery, upper limb arteries

Introduction

According to classical anatomical knowledge, the arterial supply of the upper extremity is provided by the axillary artery (AA). The AA starts at the level of the first rib and progresses to the lower border of the teres major muscle and continues as the brachial artery that divides into the radial and ulnar arteries at the elbow.

The AA is divided into three parts with regard to the pectoralis minor muscle and normally gives a total of six branches: one branch from the first, two branches from the second, and three branches from the third part. However, the frequency for the classical branching pattern of the AA was 27% in the study by Huelke.^[1]

Anatomical information regarding the branching and course of upper extremity arteries is important because these branches can be used as arterial flaps or grafts during surgical reconstruction procedures. In addition, physicians working in this field should be aware of possible variations to prevent unwanted complications and ensure successful operation during the surgery of conditions such as breast cancer, humerus fractures and dislocations, and brachial plexus and arterial injuries. This study describes multiple variations of the upper

limb arteries that have not been previously reported.^[2-4]

Case Report

During the routine dissection of the upper extremity in a 64-year-old Caucasian male donor cadaver, multiple variations were observed in the right upper extremity arteries. No surgical incisions or scar tissue were observed. The study was approved by the ethics committee and conforms to the provisions of the Declarations of Helsinki (date: May 16, 2019, number: 680).

The AA did not give any branches in the first part. The superior thoracic artery and thoracoacromial artery originated from the second part. Following these branches, the AA was divided into two terminal branches. One of these branches coursed superficial to the median nerve (MN) and was named the superficial brachial artery (SBA). The second one coursed deeper and therefore was named the deep brachial artery (DBA).^[4] SBA gave the lateral thoracic artery (LTA) and then continued as the brachial artery. The DBA gave anterior circumflex humeral artery and then trifurcated into the subscapular artery (SSA), posterior circumflex humeral artery (PCHA), and profunda brachii artery. The SSA gave the thoracodorsal artery and circumflex scapular artery. This branching pattern is shown in Figure 1. The left side

**Buse Naz Çandır,
Latif Sağlam,
İlke Ali Gürses¹,
Özcan Gayretli**

Department of Anatomy,
Istanbul Faculty of Medicine,
Istanbul University, ¹Department
of Anatomy, School of Medicine,
Koç University, Istanbul, Turkey

Article Info

Received: 20 December 2021
Accepted: 25 March 2022
Available online: ***

Address for correspondence:

Dr. Buse Naz Çandır,
Millet Caddesi, İstanbul Tıp
Fakültesi Hastanesi, Anatomi
Anabilim Dalı, 118-K, 34093
Fatih, İstanbul, Turkey.
E-mail: busenazcandir@gmail.
com

Access this article online

Website: www.jasi.org.in

DOI:
10.4103/jasi.jasi_208_21

Quick Response Code:



How to cite this article: Çandır BN, Sağlam L, Gürses IA, Gayretli Ö. Unusual multiple arterial variations of the upper limb. J Anat Soc India 2022;XX:XX-XX.

This is an open access journal, and articles are distributed under the terms of the Creative Commons Attribution-NonCommercial-ShareAlike 4.0 License, which allows others to remix, tweak, and build upon the work non-commercially, as long as appropriate credit is given and the new creations are licensed under the identical terms.

For reprints contact: WKHLRPMedknow_reprints@wolterskluwer.com

branched in the classic pattern. The classical branching pattern of the axillary artery is shown in Figure 2a and the branching pattern, in this case, is shown in Figure 2b.

Discussion

Embryological basis

Upper limb vascular development begins at the 12th stage when the upper limb bud first appears. Initially, newly developed capillary vessels enter the limb bud. As the limb bud develops, capillary vessels also develop from the distal direction. In the continuation of the development process, an artery originating from the seventh intersegmental artery becomes dominant and the other capillary vessels degenerate. This artery is named the axial (axis) artery because it develops along the central axis of the limb bud. The artery then continues to develop as the main artery supplying the upper limb. The axial artery forms the AA in the axilla in stage 15, the brachial artery in the arm at stage

17, the interosseous artery in the forearm at stage 18, and the deep palmar arch at stage 19.^[5] Other arteries of the upper extremity develop as sprouts of the axial artery.

Anomalies of the upper limb arteries are quite common and can be explained by the deviation of vascular plexuses from normal morphogenetic development and temporal sequence in the embryological period.^[6,7] Some arteries that are dominant in the initial stages of embryological development may regress later. Accordingly, SBA joining the axillary and brachial artery regresses over time.

Clinical relevance

The axillary region is of critical importance in routine clinical practice for radiologists, cardiovascular, plastic, and orthopedic surgeons who are actively interested in this region because it includes the brachial plexus, axillary lymph nodes, and axillary tail of the breast. An important weapon for a surgeon to make the necessary decisions is the knowledge of the origin, course, distribution, and anastomotic networks of the arterial branches in the region.^[8] Preparing for the presence of anatomical variations can prevent postoperative complications or unsuccessful surgery due to incorrect identification of the artery. In the literature, arterial injuries have been reported as a result of dislocation of the shoulder reduction,^[9] axillary-femoral bypass disruption,^[10] and postcatheterization.^[11] These injuries are extremely high risk as they can cause limb loss or death. This risk is further increased as a result of differences in branching patterns of the arteries in the upper extremities.

The SBA was first defined in 1928 by Adachi.^[6,12] According to this, if the brachial artery is in front of the MN, it is called the SBA.^[2,6] Therefore, in this case, the two terminal branches of the AA were defined as the SBA in front of the MN and the DBA behind it (a. brachialis profunda). The incidence of the SBA in the different populations studied ranged from 0.12% to 19.7%.^[12]

Variant superficial arteries such as SBA are more vulnerable to injury and trauma, and their damage can cause severe

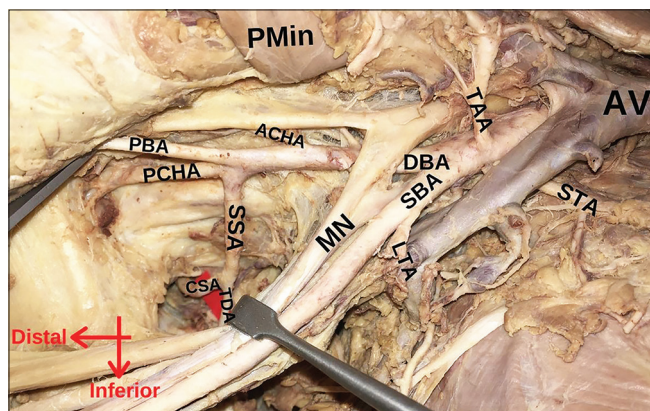


Figure 1: Branching type of the AA. ACHA: Anterior circumflex humeral artery, AV: Axillary vein, CSA: Circumflex scapular artery, DBA: Deep brachial artery, LTA: Lateral thoracic artery, MN: Median nerve, PBA: Profunda brachii artery, PCHA: Posterior circumflex humeral artery, PMin: Pectoralis minor, SBA: Superficial brachial artery, SSA: Subscapular artery, STA: Superior thoracic artery, TAA: Thoracoacromial artery, TDA: Thoracodorsal artery, AA: Axillary artery

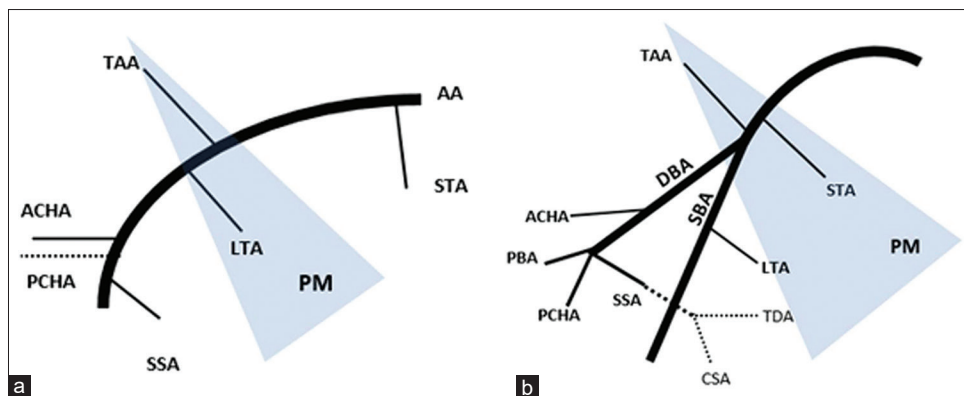


Figure 2: (a) Schematic image of the classical branching pattern of the AA. (b) Schematic image of the branching pattern in the presented case. AA: Axillary artery, PM: Pectoralis minor muscle, ACHA: Anterior circumflex humeral artery, CSA: Circumflex scapular artery, DBA: Deep brachial artery, LTA: Lateral thoracic artery, PBA: Profunda brachii artery, PCHA: Posterior circumflex humeral artery, SBA: Superficial brachial artery, SSA: Subscapular artery, STA: Superior thoracic artery, TAA: Thoracoacromial artery, TDA: Thoracodorsal artery

bleeding.^[7] During intravenous administration and catheterization, it can be considered a vein and accidentally injured. Accidental intraarterial administration of drugs can cause reflex vascular occlusion, and consequently, can lead to forearm and hand gangrene.^[13] SBA can also cause idiopathic neuropathies.^[12] In addition, it can disrupt radiological diagnostic methods such as angiography and surgeons may encounter intraoperative difficulties.^[6] Conversely, the presence of superficial arteries can provide pedicles to lift flaps for local reconstructive surgery.

LTA contributes to the supply of the breast tissue and is an important vessel as the main artery of the nipple–areolar complex.^[8,14] The nipple–areolar complex should be protected in breast surgeries such as tumor resection, reduction in gigantomastia cases, and implant placement for cosmetic or reconstruction purposes. The most important complication stated for these procedures is nipple necrosis due to arterial insufficiency.^[14] LTA is also a reliable flap option for a variety of reconstructions in terms of size, thickness, and tissue composition and is easily configurable.^[15] In this case, since LTA originates from a more distal level than its normal course, it may complicate the identification of the artery, as a result, it may disrupt the planning for reconstructive, and if damaged, it may cause problems in circulation of the breast tissue.

Circumflex arteries provide arterial supply of the humeral head, anatomical and surgical neck of the humerus, glenohumeral joint, and surrounding shoulder muscles. According to recent studies, it is suggested that the main blood supply of the humeral head is the PCHA.^[16] In deltopectoral and transdeltoid surgical approaches traditionally used for open reduction and internal fixation of proximal humeral fractures, injury to the circumflex arteries has been reported as common complications.^[16,17] Chen *et al.* aimed to define anatomical landmarks and specified reference distances for identifying and preserving the circumflex arteries.^[17] However, they stated that they analyzed these landmarks in cadavers with normal branching patterns of circumflex arteries. These reference values may not valid in our case, due to the locations and origins of the circumflex arteries.

The SSA offers a predictable and versatile donor site that can meet the needs of many microvascular reconstructions, provide any combination of subcutaneous tissue, fascia, muscle, and bone.^[18,19] It is an ideal donor artery due to its size, length, diameter, its suitable anatomical features, and is easy to harvest.^[18] Therefore, SSA flaps have been widely used in various surgeries such as upper limb restoration,^[18] repair of oromandibular and facial defects,^[20] and lower extremity soft-tissue reconstructions.^[19]

Conclusion

In conclusion, axilla is frequently used in routine clinical applications for reasons such as axillary lymph node

dissection in total and partial mastectomy, axillary lymph node biopsy, proximal humerus fractures, regional nerve block in upper extremity surgeries, and a donor area for various flaps used in reconstructive microsurgery. In these interventional procedures, knowledge of regional anatomy is important to complete surgical operations safely. Therefore, awareness on such anatomical variations and understanding that they may be more common than thought will help clinicians and surgeons achieve better and safer results.

Acknowledgment

The authors sincerely thank those who donated their bodies to science so that anatomical research could be performed.

Financial support and sponsorship

Nil.

Conflicts of interest

There are no conflicts of interest.

References

- Huelke DF. Variation in the origins of the branches of the axillary artery. *Anat Rec* 1959;135:33-41.
- Tubbs RS, Shoja MM, Loukas M, editors. *Bergman's Comprehensive Encyclopedia of Human Anatomic Variation*. Hoboken, NJ: John Wiley & Sons; 2016. p. 583-600.
- Lippert H, Pabst R. *Arterial Variations in Man: Classification and Frequency*. Munich, GER: JF Bergmann Verlag; 1985. p. 66-8.
- Adachi B. *Das Arteriensystem der Japaner*. Band 1. Kyoto, UKY, JPN: Keiserlich-Japanischen Universitat; 1928. p. 210-25.
- Rodríguez-Niedenführ M, Burton GJ, Deu J, Sañudo JR. Development of the arterial pattern in the upper limb of staged human embryos: Normal development and anatomic variations. *J Anat* 2001;199:407-17.
- Goswami P, Tigga SR, Bharihoke V. Variant course and branching of right brachial artery: A case study. *Int J Res Med Sci* 2013;1:62-5.
- Jurjus AR, Correa-De-Aruaujo R, Bohn RC. Bilateral double axillary artery: Embryological basis and clinical implications. *Clin Anat* 1999;12:135-40.
- Dimovolis I, Michalinos A, Spartalis E, Athanasiadis G, Skandalakis P, Troupis T. Tetrafurcation of the subscapular artery. Anatomical and clinical implications. *Folia Morphol (Warsz)* 2017;76:312-5.
- Eyler Y, Yılmaz Kilic T, Turgut A, Hakoglu O, Idil H. Axillary artery laceration after anterior shoulder dislocation reduction. *Turk J Emerg Med* 2019;19:87-9.
- Siani A, Marcucci G, Siani LM, Mounayergi F, Baldassarre E. A singular case of iatrogenic axillofemoral bypass disruption: A dramatic event treated by a lucky combined approach. *Ann Vasc Surg* 2009;23:413.e5-7.
- Hudorovic N, Lovricevic I, Ahel Z. *In situ* cephalic vein bypasses from axillary to the brachial artery after catheterization injuries. *Interact Cardiovasc Thorac Surg* 2010;11:103-5.
- Nkomozepi P, Xhakaza N, Swanepoel E. Superficial brachial artery: A possible cause for idiopathic median nerve entrapment neuropathy. *Folia Morphol (Warsz)* 2017;76:527-31.
- Bataineh ZM, Al-Hussain SM, Moqattash ST. Complex

- neurovascular variation in one upper limb. *Ital J Anat Embryol* 2007;112:37-44.
14. Loukas M, du Plessis M, Owens DG, Kinsella CR Jr, Litchfield CR, Nacar A, *et al.* The lateral thoracic artery revisited. *Surg Radiol Anat* 2014;36:543-9.
 15. Kim JT, Ng SW, Naidu S, Kim JD, Kim YH. Lateral thoracic perforator flap: Additional perforator flap option from the lateral thoracic region. *J Plast Reconstr Aesthet Surg* 2011;64:1596-602.
 16. Mostafa E, Imonugo O, Varacallo M. Anatomy, shoulder and upper limb, humerus. In: *StatPearls*. Treasure Island (FL): StatPearls Publishing; 2021.
 17. Chen YX, Zhu Y, Wu FH, Zheng X, Wangyang YF, Yuan H, *et al.* Anatomical study of simple landmarks for guiding the quick access to humeral circumflex arteries. *BMC Surg* 2014;14:39.
 18. Valnicek SM, Mosher M, Hopkins JK, Rockwell WB. The subscapular arterial tree as a source of microvascular arterial grafts. *Plast Reconstr Surg* 2004;113:2001-5.
 19. Karşıdağ S, Akçal A, Turgut G, Uğurlu K, Baş L. Lower extremity soft tissue reconstruction with free flap based on subscapular artery. *Acta Orthop Traumatol Turc* 2011;45:100-8.
 20. Shaw RJ, Ho MW, Brown JS. Thoracodorsal artery perforator – Scapular flap in oromandibular reconstruction with associated large facial skin defects. *Br J Oral Maxillofac Surg* 2015;53:569-71.

Milder and Later Presentation of Trisomy 13: A Case Report and Literature Review

Abstract

Patau syndrome or Trisomy 13 is the least common and most severe of the viable autosomal trisomies. The frequent clinical features include holoprosencephaly, polydactyly, flexion of the fingers, rocker-bottom feet, cleft lip and palate, neural tube defects, and heart defects, with neurological involvement being the most consistent one. It is usually recognized at birth by the typical birth defects with poor neurologic performance. About 85%–90% of cases die during infancy, with only 5% to 10% of patients alive beyond 1 year. Patients surviving beyond 1 year have a severe developmental handicap. We present here an infant who came with a relatively milder form of Patau syndrome and was confirmed by karyotyping.

Keywords: *Infancy, karyotyping, Patau syndrome, trisomy 13*

Introduction

Trisomy 13 or Patau syndrome described first in 1960, is a chromosomal disorder wherein an individual has an extra copy of chromosome 13 and occurs in about 1 in every 12,500 newborns.^[1-5] It can be caused by free trisomy of chromosome 13 in 75% of cases, and trisomy from Robertsonian translocations in 25% of cases. Clinical features include a wide spectrum of major central nervous system (CNS) anomalies (45%–55%) such as holoprosencephaly, agenesis of the corpus callosum, and cerebellar malformations; craniofacial anomalies (80%) in the form of midline defects, such as bilateral cleft lip and palate, micro and anophthalmia, and micrognathia; congenital heart disease (40%–50%) such as septation defects and dextrocardia and absent pulmonary venous return; urinary tract anomalies (30%–35%) such as cystic renal dysplasia; skeletal anomalies (20%–30%) such as postaxial polydactyly and clenched hands; and abdominal wall anomalies (30%) such as exomphalos.^[6] It is a lethal condition in the majority of cases and 95% of the survivors die in early infancy.^[6] There could be severe psychomotor delay and blindness associated with epilepsy. Patients

This is an open access journal, and articles are distributed under the terms of the Creative Commons Attribution-NonCommercial-ShareAlike 4.0 License, which allows others to remix, tweak, and build upon the work non-commercially, as long as appropriate credit is given and the new creations are licensed under the identical terms.

For reprints contact: WKHLRPMedknow_reprints@wolterskluwer.com

surviving beyond one year have a severe developmental handicap.^[7]

Case Report

A 5-month-old male baby was brought with complaints of cough, fever for 3 days, hurried breathing, and chest retractions for 1 day. The patient was the second child of a nonconsanguinously married couple, the mother being elderly (35 years old). He was born by lower-segment cesarean section at term, with uneventful antenatal and perinatal history. There was no history of seizures. His elder brother is 2 years old and is developmentally normal. On admission, the baby was found to have tachypnea with a respiratory rate of 80 breaths/min with severe chest retractions and without cyanosis. There were bilateral scattered crepitations with expiratory wheeze on auscultation. The cardiovascular system examination was normal. General physical examination revealed the presence of a long philtrum, complete cleft palate, and large open anterior fontanel (5 cm × 5 cm) with fused posterior fontanel, low-set ears, micrognathia, pectus carinatum, and overlapping of the second toe over the third toe in both feet. Hands were normal with no polydactyly observed. The baby was said to be treated at the age of 2 months for bilateral congenital talipes equinovarus. However,

How to cite this article: Rashmi. N, Kiran HS, Rajani HS. Milder and later presentation of trisomy 13: A case report and literature review. *J Anat Soc India* 2022;XX:XX-XX.

Rashmi. N,
H. S. Kiran¹,
H. S. Rajani

Departments of Pediatrics and ¹Internal Medicine, JSS Medical College and Hospital, JSSAHER, Mysuru, Karnataka, India

Article Info

Received: 26 August 2021

Revised: 21 July 2022

Accepted: 26 July 2022

Available online: ***

Address for correspondence:

Dr. Rashmi. N,
Associate Professor,
Department of Pediatrics,
JSS Medical College,
JSSAHER, Mysuru,
Karnataka, India.
E-mail: dr.rashminagaraj@gmail.com

Access this article online

Website: www.jasi.org.in

DOI:
10.4103/jasi.jasi_149_21

Quick Response Code:



he was found to have rocker-bottom feet on examination [Figure 1 - written informed consent taken].

There was generalized hypotonia with gross motor developmental delay. However, other areas of development were normal. All these features suggested a clinical suspicion of trisomy 13 presenting with bronchopneumonia.

Investigations such as complete hemogram, blood urea, serum creatinine, blood sugar, serum calcium, phosphorus, magnesium, alkaline phosphatase, liver function test, thyroid function test, serum electrolytes, serum lactate,

and serum ammonia levels were within the normal limits. The blood culture was sterile. Fundoscopy was normal and ultrasound abdomen did not reveal any abnormality.

X-ray of the chest showed right paracardiac haziness. Two-dimensional echocardiography revealed mild pulmonary arterial hypertension (37 mmHg), with intact septa. A computed tomography scan of the brain showed a persistent cavum septum pellucidum.

Karyotyping confirmed the diagnosis of Patau syndrome (trisomy 13) [Figure 2].

However, the baby was only mildly affected as against its presentation as described in the literature. The baby was treated for lung infection, including supportive treatment and rehabilitation with occupational therapy, for his developmental disabilities. He was advised to be on regular follow-up.

Discussion

Patau syndrome is characterized by the following triad: microphthalmia, cleft lip and palate, and polydactyly. The face may also be characterized by prominent glabellae, ocular hypertelorism, anophthalmia, and micrognathia. Our patient had depressed nasal bridge, low-set ears, micrognathia, hypertelorism, long philtrum but no cleft lip, prominent glabella, cleft palate, and congenital talipes equinovarus. However, he did not have microphthalmia or anophthalmia, cardiac malformations, and hemangiomas.



Figure 1: Image describing clinical features

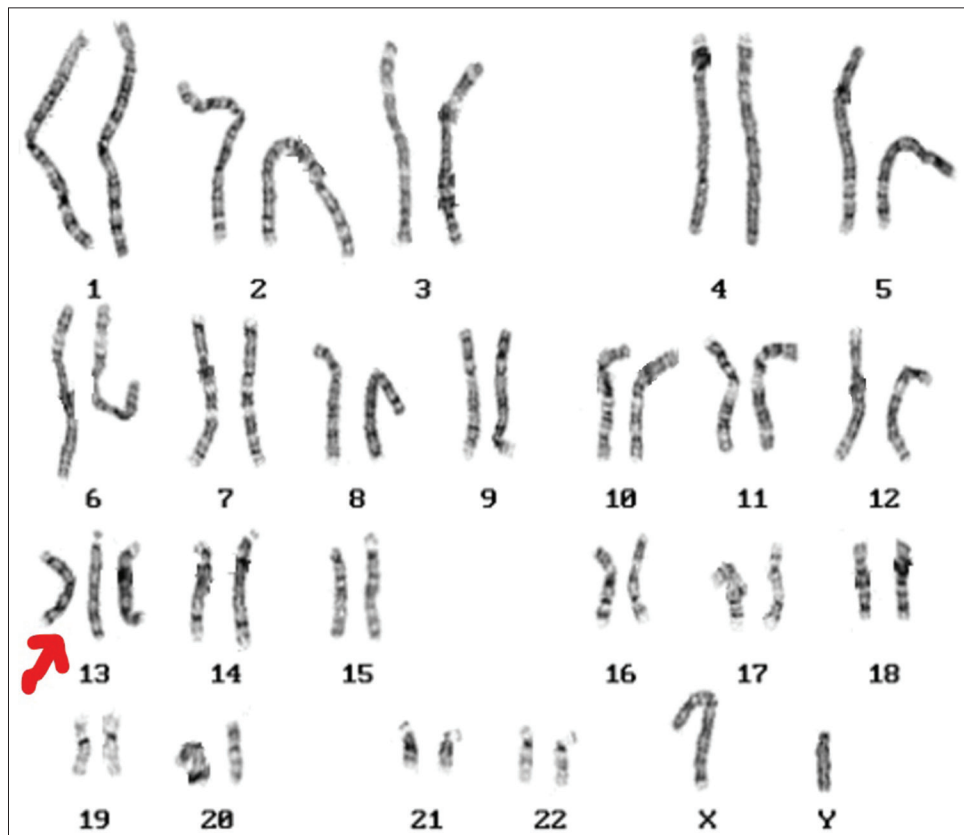


Figure 2: Image of karyotyping

The mean maternal age is increased for free trisomy 13.^[8,9] This fact was evident in our case also, the baby's mother being elderly. Twenty-eight percent of newborns with Patau syndrome die within the 1st week of life, 44% in the 1st month, and 86% by 1 year of age. The median survival age is 2.5 days, and only a small number of cases experience puberty age. Most infants with Patau syndrome have high mortality: 69% from cardiopulmonary failure, 13% from congenital heart defects, and 4% from pneumonia.^[8,9] The baby presented here did not have significant morbidity till this time and could be possibly due to the absence of cardiac defects. He also did not have seizures or CNS malformations such as holoprosencephaly which is common in this condition.

Spontaneous abortions, especially after 12 weeks of gestation, are 100 times more common in trisomy 13 than in any other condition. About half of pregnancies diagnosed with trisomy 13 are estimated to end with miscarriage or stillbirth between 12 weeks of gestation and term.^[8,9] The estimated mortality rate is about 50 times higher in this condition in comparison with the general neonatal mortality rate.^[8] Eighty-two percent die within 1 month and 85% do not live beyond 1-year survival beyond 1 year of age was found to be associated with mosaicism.^[10]

Children who survive beyond the neonatal period continue to show developmental delays with a declining developmental quotient over time. This progressively decreasing developmental quotient however does not result from loss of developmental milestones but from a worsening developmental lag when compared with other normal children. A report on a group of 21 individuals with Patau syndrome (3 mosaics and 18 nonmosaics) who survived past age 5 years showed the oldest to be aged 21 years.^[9]

Prenatal diagnosis can be made by G-banding of chromosomes from the chorionic villi, amniocytes, and peripheral leukocytes, and also by ultrasound screening done at 12–14 weeks of gestation, which can reveal an enlarged nuchal translucency.^[6]

A retrospective cohort study by Dotters-Katz *et al.* showed that the risk of certain morbidities was higher in women with a trisomy 13 pregnancy than in those with a nontrisomy 13 pregnancy, with the likelihood of gestational hypertensive disorder being 6.3 times greater and the risk for severe preeclampsia being 12.5 times higher.^[11]

The other diagnostic considerations in such cases would be Edwards syndrome, partial duplication of 13q, and pseudotrismy 13 (holoprosencephaly–polydactyly syndrome). The clinical phenotypes of Patau syndrome and Edwards syndrome may seem similar to physicians who do not frequently encounter these syndromes.

Conclusion

Patau syndrome involves a recognizable pattern of multiple congenital anomalies with increased neonatal and infant

mortality and significant intellectual disability in older children, posing challenges for primary care practitioners and specialists. However, there could be a milder presentation of the same also, as in our child. Hence, a high index of suspicion is important to make a diagnosis and intervene early, which may improve the quality of life both for parents and the child.

Declaration of patient consent

The authors certify that they have obtained all appropriate patient consent forms. In the form, the parents have given their consent for the child's images and other clinical information to be reported in the journal. The parents understand that their names and initials will not be published and due efforts will be made to conceal their identity, but anonymity cannot be guaranteed.

Financial support and sponsorship

Nil.

Conflicts of interest

There are no conflicts of interest.

References

- Irving C, Richmond S, Wren C, Longster C, Embleton ND. Changes in fetal prevalence and outcome for trisomies 13 and 18: A population-based study over 23 years. *J Matern Fetal Neonatal Med* 2011;24:137-41.
- Parker SE, Mai CT, Canfield MA, Rickard R, Wang Y, Meyer RE, *et al.* Updated national birth prevalence estimates for selected birth defects in the United States, 2004-2006. *Birth Defects Res A Clin Mol Teratol* 2010;88:1008-16.
- Savva GM, Walker K, Morris JK. The maternal age-specific live birth prevalence of trisomies 13 and 18 compared to trisomy 21 (Down syndrome). *Prenat Diagn* 2010;30:57-64.
- Vendola C, Canfield M, Daiger SP, Gambello M, Hashmi SS, King T, *et al.* Survival of Texas infants born with trisomies 21, 18, and 13. *Am J Med Genet Part A* 2010;152A: 360-6.
- Crider KS, Olney RS, Cragan JD. Trisomies 13 and 18: Population prevalences, characteristics, and prenatal diagnosis, metropolitan Atlanta, 1994-2003. *Am J Med Genet A* 2008;146A:820-6.
- Paladini D, Greco E, Sglavo G, D'Armiento MR, Penner I, Nappi C. Congenital anomalies of upper extremities: Prenatal ultrasound diagnosis, significance, and outcome. *Am J Obstet Gynecol* 2010;202:596.e1-10.
- Lin HY, Lin SP, Chen YJ, Hung HY, Kao HA, Hsu CH, *et al.* Clinical characteristics and survival of trisomy 18 in a medical center in Taipei, 1988-2004. *Am J Med Genet A* 2006;140:945-51.
- Schinzel A. *Catalogue of Unbalance Chromosome Aberration in Man*. 2nd ed. Berlin, New York: Walter de Gruyter; 2001. p. 505-10.
- Morris JK, Savva GM. The risk of fetal loss following a prenatal diagnosis of trisomy 13 or trisomy 18. *Am J Med Genet A* 2008;146A:827-32.
- Hsu HF, Hou JW. Variable expressivity in Patau syndrome is not all related to trisomy 13 mosaicism. *Am J Med Genet A* 2007;143A:1739-48.
- Dotters-Katz SK, Humphrey WM, Senz KL, Lee VR, Shaffer BL, Kuller JA, *et al.* Trisomy 13 and the risk of gestational hypertensive disorders: A population-based study. *J Matern Fetal Neonatal Med* 2018;31:1951-5.

Case Report of Persistent Left Superior Vena Cava with Absent Papillary Muscle – Unusual Coexistence

Abstract

Persistent left superior vena cava (PLSVC) is uncommon with an incidence of 0.3%–1.3%. The incidence of absent papillary muscle is unknown. Congenital anomalies of a thoracic venous system associated with absent papillary muscle are very rare. During dissection of a 55-year-old male cadaver, PLSVC with absent papillary muscle was found. Although these congenital anomalies are incidentally found, it is worthwhile following such patients to look for the evolution of any cardiac symptoms. Sound knowledge and awareness of such congenital anomalies are required for radiologists, cardiothoracic surgeons, and critical care physicians.

Keywords: Heart failure, papillary muscle, tricuspid regurgitation

Introduction

Congenital anomalies of the thoracic venous system are uncommon. These anomalies are commonly encountered incidentally, yet the knowledge of them is necessary for the prevention of misdiagnosis. Superior vena cava (SVC) is the second-largest valveless vein in the human body. It is located in the anterior right superior mediastinum with a length measuring 7 cm and a width of 24 mm. SVC is formed by the union of the right and left brachiocephalic veins, and finally, drains into the right atrium. It extends from the confluence of the brachiocephalic veins behind the first right costal cartilage, and at the level of the second costal cartilage, SVC enters the middle mediastinum piercing the fibrous pericardium and eventually drains into the right atrium, at the level of third right costal cartilage. The main function of the SVC is to drain the blood from the upper half of the body above the diaphragm into the right atrium. SVC receives tributaries from the left and right brachiocephalic veins and azygos veins. The minor tributaries such as mediastinal veins, esophageal veins, and pericardial veins drain into the azygos vein. SVC is considered to be an ideal site for the insertion of a central venous catheter for monitoring fluid levels, especially when peripheral veins are difficult to access, in

patients admitted to the intensive care unit. Variant anatomy of the SVC can lead to misplacement of central venous catheter leading to serious complications in the patient.^[1] Sound knowledge of normal anatomy and the possible variations of SVC are necessary for clinicians and radiologists.

Double SVC is an infrequent variation of the venous system. In double SVC, the most common type is persistent left superior vena cava (PLSVC), but in the general population, its incidence is reported to be around 0.3%–1.3% only.^[2-4] The prevalence increases up to 11% when it is associated with other congenital cardiac abnormalities.^[5] Although most individuals do not encounter any problems, rarely it can cause tricuspid regurgitation leading to heart failure clinically.

Papillary muscles are pillar-like muscles present in the ventricles of the heart. It attaches the cusps to the ventricular wall by chordae tendineae. The main function is to help in the tight closure of the atrioventricular valves during the systole phase. The absence of papillary muscle is an uncommon variation with unknown prevalence. Tricuspid regurgitation can be caused due to decrease in the number of the papillary muscles in the ventricles.^[6]

Numerous double SVC with congenital cardiac anomalies cases have been reported earlier. However, a congenital anomaly

Divya Umamaheswaran, Jayagandhi Sakkarai, Rema Devi

Department of Anatomy, Pondicherry Institute of Medical Sciences, Puducherry, India

Article Info

Received: 28 May 2022

Revised: 13 July 2022

Accepted: 25 July 2022

Available online: ***

Address for correspondence:

Dr. Divya Umamaheswaran, Department of Anatomy, Pondicherry Institute of Medical Sciences, Puducherry - 605 014, India.

E-mail: divilatha21@gmail.com

Access this article online

Website: www.jasi.org.in

DOI: 10.4103/jasi.jasi_81_22

Quick Response Code:



This is an open access journal, and articles are distributed under the terms of the Creative Commons Attribution-NonCommercial-ShareAlike 4.0 License, which allows others to remix, tweak, and build upon the work non-commercially, as long as appropriate credit is given and the new creations are licensed under the identical terms.

For reprints contact: WKHLRPMedknow_reprints@wolterskluwer.com

How to cite this article: Umamaheswaran D, Sakkarai J, Devi R. Case report of persistent left superior vena cava with absent papillary muscle – Unusual coexistence. *J Anat Soc India* 2022;XX:XX-XX.

with double SVC associated with absent papillary muscle has not been reported, and to the best of our knowledge, it is the first report from a cadaver.

Case Report

During routine dissection of an adult male cadaver of approximately 55 years, in the Department of Anatomy in Pondicherry Institute of Medical Sciences, on opening the thoracic cavity, two veins entering the heart were noted. Further dissection was done, and the presence of double SVC (right and PLSVC) was confirmed as shown in Figure 1a and b.

Venous system variation

The PLSVC was narrower (17 mm) than the right element. There was no variation in the length of both SVC (69 mm). The right SVC was draining into the right atrium directly and had a normal diameter of about 25 mm. It was seen as the continuation of a right brachiocephalic vein which was formed by the confluence of the right internal jugular vein and right subclavian vein. The right internal jugular vein, measuring 26 mm in diameter, was dilated. The formation of both SVC and right IJV dilatation is shown in Figure 1c. The left SVC was formed as a continuation of the left brachiocephalic vein. A confluence of the left internal jugular and left subclavian vein led to the formation of the left brachiocephalic vein. The coronary sinus was receiving the left SVC in the superior border and draining into the right atrium. Since the coronary sinus was receiving an additional venous channel, it was found to be dilated, measuring 17 mm, as shown in Figure 1d. A venous channel which acts as a communication between the right and left SVC called oblique communication during embryogenesis was observed between the left and right SVC. It was noted below the sternal angle, 60 mm below

the thyroid cartilage, and 20 mm above the aortic arch. It was narrow measuring about 9 mm in diameter.

Inferior vena cava (IVC), azygos and hemiazygos vein formation and drainage were noted. IVC formation and drainage were normal, but IVC was dilated significantly (30 mm diameter). Azygos formation and drainage were normal. The hemiazygos formation was normal, but it was draining into the left persistent SVC.

No anomalies were observed in the arterial system. The brachiocephalic trunk, common carotid artery, and left subclavian were arising from the aortic arch directly. The thoracic duct, vagus nerve, and sympathetic trunks were noted to be normal.

Variations in the heart

On exploratory dissection of the interior of the heart, the right auricle and right atrium were found to be enlarged. Dilatation of coronary sinus opening was observed. The left atrium appeared normal and four pulmonary veins were draining into it. There were no defects in the interatrial septum. The tricuspid valve appeared patulous and dilated, with the orifice measuring 45 mm × 30 mm in diameter, and with a surface area of about 10.5 cm² [Figure 2a]. Mitral orifice and mitral valves were normal. The right ventricular wall was thin. The thickness of the wall was 5 mm. Only anterior papillary muscle of ventricle was noted and appeared to be thin; thickness measured only 3 mm [Figure 2b]. Posterior and septal papillary muscles were absent. The moderator band was present, but it was very thin measuring 2 mm in thickness. The thickness of the left ventricle was normal, measuring about 20 mm. The anterior and posterior papillary muscles were present [Figure 2c]. No defects were noted in the interventricular septum. On comparing the thickness of the right ventricle and left ventricle, the left ventricle was

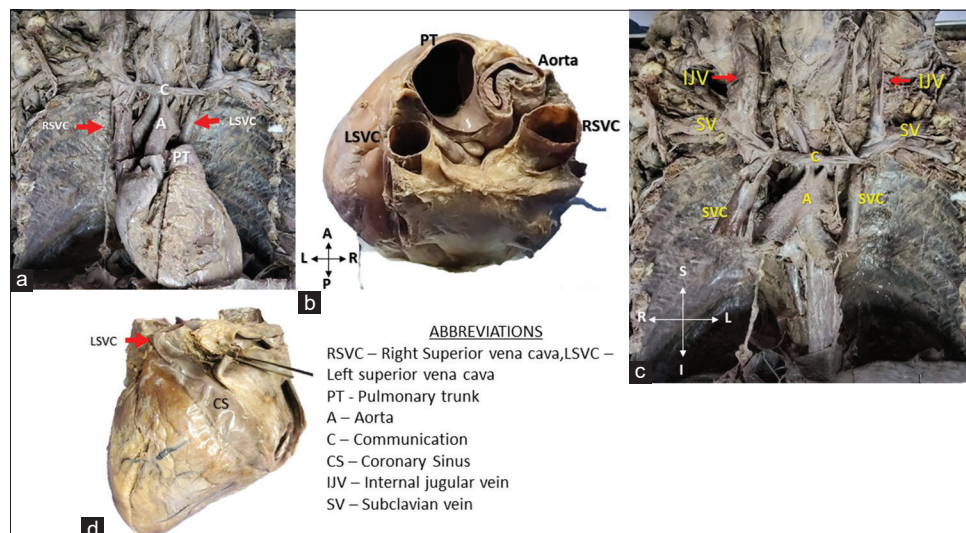


Figure 1: (a) Double SVC with heart *in situ* and pulmonary arteries removed. (b) Superior view of the heart showing double SVC. (c) Formation of both SVC with oblique communication. (d) Dilated coronary sinus. SVC: Superior vena cava

found to be four times thicker than the right ventricle which implies that there is a significant right ventricular wall dilatation.

Classifications of double superior vena cava

Numerous classifications have been proposed for double SVC based on the presence or absence of the right SVC, presence or absence of the anastomotic venous channel between the right and left SVC, and presence or absence of the paired azygos vein^[7] and in association with congenital heart diseases.^[8] In combination with all these three criteria, Uemura *et al.* concluded with 24 types of DSVC.^[9] Although these classifications provide a better understanding, considering the importance of the drainage pattern of the left SVC, Zhang *et al.* recently proposed a newer classification based on the presence or absence of the left brachiocephalic vein and drainage pattern of the left SVC.^[10]

Zhang *et al.*'s Classification

- Type I – LBCV absent, LSVC drains into the right atrium via the coronary sinus
- Type II – LBCV present, LSVC drains into the right atrium via the coronary sinus
- Type III – LBCV absent, LSVC drains into the right atrium via anastomosis
- Type IV – LBCV present, LSVC drains into the right atrium via anastomosis.

If the LSVC drains into the left atrium, it is classified as others.

Type II was found to be more prevalent than other types. This classification would also provide a better vision for clinicians to understand the hemodynamic changes better in case of a double SVC anomaly.

Discussion

In most instances, double SVC is incidentally encountered. Mc Cotters reported the first case of double SVC in 1918.^[11] About 80%–90% of PLSVC drains into the coronary sinus^[12] but 10%–20% drains into the left

atrium.^[13] This case reports double SVC with the presence of oblique connection between two SVC and also with an interesting finding of the absence of papillary muscle of the right ventricle. Schematic representation of which is shown in Figure 3. As per Zhang *et al.*^[10] classification, this anomaly can be classified as Type II with the additional presence of oblique connection making it an exceptional report. In literature, the absence or presence of one papillary muscle in the left ventricle is reported so far.^[14] However, the absence or presence of one papillary muscle in the right ventricle is not reported. There are multiple congenital anomalies and abnormalities noted in this case which is very uncommon. PLSVC can be attributed to the failure of regression of the left anterior cardinal vein, around 8 weeks of intrauterine life. An oblique connection was found which was serving as a communicating venous channel between the right and left SVC. After the regression of the left anterior and left common cardinal vein, this oblique connection is transformed into the future left brachiocephalic vein. However, the failure of regression of the above led to the persistence of this oblique connection, which is very rare in the case of PLSVC. Another congenital anomaly observed is an absence of posterior and septal papillary muscle in the right ventricle which is due to the failure of formation of trabecular cord from the ventricular surface, around 7–19 weeks.

In this case, there are also some evident features of right heart failure such as enlargement of the right atrium, right ventricle, dilatation of the right internal jugular vein, and IVC which are all due to the presence of the abovementioned congenital anomalies. PLSVC draining into the coronary sinus has caused coronary sinus dilatation. Coronary sinus was draining into the right atrium which caused an overload in the right atrium leading to enlargement. The absence of posterior and septal papillary muscle in the right ventricle caused improper closure of the valve leading to loss of patency of the tricuspid valve. A patulous valve and overloaded right atrium may have caused tricuspid regurgitation which explains the right ventricular dilatation as evidenced by the thinning of the right ventricular wall.

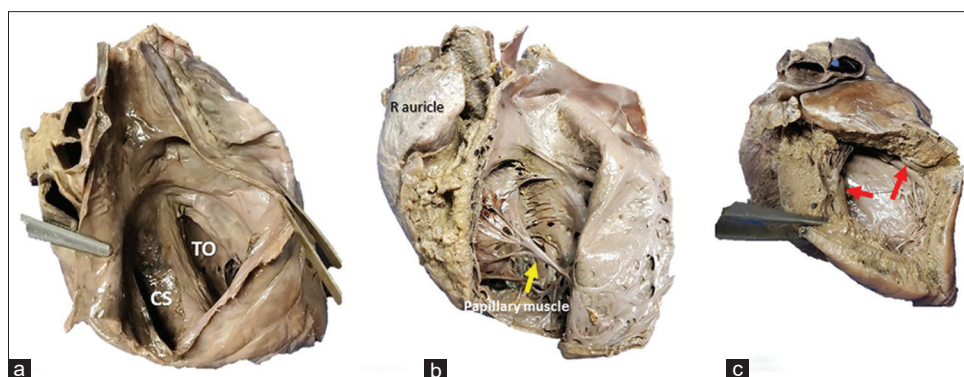


Figure 2: (a) The interior of the right atrium with dilated coronary sinus ostium and patulous tricuspid valve. (b) Thinned right ventricular wall and the yellow arrow show the anterior papillary muscle. (c) The interior of the left ventricle and red arrow showing anterior and posterior papillary muscles

Eventually, it led to heart failure as was seen by the right internal jugular vein and IVC dilatation. Since persistent left superior vena and absent papillary muscle can account for tricuspid regurgitation,^[6,14] in this case, this combined congenital anomaly caused heart failure which is evident by the features. Flowchart explaining the findings of heart failure is shown in Figure 4.

Heart embryogenesis starts around 3 weeks. NK 2 is the master gene for the development of the heart. It is expressed by combined activity bone morphogenetic protein (BMP 3) expression and suppression of WNT. A defect in the NK 2.5 gene would have caused improper development of the heart leading to failure of development of papillary muscle. Venous development is regulated by notch signaling which upregulates the expression of the EPHD 4 gene, which is

responsible for the development of veins. Alterations in the expression would have led to anomalies in the thoracic venous system. Development of the venous system and papillary muscle is around 5–19 weeks. Some disturbance in the process of organogenesis during around 5–19 weeks might have caused these multiple congenital anomalies.

Conclusion

Although many PLSVC case reports are reported earlier, to the best of our knowledge, this is the first cadaveric case report showing PLSVC associated with absent papillary muscle with evident features of tricuspid regurgitation and heart failure. To conclude, persistent double SVC in most of the instances found incidentally, those patients can be followed up to diagnose and prevent heart failure in future.

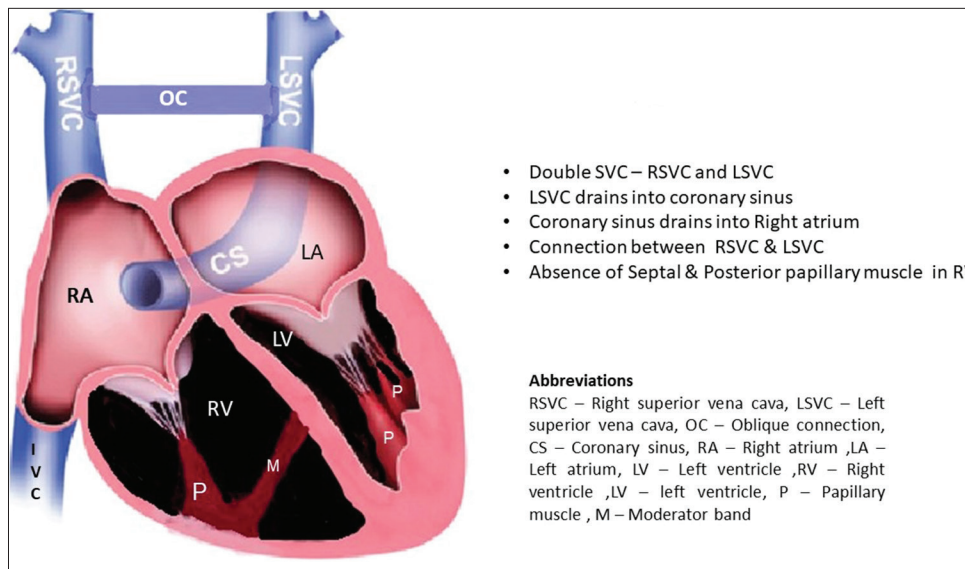


Figure 3: The schematic representation of this report

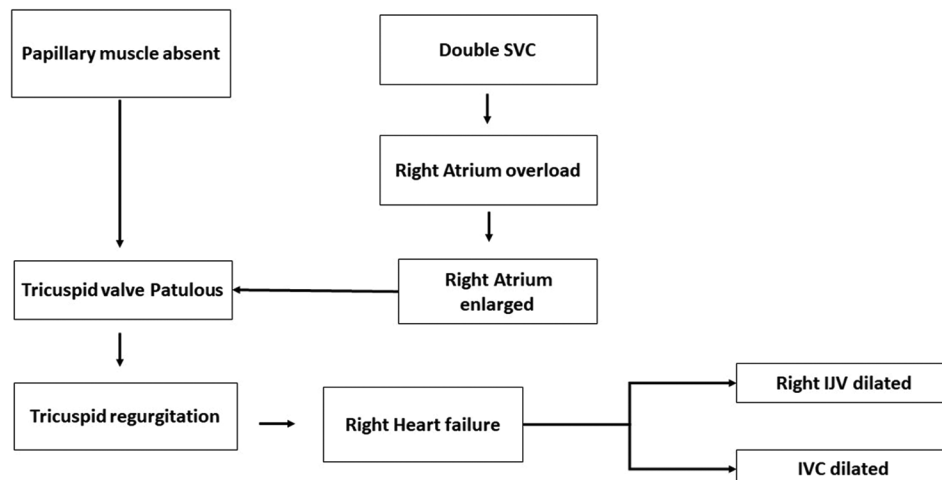


Figure 4: Flowchart explaining evident features of heart failure (tricuspid regurgitation)

Knowledge and awareness of anatomical variation of SVC and papillary muscle are required for radiologists to prevent misdiagnosis, cardiothoracic surgeons, and critical care physicians for better patient management.

Acknowledgments

The authors sincerely thank those who donated their bodies to science so that anatomical research could be performed. Results from such research can potentially increase humankind's overall knowledge that can then improve patient care. These body donors and their families deserve our highest gratitude. The authors also thank all the faculties of the department of anatomy and the nonteaching staff of the department.

Financial support and sponsorship

Nil.

Conflicts of interest

There are no conflicts of interest.

References

- Schummer W, Schummer C, Fröber R. Persistent left superior vena cava and central venous catheter position: Clinical impact illustrated by four cases. *Surg Radiol Anat* 2003;25:315-21.
- Perles Z, Nir A, Gavri S, Golender J, Tashma A, Ergaz Z, *et al.* Prevalence of persistent superior vena cava and association with congenital heart anomalies. *Am J Cardiol* 2013;112:1214-8.
- Nagasawa H, Kuwabara N, Goto H, Omoya K, Yamamoto T, Terazawa A, *et al.* Incidence of persistent left superior vena cava in the normal population and in patients with congenital heart diseases detected using echocardiography. *Pediatr Cardiol* 2018;39:484-90.
- Peltier J, Destrieux C, Desme J, Renard C, Remond A, Velut S. The persistent left superior vena cava: Anatomical study, pathogenesis and clinical considerations. *Surg Radiol Anat* 2006;28:206-10.
- Eldin GS, El-Segaier M, Galal MO. High prevalence rate of left superior vena cava determined by echocardiography in patients with congenital heart disease in Saudi Arabia. *Libyan J Med* 2013;8:21679.
- Tian C, Pan S. Congenital absence of anterior papillary muscle of the tricuspid valve and surgical repair with artificial chordae. *Interact Cardiovasc Thorac Surg* 2017;24:299-300.
- Nandy K, Blair CB Jr. Double superior venae cavae with completely paired azygos veins. *Anat Rec* 1965;151:1-9.
- Steinberg I, Dubilier W Jr., Lukas DS. Persistence of left superior vena cava. *Dis Chest* 1953;24:479-88.
- Uemura M, Suwa F, Takemura A, Toda I, Morishita A. Classification of persistent left superior vena cava considering presence and development of both superior venae cavae, the anastomotic ramus between superior venae cavae, and the azygos venous system. *Anat Sci Int* 2012;87:212-22.
- Zhang L, Ling G, Gang Y, Yang Z, Lu Z, Gan X, *et al.* Classification and quantification of double superior vena cava evaluated by computed tomography imaging. *Quant Imaging Med Surg* 2022;12:1405-14.
- McCotter: Left Superior Vena Cava – Google Scholar. Available from: https://scholar.google.com/scholar_lookup?journal=Anat+Rec&title=Three+cases+of+the+persistence+of+the+left+superior+vena+cava&author=RE+McCotter&volume=10&publication_year=1916&pages=371-383&doi=10.1002/ar.1090100503&. [Last accessed on 2022 Jul 13].
- Goyal SK, Punnam SR, Verma G, Ruberg FL. Persistent left superior vena cava: A case report and review of literature. *Cardiovasc Ultrasound* 2008;6:50.
- Dinasarapu CR, Adiga GU, Malik S. Recurrent cerebral embolism associated with indwelling catheter in the presence of anomalous neck venous structures. *Am J Med Sci* 2010;340:421-3.
- Baird CW, Bengur AR, Bensky A, Watts LT. Congenital absence of posteromedial papillary muscle and anterior mitral leaflet chordae: The use of three-dimensional echocardiography and approach in complex pediatric mitral valve disease. *J Thorac Cardiovasc Surg* 2010;139:e75-7.

The Editorial Process

A manuscript will be reviewed for possible publication with the understanding that it is being submitted to Journal of the Anatomical Society of India alone at that point in time and has not been published anywhere, simultaneously submitted, or already accepted for publication elsewhere. The journal expects that authors would authorize one of them to correspond with the Journal for all matters related to the manuscript. All manuscripts received are duly acknowledged. On submission, editors review all submitted manuscripts initially for suitability for formal review. Manuscripts with insufficient originality, serious scientific or technical flaws, or lack of a significant message are rejected before proceeding for formal peer-review. Manuscripts that are unlikely to be of interest to the Journal of the Anatomical Society of India readers are also liable to be rejected at this stage itself.

Manuscripts that are found suitable for publication in Journal of the Anatomical Society of India are sent to two or more expert reviewers. During submission, the contributor is requested to provide names of two or three qualified reviewers who have had experience in the subject of the submitted manuscript, but this is not mandatory. The reviewers should not be affiliated with the same institutes as the contributor/s. However, the selection of these reviewers is at the sole discretion of the editor. The journal follows a double-blind review process, wherein the reviewers and authors are unaware of each other's identity. Every manuscript is also assigned to a member of the editorial team, who based on the comments from the reviewers takes a final decision on the manuscript. The comments and suggestions (acceptance/ rejection/ amendments in manuscript) received from reviewers are conveyed to the corresponding author. If required, the author is requested to provide a point by point response to reviewers' comments and submit a revised version of the manuscript. This process is repeated till reviewers and editors are satisfied with the manuscript.

Manuscripts accepted for publication are copy edited for grammar, punctuation, print style, and format. Page proofs are sent to the corresponding author. The corresponding author is expected to return the corrected proofs within three days. It may not be possible to incorporate corrections received after that period. The whole process of submission of the manuscript to final decision and sending and receiving proofs is completed online. To achieve faster and greater dissemination of knowledge and information, the journal publishes articles online as 'Ahead of Print' immediately on acceptance.

Clinical trial registry

Journal of the Anatomical Society of India favors registration of clinical trials and is a signatory to the Statement on publishing clinical trials in Indian biomedical

journals. Journal of the Anatomical Society of India would publish clinical trials that have been registered with a clinical trial registry that allows free online access to public. Registration in the following trial registers is acceptable: <http://www.ctri.in/>; <http://www.actr.org.au/>; <http://www.clinicaltrials.gov/>; <http://isrctn.org/>; <http://www.trialregister.nl/trialreg/index.asp>; and <http://www.umin.ac.jp/ctr>. This is applicable to clinical trials that have begun enrollment of subjects in or after June 2008. Clinical trials that have commenced enrollment of subjects prior to June 2008 would be considered for publication in Journal of the Anatomical Society of India only if they have been registered retrospectively with clinical trial registry that allows unhindered online access to public without charging any fees.

Authorship Criteria

Authorship credit should be based only on substantial contributions to each of the three components mentioned below:

1. Concept and design of study or acquisition of data or analysis and interpretation of data;
2. Drafting the article or revising it critically for important intellectual content; and
3. Final approval of the version to be published.

Participation solely in the acquisition of funding or the collection of data does not justify authorship. General supervision of the research group is not sufficient for authorship. Each contributor should have participated sufficiently in the work to take public responsibility for appropriate portions of the content of the manuscript. The order of naming the contributors should be based on the relative contribution of the contributor towards the study and writing the manuscript. Once submitted the order cannot be changed without written consent of all the contributors. The journal prescribes a maximum number of authors for manuscripts depending upon the type of manuscript, its scope and number of institutions involved (vide infra). The authors should provide a justification, if the number of authors exceeds these limits.

Contribution Details

Contributors should provide a description of contributions made by each of them towards the manuscript. Description should be divided in following categories, as applicable: concept, design, definition of intellectual content, literature search, clinical studies, experimental studies, data acquisition, data analysis, statistical analysis, manuscript preparation, manuscript editing and manuscript review. Authors' contributions will be printed along with the article. One or more author should take responsibility for the integrity of the work as a whole from inception to published article and should be designated as 'guarantor'.

Conflicts of Interest/ Competing Interests

All authors of must disclose any and all conflicts of interest they may have with publication of the manuscript or an institution or product that is mentioned in the manuscript and/or is important to the outcome of the study presented. Authors should also disclose conflict of interest with products that compete with those mentioned in their manuscript.

Submission of Manuscripts

All manuscripts must be submitted on-line through the website <https://review.jow.medknow.com/jasi>. First time users will have to register at this site. Registration is free but mandatory. Registered authors can keep track of their articles after logging into the site using their user name and password.

- If you experience any problems, please contact the editorial office by e-mail at editor@jasi.org.in

The submitted manuscripts that are not as per the "Instructions to Authors" would be returned to the authors for technical correction, before they undergo editorial/peer-review. Generally, the manuscript should be submitted in the form of two separate files:

[1] Title Page/First Page File/covering letter:

This file should provide

1. The type of manuscript (original article, case report, review article, Letter to editor, Images, etc.) title of the manuscript, running title, names of all authors/ contributors (with their highest academic degrees, designation and affiliations) and name(s) of department(s) and/ or institution(s) to which the work should be credited, . All information which can reveal your identity should be here. Use text/rtf/doc files. Do not zip the files.
2. The total number of pages, total number of photographs and word counts separately for abstract and for the text (excluding the references, tables and abstract), word counts for introduction + discussion in case of an original article;
3. Source(s) of support in the form of grants, equipment, drugs, or all of these;
4. Acknowledgement, if any. One or more statements should specify 1) contributions that need acknowledging but do not justify authorship, such as general support by a departmental chair; 2) acknowledgments of technical help; and 3) acknowledgments of financial and material support, which should specify the nature of the support. This should be included in the title page of the manuscript and not in the main article file.
5. If the manuscript was presented as part at a meeting, the organization, place, and exact date on which it was read. A full statement to the editor about all submissions and previous reports that might be regarded as

redundant publication of the same or very similar work. Any such work should be referred to specifically, and referenced in the new paper. Copies of such material should be included with the submitted paper, to help the editor decide how to handle the matter.

6. Registration number in case of a clinical trial and where it is registered (name of the registry and its URL)
7. Conflicts of Interest of each author/ contributor. A statement of financial or other relationships that might lead to a conflict of interest, if that information is not included in the manuscript itself or in an authors' form
8. Criteria for inclusion in the authors'/ contributors' list
9. A statement that the manuscript has been read and approved by all the authors, that the requirements for authorship as stated earlier in this document have been met, and that each author believes that the manuscript represents honest work, if that information is not provided in another form (see below); and
10. The name, address, e-mail, and telephone number of the corresponding author, who is responsible for communicating with the other authors about revisions and final approval of the proofs, if that information is not included on the manuscript itself.

[2] Blinded Article file: The main text of the article, beginning from Abstract till References (including tables) should be in this file. The file must not contain any mention of the authors' names or initials or the institution at which the study was done or acknowledgements. Page headers/ running title can include the title but not the authors' names. Manuscripts not in compliance with the Journal's blinding policy will be returned to the corresponding author. Use rtf/doc files. Do not zip the files. **Limit the file size to 1 MB.** Do not incorporate images in the file. If file size is large, graphs can be submitted as images separately without incorporating them in the article file to reduce the size of the file. The pages should be numbered consecutively, beginning with the first page of the blinded article file.

[3] Images: Submit good quality color images. **Each image should be less than 2 MB in size.** Size of the image can be reduced by decreasing the actual height and width of the images (keep up to 1600 x 1200 pixels or 5-6 inches). Images can be submitted as jpeg files. Do not zip the files. Legends for the figures/images should be included at the end of the article file.

[4] The contributors' / copyright transfer form (template provided below) has to be submitted in original with the signatures of all the contributors within two weeks of submission via courier, fax or email as a scanned image. Print ready hard copies of the images (one set) or digital images should be sent to the journal office at the time of submitting revised manuscript. High resolution images (up to 5 MB each) can be sent by email.

Contributors' form / copyright transfer form can be submitted online from the authors' area on <https://review.jow.medknow.com/jasi>.

Preparation of Manuscripts

Manuscripts must be prepared in accordance with "Uniform requirements for Manuscripts submitted to Biomedical Journals" developed by the International Committee of Medical Journal Editors (October 2008). The uniform requirements and specific requirement of Journal of the Anatomical Society of India are summarized below. Before submitting a manuscript, contributors are requested to check for the latest instructions available. Instructions are also available from the website of the journal (www.jasi.org.in) and from the manuscript submission site <https://review.jow.medknow.com/jasi>.

Journal of the Anatomical Society of India accepts manuscripts written in American English.

Copies of any permission(s)

It is the responsibility of authors/ contributors to obtain permissions for reproducing any copyrighted material. A copy of the permission obtained must accompany the manuscript. Copies of any and all published articles or other manuscripts in preparation or submitted elsewhere that are related to the manuscript must also accompany the manuscript.

Types of Manuscripts

Original articles:

These include randomized controlled trials, intervention studies, studies of screening and diagnostic test, outcome studies, cost effectiveness analyses, case-control series, and surveys with high response rate. The text of original articles amounting to up to 3000 words (excluding Abstract, references and Tables) should be divided into sections with the headings Abstract, Keywords, Introduction, Material and Methods, Results, Discussion and Conclusion, References, Tables and Figure legends.

An abstract should be in a structured format under following heads: **Introduction, Material and Methods, Results, and Discussion and Conclusion.**

Introduction: State the purpose and summarize the rationale for the study or observation.

Material and Methods: It should include and describe the following aspects:

Ethics: When reporting studies on human beings, indicate whether the procedures followed were in accordance with the ethical standards of the responsible committee on human experimentation (institutional or regional) and with the Helsinki Declaration of 1975, as revised in 2000

(available at http://www.wma.net/e/policy/17-c_e.html). For prospective studies involving human participants, authors are expected to mention about approval of (regional/ national/ institutional or independent Ethics Committee or Review Board, obtaining informed consent from adult research participants and obtaining assent for children aged over 7 years participating in the trial. The age beyond which assent would be required could vary as per regional and/ or national guidelines. Ensure confidentiality of subjects by desisting from mentioning participants' names, initials or hospital numbers, especially in illustrative material. When reporting experiments on animals, indicate whether the institution's or a national research council's guide for, or any national law on the care and use of laboratory animals was followed. Evidence for approval by a local Ethics Committee (for both human as well as animal studies) must be supplied by the authors on demand. Animal experimental procedures should be as humane as possible and the details of anesthetics and analgesics used should be clearly stated. The ethical standards of experiments must be in accordance with the guidelines provided by the CPCSEA and World Medical Association Declaration of Helsinki on Ethical Principles for Medical Research Involving Humans for studies involving experimental animals and human beings, respectively). The journal will not consider any paper which is ethically unacceptable. A statement on ethics committee permission and ethical practices must be included in all research articles under the 'Materials and Methods' section.

Study design:

Selection and Description of Participants: Describe your selection of the observational or experimental participants (patients or laboratory animals, including controls) clearly, including eligibility and exclusion criteria and a description of the source population. *Technical information:* Identify the methods, apparatus (give the manufacturer's name and address in parentheses), and procedures in sufficient detail to allow other workers to reproduce the results. Give references to established methods, including statistical methods (see below); provide references and brief descriptions for methods that have been published but are not well known; describe new or substantially modified methods, give reasons for using them, and evaluate their limitations. Identify precisely all drugs and chemicals used, including generic name(s), dose(s), and route(s) of administration.

Reports of randomized clinical trials should present information on all major study elements, including the protocol, assignment of interventions (methods of randomization, concealment of allocation to treatment groups), and the method of masking (blinding), based on the CONSORT Statement (<http://www.consort-statement.org>).

Reporting Guidelines for Specific Study Designs

Initiative	Type of Study	Source
CONSORT	Randomized controlled trials	http://www.consort-statement.org
STARD	Studies of diagnostic accuracy	http://www.consort-statement.org/stardstatement.htm
QUOROM	Systematic reviews and meta-analyses	http://www.consort-statement.org/Initiatives/MOOSE/moose.pdf
STROBE	Observational studies in epidemiology	http://www.strobe-statement.org
MOOSE	Meta-analyses of observational studies in epidemiology	http://www.consort-statement.org/Initiatives/MOOSE/moose.pdf

Statistics: Whenever possible quantify findings and present them with appropriate indicators of measurement error or uncertainty (such as confidence intervals). Authors should report losses to observation (such as, dropouts from a clinical trial). When data are summarized in the Results section, specify the statistical methods used to analyze them. Avoid non-technical uses of technical terms in statistics, such as ‘random’ (which implies a randomizing device), ‘normal’, ‘significant’, ‘correlations’, and ‘sample’. Define statistical terms, abbreviations, and most symbols. Specify the computer software used. Use upper italics (P 0.048). For all P values include the exact value and not less than 0.05 or 0.001. Mean differences in continuous variables, proportions in categorical variables and relative risks including odds ratios and hazard ratios should be accompanied by their confidence intervals.

Results: Present your results in a logical sequence in the text, tables, and illustrations, giving the main or most important findings first. Do not repeat in the text all the data in the tables or illustrations; emphasize or summarize only important observations. Extra- or supplementary materials and technical detail can be placed in an appendix where it will be accessible but will not interrupt the flow of the text; alternatively, it can be published only in the electronic version of the journal.

When data are summarized in the Results section, give numeric results not only as derivatives (for example, percentages) but also as the absolute numbers from which the derivatives were calculated, and specify the statistical methods used to analyze them. Restrict tables and figures to those needed to explain the argument of the paper and to assess its support. Use graphs as an alternative to tables with many entries; do not duplicate data in graphs and tables. Where scientifically appropriate, analyses of the data by variables such as age and sex should be included.

Discussion: Include summary of *key findings* (primary outcome measures, secondary outcome measures, results

as they relate to a prior hypothesis); *Strengths and limitations* of the study (study question, study design, data collection, analysis and interpretation); *Interpretation and implications* in the context of the totality of evidence (is there a systematic review to refer to, if not, could one be reasonably done here and now?, what this study adds to the available evidence, effects on patient care and health policy, possible mechanisms); *Controversies* raised by this study; and *Future research directions* (for this particular research collaboration, underlying mechanisms, clinical research).

Do not repeat in detail data or other material given in the Introduction or the Results section. In particular, contributors should avoid making statements on economic benefits and costs unless their manuscript includes economic data and analyses. Avoid claiming priority and alluding to work that has not been completed. New hypotheses may be stated if needed, however they should be clearly labeled as such. About 30 references can be included. These articles generally should not have more than six authors.

Review Articles:

These are comprehensive review articles on topics related to various fields of Anatomy. The entire manuscript should not exceed 7000 words with no more than 50 references and two authors. Following types of articles can be submitted under this category:

- Newer techniques of dissection and histology
- New methodology in Medical Education
- Review of a current concept

Please note that generally review articles are by invitation only. But unsolicited review articles will be considered for publication on merit basis.

Case reports:

New, interesting and rare cases can be reported. They should be unique, describing a great diagnostic or therapeutic challenge and providing a learning point for the readers. Cases with clinical significance or implications will be given priority. These communications could be of up to 1000 words (excluding Abstract and references) and should have the following headings: Abstract (unstructured), Key-words, Introduction, Case report, Discussion and Conclusion, Reference, Tables and Legends in that order.

The manuscript could be of up to 1000 words (excluding references and abstract) and could be supported with up to 10 references. Case Reports could be authored by up to four authors.

Letter to the Editor:

These should be short and decisive observations. They should preferably be related to articles previously published in the Journal or views expressed in the journal. They should not be preliminary observations that need a later

paper for validation. The letter could have up to 500 words and 5 references. It could be generally authored by not more than four authors.

Book Review: This consists of a critical appraisal of selected books on Anatomy. Potential authors or publishers may submit books, as well as a list of suggested reviewers, to the editorial office. The author/publisher has to pay INR 10,000 per book review.

Other:

Editorial, Guest Editorial, Commentary and Opinion are solicited by the editorial board.

References

References should be *numbered* consecutively in the order in which they are first mentioned in the text (not in alphabetic order). Identify references *in text*, tables, and legends by Arabic numerals in superscript with square bracket after the punctuation marks. *References cited only* in tables or figure legends should be numbered in accordance with the sequence established by the first identification in the text of the particular table or figure. Use the style of the examples below, which are based on the formats used by the NLM *in Index Medicus*. The titles of journals *should be abbreviated* according to the style used in Index Medicus. Use complete name of the journal for non-indexed journals. Avoid using abstracts as references. Information from manuscripts submitted but not accepted should be cited in the text as “unpublished observations” with written permission from the source. Avoid citing a “personal communication” unless it provides essential information not available from a public source, in which case the name of the person and date of communication should be cited in parentheses in the text. The commonly cited types of references are shown here, for other types of references such as newspaper items please refer to ICMJE Guidelines (<http://www.icmje.org> or http://www.nlm.nih.gov/bsd/uniform_requirements.html).

Articles in Journals

1. Standard journal article (for up to six authors): Parija S C, Ravinder PT, Shariff M. Detection of hydatid antigen in the fluid samples from hydatid cysts by coagglutination. *Trans. R.Soc. Trop. Med. Hyg.*1996; 90:255–256.
2. Standard journal article (for more than six authors): List the first six contributors followed by *et al.*

Roddy P, Gouri J, Flevaud L, Palma PP, Morote S, Lima N. *et al.*, Field Evaluation of a Rapid Immunochromatographic Assay for Detection of *Trypanosoma cruzi* Infection by Use of Whole Blood. *J. Clin. Microbiol.* 2008; 46: 2022-2027.

3. Volume with supplement: Otranto D, Capelli G, Genchi C: Changing distribution patterns of canine vector borne diseases in Italy: leishmaniosis vs. dirofilariosis.

Parasites & Vectors 2009; Suppl 1:S2.

Books and Other Monographs

1. Personal author(s): Parija SC. Textbook of Medical Parasitology. 3rd ed. All India Publishers and Distributors. 2008.
2. Editor(s), compiler(s) as author: Garcia LS, Filarial Nematodes In: Garcia LS (editor) Diagnostic Medical Parasitology ASM press Washington DC 2007: pp 319-356.
3. Chapter in a book: Nesheim M C. Ascariasis and human nutrition. In Ascariasis and its prevention and control, D. W. T. Crompton, M. C. Nesbemi, and Z. S. Pawlowski (eds.). Taylor and Francis, London, U.K.1989, pp. 87–100.

Electronic Sources as reference

Journal article on the Internet: Parija SC, Khairnar K. Detection of excretory *Entamoeba histolytica* DNA in the urine, and detection of *E. histolytica* DNA and lectin antigen in the liver abscess pus for the diagnosis of amoebic liver abscess. *BMC Microbiology* 2007, 7:41. doi:10.1186/1471-2180-7-41. <http://www.biomedcentral.com/1471-2180/7/41>

Tables

- Tables should be self-explanatory and should not duplicate textual material.
- Tables with more than 10 columns and 25 rows are not acceptable.
- Number tables, in Arabic numerals, consecutively in the order of their first citation in the text and supply a brief title for each.
- Place explanatory matter in footnotes, not in the heading.
- Explain in footnotes all non-standard abbreviations that are used in each table.
- Obtain permission for all fully borrowed, adapted, and modified tables and provide a credit line in the footnote.
- For footnotes use the following symbols, in this sequence: *, †, ‡, §, ||, ¶, **, ††, ‡‡
- Tables with their legends should be provided at the end of the text after the references. The tables along with their number should be cited at the relevant place in the text

Illustrations (Figures)

- Upload the images in JPEG format. The file size should be within 1024 kb in size while uploading.
- Figures should be numbered consecutively according to the order in which they have been first cited in the text.
- Labels, numbers, and symbols should be clear and of uniform size. The lettering for figures should be large enough to be legible after reduction to fit the width of a printed column.
- Symbols, arrows, or letters used in photomicrographs

should contrast with the background and should be marked neatly with transfer type or by tissue overlay and not by pen.

- Titles and detailed explanations belong in the legends for illustrations not on the illustrations themselves.
- When graphs, scatter-grams or histograms are submitted the numerical data on which they are based should also be supplied.
- The photographs and figures should be trimmed to remove all the unwanted areas.
- If photographs of individuals are used, their pictures must be accompanied by written permission to use the photograph.
- If a figure has been published elsewhere, acknowledge the original source and submit written permission from the copyright holder to reproduce the material. A credit line should appear in the legend for such figures.
- Legends for illustrations: Type or print out legends (maximum 40 words, excluding the credit line) for illustrations using double spacing, with Arabic numerals corresponding to the illustrations. When symbols, arrows, numbers, or letters are used to identify parts of the illustrations, identify and explain each one in the legend. Explain the internal scale (magnification) and identify the method of staining in photomicrographs.
- Final figures for print production: Send sharp, glossy, un-mounted, color photographic prints, with height of 4 inches and width of 6 inches at the time of submitting the revised manuscript. Print outs of digital photographs are not acceptable. If digital images are the only source of images, ensure that the image has minimum resolution of 300 dpi or 1800 x 1600 pixels in TIFF format. Send the images on a CD. Each figure should have a label pasted (avoid use of liquid gum for pasting) on its back indicating the number of the figure, the running title, top of the figure and the legends of the figure. Do not write the contributor/s' name/s. Do not write on the back of figures, scratch, or mark them by using paper clips.
- The Journal reserves the right to crop, rotate, reduce, or enlarge the photographs to an acceptable size.

Protection of Patients' Rights to Privacy

Identifying information should not be published in written descriptions, photographs, sonograms, CT scans, etc., and pedigrees unless the information is essential for scientific purposes and the patient (or parent or guardian, wherever applicable) gives informed consent for publication. Authors should remove patients' names from figures unless they have obtained informed consent from the patients. The journal abides by ICMJE guidelines:

1. Authors, not the journals nor the publisher, need to obtain the patient consent form before the publication and have the form properly archived. The consent

forms are not to be uploaded with the cover letter or sent through email to editorial or publisher offices.

2. If the manuscript contains patient images that preclude anonymity, or a description that has obvious indication to the identity of the patient, a statement about obtaining informed patient consent should be indicated in the manuscript.

Sending a revised manuscript

The revised version of the manuscript should be submitted online in a manner similar to that used for submission of the manuscript for the first time. However, there is no need to submit the "First Page" or "Covering Letter" file while submitting a revised version. When submitting a revised manuscript, contributors are requested to include, the 'referees' remarks along with point to point clarification at the beginning in the revised file itself. In addition, they are expected to mark the changes as underlined or colored text in the article.

Reprints and proofs

Journal provides no free printed reprints. Authors can purchase reprints, payment for which should be done at the time of submitting the proofs.

Publication schedule

The journal publishes articles on its website immediately on acceptance and follows a 'continuous publication' schedule. Articles are compiled in issues for 'print on demand' quarterly.

Copyrights

The entire contents of the Journal of the Anatomical Society of India are protected under Indian and international copyrights. The Journal, however, grants to all users a free, irrevocable, worldwide, perpetual right of access to, and a license to copy, use, distribute, perform and display the work publicly and to make and distribute derivative works in any digital medium for any reasonable non-commercial purpose, subject to proper attribution of authorship and ownership of the rights. The journal also grants the right to make small numbers of printed copies for their personal non-commercial use under Creative Commons Attribution-Noncommercial-Share Alike 4.0 Unported License.

Checklist

Covering letter

- Signed by all contributors
- Previous publication / presentations mentioned
- Source of funding mentioned
- Conflicts of interest disclosed

Authors

- Last name and given name provided along with Middle name initials (where applicable)
- Author for correspondence, with e-mail address provided
- Number of contributors restricted as per the instructions
- Identity not revealed in paper except title page (e.g. name of the institute in Methods, citing previous study as ‘our study’, names on figure labels, name of institute in photographs, etc.)

Presentation and format

- Double spacing
- Margins 2.5 cm from all four sides
- Page numbers included at bottom
- Title page contains all the desired information
- Running title provided (not more than 50 characters)
- Abstract page contains the full title of the manuscript
- Abstract provided (structured abstract of 250 words for original articles, unstructured abstracts of about 150 words for all other manuscripts excluding letters to the Editor)
- Key words provided (three or more)
- Introduction of 75-100 words
- Headings in title case (not ALL CAPITALS)
- The references cited in the text should be after punctuation marks, in superscript with square bracket.
- References according to the journal’s instructions, punctuation marks checked

- Send the article file without ‘Track Changes’

Language and grammar

- Uniformly American English
- Write the full term for each abbreviation at its first use in the title, abstract, keywords and text separately unless it is a standard unit of measure. Numerals from 1 to 10 spelt out
- Numerals at the beginning of the sentence spelt out
- Check the manuscript for spelling, grammar and punctuation errors
- If a brand name is cited, supply the manufacturer’s name and address (city and state/country).
- Species names should be in italics

Tables and figures

- No repetition of data in tables and graphs and in text
- Actual numbers from which graphs drawn, provided
- Figures necessary and of good quality (colour)
- Table and figure numbers in Arabic letters (not Roman)
- Labels pasted on back of the photographs (no names written)
- Figure legends provided (not more than 40 words)
- Patients’ privacy maintained (if not permission taken)
- Credit note for borrowed figures/tables provided
- Write the full term for each abbreviation used in the table as a footnote



Journal of The Anatomical Society of India

Salient Features:

- Publishes research articles related to all aspects of Anatomy and Allied medical/surgical sciences.
- Pre-Publication Peer Review and Post-Publication Peer Review
- Online Manuscript Submission System
- Selection of articles on the basis of MRS system
- Eminent academicians across the globe as the Editorial board members
- Electronic Table of Contents alerts
- Available in both online and print form.

The journal is registered with the following abstracting partners:

Baidu Scholar, CNKI (China National Knowledge Infrastructure), EBSCO Publishing's Electronic Databases, Ex Libris – Primo Central, Google Scholar, Hinari, Infotrieve, Netherlands ISSN center, ProQuest, TdNet, Wanfang Data

The journal is indexed with, or included in, the following:

SCOPUS, Science Citation Index Expanded, IndMed, MedInd, Scimago Journal Ranking, Emerging Sources Citation Index.

Impact Factor® as reported in the 2018 Journal Citation Reports® (Clarivate Analytics, 2019): 0.168

Editorial Office:

Dr. Vishram Singh, Editor-in-Chief, JASI
OC-5/103, 1st floor, Orange County Society,
Ahinsa Khand-I, Indrapuram, Ghaziabad,
Delhi, NCR- 201014.
Email: editorjasi@gmail.com
(O) | Website: www.asiindia.in

The journal is owned and run by The Anatomical Society of India